

HYDROLYSIS OF GRASS XYLAN BY XYLANASES FROM *Aureobasidium pullulans* FOR
XYLOOLIGOSACCHARIDE AND XYLITOL PRODUCTIONS



A Dissertation Submitted in Partial Fulfillment of the Requirements
for the Degree of Doctor of Philosophy in Biotechnology
FACULTY OF SCIENCE
Chulalongkorn University
Academic Year 2022
Copyright of Chulalongkorn University

ไฮโดรไลซิสของไซแลนหญ้าโดยไซแลเนสจาก *Aureobasidium pullulans* เพื่อการผลิต
ไซโกลอลิโกแซ็กคาไรด์และไซลิทอล



วิทยานิพนธ์นี้เป็นส่วนหนึ่งของการศึกษาตามหลักสูตรปริญญาวิทยาศาสตรดุษฎีบัณฑิต

สาขาวิชาเทคโนโลยีชีวภาพ ไม่สังกัดภาควิชา/เทียบเท่า

คณะวิทยาศาสตร์ จุฬาลงกรณ์มหาวิทยาลัย

ปีการศึกษา 2565

ลิขสิทธิ์ของจุฬาลงกรณ์มหาวิทยาลัย

Thesis Title HYDROLYSIS OF GRASS XYLAN BY XYLANASES FROM
Aureobasidium pullulans FOR XYLOOLIGOSACCHARIDE
AND XYLITOL PRODUCTIONS

By Acting SubLt. Sorawit Na Nongkhai

Field of Study Biotechnology

Thesis Advisor Associate Professor SEHANAT PRASONGSUK, Ph.D.

Thesis Co Advisor Associate Professor PONGTHARIN LOTRAKUL, Ph.D.

Accepted by the FACULTY OF SCIENCE, Chulalongkorn University in Partial
Fulfillment of the Requirement for the Doctor of Philosophy

..... Dean of the FACULTY OF SCIENCE
(Professor POLKIT SANGVANICH, Ph.D.)

DISSERTATION COMMITTEE

..... Chairman
(Assistant Professor JITTRA PIAPUKIEW, Ph.D.)

..... Thesis Advisor
(Associate Professor SEHANAT PRASONGSUK, Ph.D.)

..... Thesis Co-Advisor
(Associate Professor PONGTHARIN LOTRAKUL, Ph.D.)

..... Examiner
(Associate Professor APHICHART KARNCHANATAT, Ph.D.)

..... Examiner
(Assistant Professor KRISANA SIRALERTMUKUL, Ph.D.)

..... Examiner
(WICHANEE BANKEEREE, Ph.D.)

..... External Examiner
(Associate Professor Duangporn Premjet, Ph.D.)

สรวิชัย ฌ นหนองคาย : ไฮโดรไลซิสของไซแลนหญ้าโดยไซแลเนสจาก *Aureobasidium pullulans* เพื่อการผลิตไซโลอลิโกแซ็กคาไรด์และไซลิทอล. (HYDROLYSIS OF GRASS XYLAN BY XYLANASES FROM *Aureobasidium pullulans* FOR XYLOOLIGOSACCHARIDE AND XYLITOL PRODUCTIONS) อ.ที่ปรึกษาหลัก : รศ. ดร.สีหนาท ประสงค์สุข, อ.ที่ปรึกษาร่วม : รศ. ดร.พงศ์ธาริน โฉมตระกูล

เมื่อสกัดไซแลนจากหญ้า 10 ตัวอย่าง พบว่าหญ้า 5 ตัวอย่างมีศักยภาพเป็นแหล่งของไซแลน ได้แก่ ใบอ้อย หญ้ากีนีสีม่วง หญ้าเนเปียร์ หญ้าซาบิและหญ้าแฝก จากนั้นเมื่อหาภาวะที่เหมาะสม พบว่าใบอ้อยให้ร้อยละการได้ไซแลนกลับคืนสูงสุดที่ 99.42 เมื่อใช้ไซโตเดียมไฮกรอกไซโตร้อยละ 14.32 (น้ำหนักต่อปริมาตร) สัดส่วนของเหลวต่อของแข็งที่ 13.25:1 และเวลาสกัด 32.36 นาที เมื่อวิเคราะห์โครงสร้างและองค์ประกอบน้ำตาลของไซแลนที่สกัดได้พบว่า ไซแลนจากใบอ้อยเป็นอะราบิโนไซแลน ในขณะที่ไซแลนจากหญ้าอีก 4 ชนิดเป็น กลูคูโรอะราบิโนไซแลน นำไซแลนจากใบอ้อย หญ้ากีนีสีม่วงและหญ้าเนเปียร์ที่ถูกต้องเลือกบนพื้นฐานของค่าการได้ไซแลนกลับคืนสูง มาศึกษาการย่อยโดยใช้เอนไซม์ รวมถึงการผลิตไซโลอลิโกแซ็กคาไรด์และไซลิทอล โดยเริ่มจากการคัดกรองเชื้อที่ผลิตเอนไซม์ย่อยสลายไซแลนได้ดีที่สุดและพบว่า *Aureobasidium pullulans* NRRL 58523 และ *A. pullulans* CBS 135684 เป็นสายพันธุ์ที่ถูกคัดเลือกเพื่อนำมาผลิตเอนไซม์เอนโดไซแลเนส และปีตาไซโลซิเดสหยาบ สำหรับใช้ในการย่อยแบบบางส่วนและแบบสมบูรณ์ จากการย่อยไซแลนแบบบางส่วนภายใต้ภาวะที่เหมาะสม (ใช้เอนไซม์เอนโดไซแลเนสที่อัตรา 65.32 ยูนิตต่อกรัมไซแลน และบ่มนาน 52.89 ชั่วโมง) สามารถผลิตไซโลอลิโกแซ็กคาไรด์ได้สูงสุดจากไซแลนที่สกัดจากใบอ้อยที่ 0.27 กรัมต่อกรัมไซแลนเริ่มต้น ในขณะที่การย่อยไซแลนแบบสมบูรณ์ภายใต้ภาวะที่เหมาะสม (ใช้เอนไซม์ผสมระหว่างเอนโดไซแลเนสและปีตาไซโลซิเดสที่อัตรา 66.93 และ 67.85 ยูนิตต่อกรัมไซแลนตามลำดับ และบ่มนาน 17.71 ชั่วโมง) สามารถผลิตไซโลสได้สูงสุดจากไซแลนที่สกัดจากใบอ้อยเช่นกันที่ 0.20 กรัมต่อกรัมไซแลนเริ่มต้น ไซโลอลิโกแซ็กคาไรด์ที่ผลิตได้แสดงสมบัติฟิโบริโอติกอย่างจำเพาะกับแบคทีเรียในสกุล *Lactobacillus* อย่างมีนัยสำคัญ และเมื่อนำไซโลอลิโกแซ็กคาไรด์มาทดสอบกับ DPPH พบฤทธิ์การต้านอนุมูลอิสระในระดับต่ำ สำหรับการผลิตไซลิทอลโดยใช้ไซโลสที่ได้จากการย่อยแบบสมบูรณ์ด้วย *Candida tropicalis* FS 10 สามารถผลิตไซลิทอลได้สูงสุดที่ร้อยละ 28.78 เมื่อเติมไซโลสจากใบอ้อยที่ความเข้มข้น 56.69 กรัมต่อลิตรในอาหารสูตรผลิตประกอบด้วยกลูโคสที่ความเข้มข้น 5.44 กรัมต่อลิตรและยีสต์สกัดที่ความเข้มข้น 4.71 กรัมต่อลิตร

สาขาวิชา	เทคโนโลยีชีวภาพ	ลายมือชื่อนิติ
ปีการศึกษา	2565	ลายมือชื่อ อ.ที่ปรึกษาหลัก
		ลายมือชื่อ อ.ที่ปรึกษาร่วม

5772851623 : MAJOR BIOTECHNOLOGY

KEYWORD: Xylan, Grass, Endoxylanase, β -xylosidase, Xylooligosaccharides, Xylose, Xylitol

Sorawit Na Nongkhai : HYDROLYSIS OF GRASS XYLAN BY XYLANASES FROM *Aureobasidium pullulans* FOR XYLOOLIGOSACCHARIDE AND XYLITOL PRODUCTIONS.

Advisor: Assoc. Prof. SEHANAT PRASONGSUK, Ph.D. Co-advisor: Assoc. Prof. PONGTHARIN LOTRAKUL, Ph.D.

Ten grass samples were screened for potential as a xylan source and five including sugarcane leaf, purple guinea grass, Napier grass, sabi grass and vetiver grass were selected for optimization of xylan extraction. After optimization, sugarcane leaf gave the highest xylan recovery at 99.42% when it was extracted by 14.32% (w/v) NaOH at 13.25:1 liquid: solid ratio with 32.36-min steaming time. From the xylan structural and sugar composition analyses, the major xylan from sugarcane leaf was arabinoxylan whereas those from the other grass samples were (glucurono)arabinoxylan. Xylans from sugarcane leaf, purple guinea grass and Napier grass were selected for further enzymatic hydrolysis and xylooligosaccharide and xylitol production based on their high xylan recovery. After screening for the best xylanolytic enzymes producers, crude endoxylanase and β -xylosidase were produced from *Aureobasidium pullulans* NRRL 58523 and *A. pullulans* CBS 135684, respectively, and used for the partial and complete xylan saccharification. After optimization, the maximum yield of xylooligosaccharides at 0.27 g/g initial xylan was received from sugarcane leaf through partial hydrolysis with 65.32 U/g xylan endoxylanase dosage and 52.89-h incubation time. Sugarcane leaf also gave the maximum xylose yield at 0.20 g/g initial xylan through the optimized completed hydrolysis with a cocktail of 69.93 U/g xylan endoxylanase and 67.85 U/g xylan β -xylosidase and 17.71-h incubation time. Xylooligosaccharides from all digested xylans showed significant species-specific prebiotic activity toward *Lactobacillus* spp. Insignificant antioxidant activity was also observed from all grass xylans via DPPH assay. Xylose obtained from the complete hydrolysis was used for xylitol production by *Candida tropicalis* FS 10. The highest xylitol conversion efficiency at 28.78% was obtained when xylose from sugarcane leaf was added at 56.69 g/L to the optimized production medium containing 5.44 g/L glucose and 4.71 g/L yeast extract.

Field of Study: Biotechnology

Student's Signature

Academic Year: 2022

Advisor's Signature

Co-advisor's Signature

ACKNOWLEDGEMENTS

First of all, I would like to express my gratitude to my advisor, Assoc. Prof. Dr. Sehanat Prasongsuk for his kindness, support and expert guidance for editing works and scholarship applications during my PhD study in Chulalongkorn University. Moreover, I would like to express the deepest appreciation to my co-advisor Assoc. Prof. Dr. Pongtharin Lotrakul for his suggestion and editing publications and this thesis.

I would like to thank Assist. Prof. Dr. Jittra Piapukiew, Assoc. Prof. Dr. Aphichart Karnchanatat, Assist. Prof. Dr. Krisana Siralermukul, Dr. Wichanee Bankeeree and Assoc. Prof. Dr. Duangporn Premjet to provide opportunity on my thesis committees for their valuable suggestions.

I wish to express my appreciation to Graduate School, Chulalongkorn University for scholarships including the 100th Anniversary Chulalongkorn University Fund for Doctoral Scholarship, the 90th Anniversary of Chulalongkorn University Fund (Ratchadaphiseksomphot Endowment Fund) and the Overseas Research Experience Scholarship for Graduate Student for my research experience at Yamaguchi University, Japan.

I specially thank to Nakhon Ratchasima/ Phetchaburi Animal Nutrition Research and Development Center, Department of Livestock Development, Ministry of Agriculture and Cooperatives, Pakchong Technology Research and Training Center, Department of Lands, Ministry of Interior and Department of Agronomy, Kasetsart University for grass samples supporting in this study.

Finally, I would like to express my special gratitude to my colleagues from the Plant Biomass Utilization Research Unit (PBURU) to support my research and private life. Moreover, I would like to provide my special gratitude to my family, especially my wife and my son, to encourage me during my PhD working.

Sorawit Na Nongkhai

TABLE OF CONTENTS

	Page
ABSTRACT (THAI).....	iii
ABSTRACT (ENGLISH)	iv
ACKNOWLEDGEMENTS.....	v
TABLE OF CONTENTS.....	vi
LIST OF TABLES.....	ix
LIST OF FIGURES	xii
Chapter I Introduction	1
1.1 Rationale.....	1
1.2 Objectives of this study	2
1.3 Research Procedure.....	3
1.4 Anticipated benefits.....	3
Chapter II Literature review.....	4
2.1 Plant biomass potential	4
2.2 Hemicellulose	5
2.3 Xylanolytic enzymes	10
2.4 Enzymatic hydrolysis of xylan	17
2.5 Xylooligosaccharides	20
2.6 Bioconversion of xylose to xylitol.....	24
Chapter III Materials and Methods.....	28
3.1 Equipments.....	28
3.2 Chemicals	28

3.3 Microorganisms	30
3.4 Optimization of xylan extraction from grasses	32
3.4 Production of endoxylanase and β -xylosidase from <i>A. pullulans</i>	34
3.5 Determination of molecular weight, degree of polymerization and viscosity property	36
3.6 Enzymatic hydrolysis of xylan	37
3.7 Prebiotic property of XOs	39
3.8 Antioxidant activity of XOs.....	39
3.9 Xylitol production	40
Chapter IV Results.....	43
4.1 Biomass composition of grass samples	43
4.2 Optimization of xylan extraction from grasses	44
4.3 Endoxylanase and β -xylosidase production from <i>A. pullulans</i>	58
4.4 Determination of molecular weight, average DP and viscosity property	64
4.5 XOs production.....	65
4.6 Xylose production.....	71
4.7 Prebiotic property of XOs	78
4.8 Antioxidant activity of XOs.....	79
4.9 Xylitol production	80
Chapter V Discussion.....	90
5.1 Xylan extraction	90
5.2 Endoxylanase and β -xylosidase production	92
5.3 Molecular weight, average DP and viscosity property	93

5.4 Enzymatic xylan hydrolysis	94
5.5 Prebiotic property	96
5.6 Antioxidant activity.....	97
5.7 Xylitol production	97
Chapter VI Conclusion and prospect.....	100
REFERENCES.....	102
APPENDIX	126
VITA	159



LIST OF TABLES

	Page
Table 1 Composition of different plant biomasses	4
Table 2 Comparative xylan extractions using NaOH and KOH in different biomasses.....	8
Table 3 Viscosities of various xylans and their applications	10
Table 4 Previously reported microbial endoxylanases and their activities	11
Table 5 Previously reported microbial β -xylosidases and their activities.....	13
Table 6 XO _s production from lignocellulosic biomasses by endoxylanase.....	18
Table 7 Xylose production from lignocellulosic biomasses via enzyme hydrolysis.....	19
Table 8 Radical scavenging activity of XO _s from xylan through DPPH assay.....	23
Table 9 Xylitol production by <i>Candida</i> spp. using lignocellulosic hydrolysate.....	26
Table 10 36 strains of <i>Aureobasidium</i> spp.	31
Table 11 Grass samples in this study	32
Table 12 Code and actual levels of three variables	34
Table 13 Code and actual levels of two variables for optimization of XO _s production ...	37
Table 14 Code and actual levels of three variables for optimization of xylose production	39
Table 15 Fourteen strains of xylitol-producing yeasts	40
Table 16 Code and actual levels of three variables for optimization of xylitol production	41
Table 17 Biomass composition of the grass samples	43
Table 18 Sugar composition of xylan samples	45

Table 19 BBD matrix with experimental and RSM predicted values of relative xylan recovery from sugarcane leaf	48
Table 20 BBD matrix with experimental and RSM predicted values of relative xylan recovery from napier grass	50
Table 21 BBD matrix with experimental and RSM predicted values of relative xylan recovery from purple guinea grass	52
Table 22 BBD matrix with experimental and RSM predicted values of relative xylan recovery from vetiver grass	54
Table 23 BBD matrix with experimental and RSM predicted values of relative xylan recovery from sabi grass	56
Table 24 Comparison of five grasses xylan extraction under optimize condition	57
Table 25 CCD and RSM predicted values of reducing sugars from partial hydrolysis of sugarcane leaf xylan	67
Table 26 CCD and RSM predicted values of reducing sugars from partial hydrolysis of purple guinea grass xylan	69
Table 27 CCD and RSM predicted values of reducing sugars from partial hydrolysis of napier grass xylan	70
Table 28 BBD and RSM predicted values of xylose production from sugarcane leaf xylan	73
Table 29 BBD and RSM predicted values of xylose production from purple guinea grass xylan	75
Table 30 BBD and RSM predicted values of xylose production from napier grass xylan	77
Table 31 Growth of <i>Lactobacillus</i> spp. and <i>Bifidobacterium</i> spp. in MRS medium with carbon sources including XOs and other compounds (2 mg carbon /mL)	78

Table 32 BBD and RSM predicted the percentages of xylitol conversion from commercial xylose.....	83
Table 33 BBD and RSM predicted the percentages of xylitol conversion from sugarcane leaf.....	85
Table 34 BBD and RSM predicted the percentages of xylitol conversion from xylose-purple guinea grass	87
Table 35 BBD and RSM predicted the percentages of xylitol conversion from xylose-napier grass.....	89



LIST OF FIGURES

	Page
Figure 1 Structure of homoxylan	5
Figure 2 Structure of glucuronoxylan	6
Figure 3 Structure of (arabino)glucuronoxylan	6
Figure 4 Structure of arabinoxylan	7
Figure 5 Structure of (glucurono)arabinoxylan	7
Figure 6 Degradation of xylan backbone and different side chains by xylanolytic enzymes. Certain enzyme groups are framed and cleavage positions are arrowed	14
Figure 7 Morphological characteristic forms of <i>A. pullulans</i> with the development stage including (A) blastospore, (B) germinating blastospore, (C) initial hyphae, (D) chlamydo spores, (E) germinating chlamydo spores, (F) swollen cell and (G) septate swollen cell	16
Figure 8 Structure of XOs	20
Figure 9 Benefits occurrence of prebiotic (XOs) in the colon	21
Figure 10 Metabolic pathways for xylitol production by yeast	25
Figure 11 Relative xylan recovery (%) of ten grass samples after alkali extraction. Different letters above the bar graphs indicate significant differences according to DMRT at $p \leq 0.05$. Bar indicated standard deviation derived from three replicates	44
Figure 12 The FT-IR spectra pattern of the xylan samples	46
Figure 13 Response surface plots of optimal condition for xylan extraction from sugarcane leaf. (A) Effects of NaOH concentration and steaming time, (B) Effects of NaOH concentration and solid to liquid ratio and (C) Effect of steaming time and solid to liquid ratio	47

Figure 14 Response surface plots of optimal condition for xylan extraction from napier grass. (A) Effects of NaOH concentration and steaming time, (B) Effects of NaOH concentration and solid to liquid ratio and (C) Effect of steaming time and solid to liquid ratio	49
Figure 15 Response surface plots of optimal condition for xylan extraction from purple guinea grass. (A) Effects of NaOH concentration and steaming time, (B) Effects of NaOH concentration and solid to liquid ratio and (C) Effect of steaming time and solid to liquid ratio	51
Figure 16 Response surface plots of optimal condition for xylan extraction from vetiver grass. (A) Effects of NaOH concentration and steaming time, (B) Effects of NaOH concentration and solid to liquid ratio and (C) Effect of steaming time and solid to liquid ratio	53
Figure 17 Response surface plots of optimal condition for xylan extraction from sabi grass. (A) Effects of NaOH concentration and steaming time, (B) Effects of NaOH concentration and solid to liquid ratio and (C) Effect of steaming time and solid to liquid ratio	55
Figure 18 Endoxylanase activity of <i>Aureobasidium</i> spp. Different letters above the bar graphs indicate significant differences according to DMRT at $p \leq 0.05$. Bar indicated standard deviation derived from three replicates.....	58
Figure 19 β -xylosidase activity of <i>Aureobasidium</i> spp. Different letters above the bar graphs indicate significant differences according to DMRT at $p \leq 0.05$. Bar indicated standard deviation derived from three replicates.....	59
Figure 20 Optimum pH and temperature of endoxylanases from (A) <i>A. pullulans</i> NRRL 58519; (B) <i>A. pullulans</i> NRRL 58523 and (C) <i>A. pullulans</i> NRRL 58536	60
Figure 21 Optimum pH and temperature of β -xylosidase from (A) <i>A. pullulans</i> CBS135684; (B) <i>A. pullulans</i> NRRL 58559, (C) <i>A. melanogenum</i> PBUAP 37 and (D) <i>A. melanogenum</i> PBUAP 13.....	61

Figure 22 Thermostability of endoxylanase from: (A) <i>A. pullulans</i> NRRL58519, (B) <i>A. pullulans</i> NRRL58523, (C) <i>A. pullulans</i> NRRL58536	62
Figure 23 Thermostability of β -xylosidase: (A) <i>A. pullulans</i> CBS 135684, (B) <i>A. melanogenum</i> PBUAP 37, (C) <i>A. pullulans</i> NRRL 58559 and (D) <i>A. melanogenum</i> PBUAP 13	63
Figure 24 Viscosity at shear rate 100 s^{-1} and the average DP of (A) sugarcane leaf xylan, (B) purple guinea grass xylan and (C) napier grass xylan before and after endoxylanase disruption at different dosages treatment(0, 25, 50, 100 U/g substrate) .	64
Figure 25 Amount of the reducing sugars obtained from the hydrolysis of three xylans. Different letters above the bar graphs indicate significant differences according to DMRT at $p \leq 0.05$. Bar indicated standard deviation derived from three replicates.	65
Figure 26 Response surface plots for optimal condition of partial xylan hydrolysis of (A) sugarcane leaf xylan, (B) Purple guinea grass xylan and (C) Napier grass xylan for determination of the releasing of reducing sugars	66
Figure 27 Comparison of different hydrolysis protocols for complete hydrolysis of xylans: (A) commercial beechwood xylan, (B) sugarcane leaf xylan, (C) purple guinea grass xylan and (D) napier grass xylan. Different letters above the bar graphs indicate significant differences according to DMRT at $p \leq 0.05$. Bar indicated standard deviation derived from three replicates.	71
Figure 28 Response surface plots for optimal condition of xylose production from sugarcane leaf xylan. (A) Effect of β -xylosidase and endoxylanase dosages, (B) Effect of incubation time and endoxylanase dosage and (C) Effect of incubation time and β -xylosidase dosage	73
Figure 29 Response surface plots for optimal condition of xylose production from purple guinea grass xylan. (A) Effect of β -xylosidase and endoxylanase dosages, (B) Effect of incubation time and endoxylanase dosage and (C) Effect of incubation time and β -xylosidase dosage	75

Figure 30 Response surface plots for optimal condition of xylose production from napier grass xylan. (A) Effect of β -xylosidase and endoxylanase dosages, (B) Effect of incubation time and endoxylanase dosage and (C) Effect of incubation time and β -xylosidase dosage	77
Figure 31 DPPH radical scavenging activity of: (A) gallic acid, (B) ascorbic acid, (C) XOs-Sugarcane leaf, (D) XOs-Napier grass and (E) XOs-Purple guinea grass	79
Figure 32 Xylitol conversion of 14 strains of <i>Candida</i> spp. using commercial xylose. Different letters above the bar graphs indicate significant differences according to DMRT at $p \leq 0.05$. Bar indicated standard deviation derived from three replicates	80
Figure 33 Effect on temperature and incubation time on xylitol production by <i>C. tropicalis</i> FS10 and The relative xylitol conversion was calculated as the percentage of the maximum xylitol conversion. Experiments were performed in triplicate and bars indicate standard deviations.	81
Figure 34 The percentage of xylitol conversion from commercial xylose and xylose from sugarcane leaf, purple guinea grass and napier grass. Different letters above the bar graphs indicate significant differences according to DMRT at $p \leq 0.05$. Bar indicated standard deviation derived from three replicates	81
Figure 35 Response surface plots for optimal condition of xylitol conversion from commercial xylose. (A) Effect of xylose and glucose concentrations, (B) Effect of xylose and yeast extract concentrations and (C) Effect of glucose and yeast extract concentrations	83
Figure 36 Response surface plots for optimal condition of xylitol conversion from xylose-sugarcane leaf. (A) Effect of xylose and glucose concentrations, (B) Effect of xylose and yeast extract concentrations and (C) Effect of glucose and yeast extract concentrations	85
Figure 37 Response surface plots for optimal condition of xylitol conversion from xylose-purple guinea grass. (A) Effect of xylose and glucose concentrations, (B) Effect of	

xylose and yeast extract concentrations and (C) Effect of glucose and yeast extract concentrations 87

Figure 38 Response surface plots for optimal condition of xylitol conversion from xylose-napier grass. (A) Effect of xylose and glucose concentrations, (B) Effect of xylose and yeast extract concentrations and (C) Effect of glucose and yeast extract concentrations 89



Chapter I

Introduction

1.1 Rationale

Non-renewable fossil fuel is limited and has become increasingly expensive. It also causes negative environmental impacts. Therefore, utilization of renewable and alternative resources such as plant biomass, both food and non-food materials, has been increased (Hood et al., 2011). Recently, due to the more frequently happening food crises, focus has been shifted toward non-food lignocellulosic biomass and agricultural residues (Miret et al., 2016). Non-food plant biomass comprises cellulose, hemicellulose and lignin as the major components in cell wall. They are the precursors for the production of value-added products through hydrolysis and fermentation (Mansor et al., 2019). As an answer to high feedstock demand and production cost, fast growing weeds and plantation grasses which are available throughout the year in every region with little to no value have high potential as an alternative lignocellulosic resource for the production of fuels, chemicals and energy (Liang et al., 2012).

Hemicellulose is the second most abundant polysaccharides in plant biomass (Peng et al., 2012). Xylan, the major component of most hemicellulose, has many interesting properties and has been used in many industrial applications. Due to its high viscosity, xylan has also been used as solution thickener, super gel for wound dressing, drug carrier and etc. (Ünlü et al., 2015). Viscosity is usually related to molecular weight and chain length for most polymeric carbohydrates. However, it is still not clear how xylan chain length affects its viscosity.

Xylan can be hydrolyzed by xylanolytic enzymes including endo-1,4- β -xylanase (endoxylanase) and β -xylosidase to xylooligosaccharides and xylose (Ohta et al., 2010; Michelin et al., 2012). Many bacteria and fungi can produce xylanolytic enzymes with a wide range of yield and properties. *Aureobasidium pullulans*, a black yeast commonly found worldwide, has been reported as a good xylanolytic enzyme producer. In Thailand, a number of xylanase-overproducing color-variant strains have been isolated and their enzymes have been shown promising potential in xylan hydrolysis (Leathers, 1986; Christov et al., 1997; Manitchotpisit et al., 2009; Yanwisetpakdee et al., 2016; Bankeeree et al., 2018; Prasongsuk et al., 2018; Patipong et al., 2019). However, most

studies have been conducted using purified hardwood xylan, an expensive substrate (Karni et al., 1993; Buthelezi et al., 2011; Nasr et al., 2013; Bankeeree et al., 2014). Therefore, it is of interest to use these enzymes for hydrolysis of cheaper hemicellulosic substrates such as weed or grass xylans.

Xylooligosaccharides have been reported as prebiotics and can enhance growth and activity of beneficial bacteria in the colon such as bifidobacteria and lactobacilli. (Chapla et al., 2012; Samanta et al., 2015). Moreover, it has antioxidant activity that can prevent similar to sucrose, but giving much lower calories. Thus, it has been widely used as sugar substitute in foods/drinks for diabetics and healthy snacks that can promote the effects of free radicals that cause many chronic diseases (Gowdhaman and Ponnusami, 2015; Jayathilake et al., 2016). For xylose, it can be converted to either ethanol or a range of high value products such as xylitol through different yeast fermentations. Xylitol can be applied in pharmaceutical and food industries because it has sweet taste oral health and to prevent dental caries (Prakash et al., 2011; Ping et al., 2013).

Therefore, the objectives of this study are (i) to optimize xylan extraction from grasses and investigate some properties of a selected xylan including viscosity, (ii) to produce xylooligosaccharides via enzymatic hydrolysis of a selected grass xylan and detect its prebiotic and antioxidant activities, (iii) to optimize xylan hydrolysis using combinations of *A. pullulans* endoxylanase and β -xylosidase to produce xylose and (iv) to optimize the xylitol production. Results obtained from this study will be a basis for larger/industrial-scale process development for xylooligosaccharide and xylitol production from grass xylan.

1.2 Objectives of this study

- 1.2.1. To optimize xylan extraction from grass and characterize selected properties of the obtained xylan
- 1.2.2. To produce xylooligosaccharides via enzymatic hydrolysis of grass xylan and to study its prebiotic and antioxidant properties
- 1.2.3. To optimize xylan hydrolysis by the combinations of *A. pullulans* endoxylanase and β -xylosidase for xylose production
- 1.2.4. To optimize the xylitol production

1.3 Research Procedure

1.3.1. Literature review

1.3.2. Optimization of xylan extraction from grasses

1.3.3. Production of endoxylanase and β -xylosidase from *A. pullulans*

1.3.4. Production of xylans with different chain lengths and viscosity determination

1.3.5. Determination of prebiotic and antioxidant properties of xylooligosaccharide

1.3.6. Optimization of xylan hydrolysis using the combinations of endoxylanase and β -xylosidase

1.3.7. Optimization of xylitol bioconversion

1.3.8. Statistical analysis

1.3.9. Manuscript preparation, publication and dissertation writing

1.4 Anticipated benefits

New processes for grass xylan utilization and production of xylooligosaccharide and xylitol are obtained.



Chapter II

Literature review

2.1 Plant biomass potential

Non-renewable fossil fuel is limited and increasingly expensive. It also produces negative environmental impacts. Therefore, utilization of renewable and alternative resources such as plant biomass, both food and non-food materials, has been increased (Hood et al., 2011). Plant biomass composes of cellulose, hemicellulose and lignin in cell wall. They are the precursors to produce value added products (Mansor et al., 2019). Different compositions of these compounds are reported based on types of plant biomasses (Samanta et al., 2015). Composition of different plant biomasses was shown in Table 1.

Table 1 Composition of different plant biomasses

Biomasses	Biomass composition (%)			References
	Cellulose	Hemicellulose	Lignin	
Rice straw	43.0	28.6	19.1	Kumari and Singh (2022)
Sugarcane bagasse	42.1	28.4	19.2	Kaur et al. (2019)
Cogon grass	34.2	33.6	5.6	Patipong et al. (2019)
Wheat straw	38.0	32.0	19.0	Tayyab et al. (2017)
Corn cob	65.2	24.7	4.3	Boonchuay et al. (2014)
Corn stover	46.0	35.0	19.0	Ho et al. (2014)
<i>Sehima nervosum</i> grass	37.3	28.1	4.8	Samanta et al. (2012)
Switch grass	35.0	26.6	6.7	Stoklosa and Hodge (2012)
Sawdust	48.0	15.0	32.0	Du et al. (2010)
Rice husk	22.7	17.5	33.9	Gullón Estévez et al. (2008)

In term of utilization, plant biomasses can be categorized into 2 groups namely the first- and second- generation biomasses (Naik et al., 2010). For the first generation, they are edible biomasses such as corn, sugarcane and wheat. Due to the more frequent food crises happening recently (Rai et al., 2022), focus has been shifted toward the second generation of plant biomass including the non-food lignocellulosic biomasses

and agricultural residues (Miret et al., 2016). Several reports have been demonstrated that these second-generation biomasses have high potential for biofuel and biorefinery production through various chemical and enzymatic processes (Parameswaran et al., 2018; Wawro et al., 2019; Hruřová et al., 2020; Singhanian et al., 2022; Kucharska et al., 2020; Olivieri et al., 2021). However, to make such utilization plausible in industrial scale, the biomass feedstock must be abundant and available year-round (Williams et al., 2016).

As an answer to high feedstock demand and production cost, fast growing weeds and plantation grasses which are available throughout the year in every region with little to no value have high potential as an alternative lignocellulosic resource for the production of fuels, chemicals and energy (Liang et al., 2012).

2.2 Hemicellulose

2.2.1 Hemicellulose structure

In plant cell wall, hemicellulose is the second most abundant polysaccharide after cellulose. The majority of hemicellulose chains are formed by β -(1 \rightarrow 4)-linked D-xylopyranoside monomer units, and they are generally called xylan. Xylan can be divided into 6 groups according to the differences in side chain types, distribution, and localization and glycoside linkage types and their distribution in the main chain.

2.2.1.1 Homoxylan

It is linear polysaccharides composed of D-xylopyranosyl residues linked by β -(1 \rightarrow 3)-linkages, β -(1 \rightarrow 4)-linkages and mixed β -(1 \rightarrow 3, 1 \rightarrow 4)-linkages. It is common in seaweeds, green algae and guar seed husks (Figure 1) (Ebringerová, 2006).

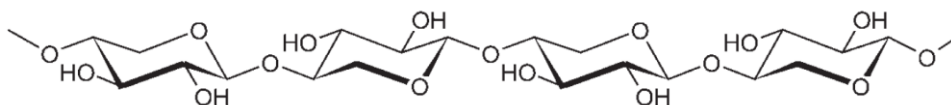


Figure 1 Structure of homoxylan (Ebringerová, 2006)

2.2.1.2 Glucuronoxylan

The linear xylopyranan backbone has side chains of α -D-glucuronic acid and/or its 4-O-methyl derivative attaching at C2 of the backbone. It is present in hardwoods and herbal plants of the temperate zone (Figure 2) (Ebringerova', 2006).

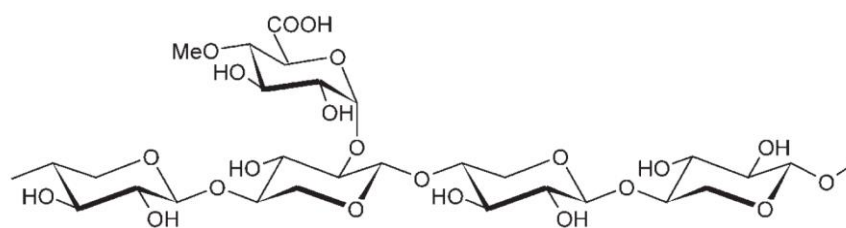


Figure 2 Structure of glucuronoxylan (Ebringerova', 2006)

2.2.1.3 (Arabino)glucuronoxylan

In this group, α -L-arabinofuranosyl residues are attached to C3 of the β -(1 \rightarrow 4)-xylopyranan backbone, in addition to the glucuronic side chains. It is hemicellulose component in softwood (Figure 3) (Ebringerova', 2006).

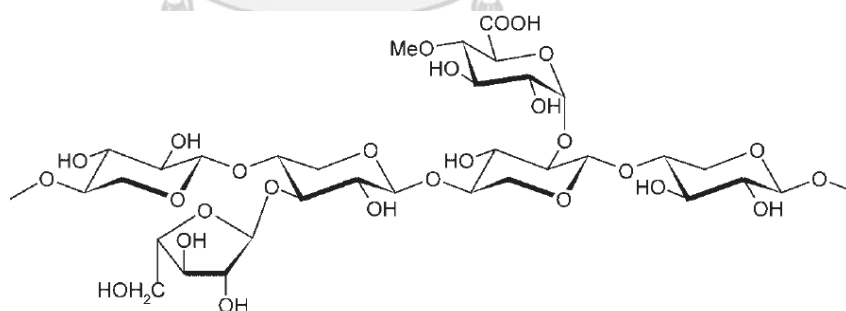


Figure 3 Structure of (arabino)glucuronoxylan (Ebringerova', 2006)

2.2.1.4 Arabinoxylan

The β -(1 \rightarrow 4)-xylopyranan backbone has α -L-arabinofuranosyl residues attached to C2 or C3. It is found in grasses and bamboo shoots (Figure 4) (Ebringerova', 2006).

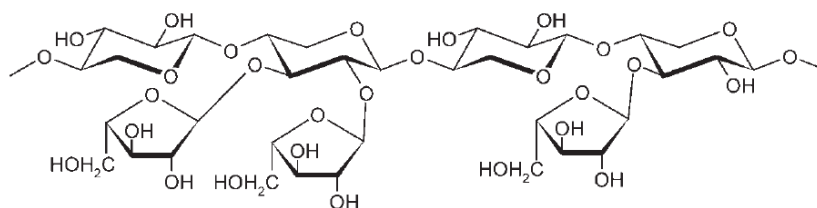


Figure 4 Structure of arabinoxylan (Ebringerova', 2006)

2.2.1.5 (Glucurono)arabinoxylan

(Glucurono)arabinoxylan has acetyl, glucuronic acid and arabinose residues as the side chains attaching at C2 and C3 of the backbone. it is the dominant hemicellulose in grasses and cereals (Figure 5) (Ebringerova', 2006).

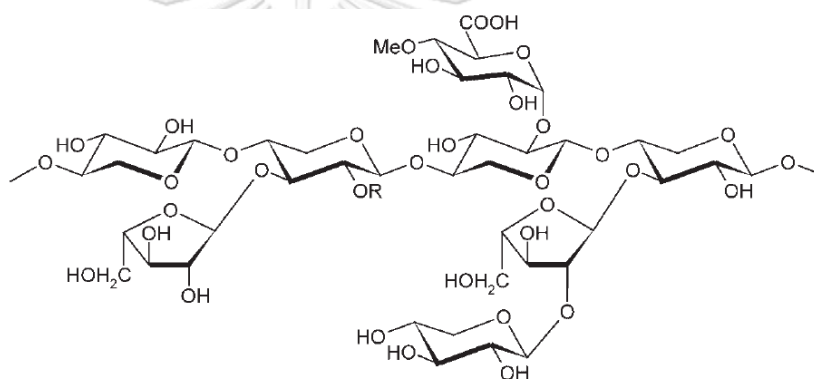


Figure 5 Structure of (glucurono)arabinoxylan (Ebringerova', 2006)

2.2.1.6 Heteroxylan

Xylan in this group has its β -(1 \rightarrow 4)-xylopyranan backbone heavily substituted with a variety of monosaccharide and oligosaccharide side chains. It is found in cereal bran, date palm seed, gum exudates and various mucilages (Ebringerova', 2006).

2.2.2 Xylan extraction

Xylan has been extracted from various sources including hardwoods, softwoods and agricultural residues such as aspen, eucalyptus, larch, spruce, poplar, willow, corn cob, barely hull, corn stalk, rice husk, rice straw, rye straw and sunflower stalk (Kämpfi et al., 2010; Deutschmann and Dekker, 2012; Hauli et al., 2013; Salmén, 2022). Although the net content of xylan in each plant is not known, the hemicellulose

contents in many plant biomasses have been reported such as hardwood (24-40 %), softwood (25-35 %), corn cobs (35%), wheat straw (50 %) and etc (Kumar et al., 2009). In general, hardwood plants grow slowly and have lower yield capacity which make them less attractive as a xylan source (Kamoga et al., 2013). Hardwood biomasses also contain significantly high amount of lignin that hinders xylan extraction (Tunc et al., 2010). In contrast with hardwoods, many herbaceous monocots such as grasses from the family Poaceae, grow and produce biomass rapidly and adapt well over a wide environmental conditions (Mafuleka and Kana, 2015). Moreover, grass biomass has high cellulose and hemicellulose contents, but low lignin content. The hemicellulose contents have been reported to be about 35-50 % for grasses (Kumar et al., 2009). Despite its high potential, studies on grass xylan extraction and its utilization have not drawn much research interest, unlike hardwood xylan (Samanta et al., 2012), and many grass species, either cultivated species or weeds, have not been fully studied (Banka et al., 2014).

To extract xylan from a plant biomass, acid and alkali extraction methods are the most widely used. However, xylans exhibit higher solubility in alkaline solutions than acid solutions, and there is less degradation and formation of furfural, a toxic derivative of dehydrated xylose (Cheng et al., 2010). Sodium hydroxide and potassium hydroxide are commonly used in alkali extraction (Deutschmann and Dekker, 2012), although sodium hydroxide is reportedly a more potent one (Table 2).

Table 2 Comparative xylan extractions using NaOH and KOH in different biomasses

Biomass sources	Xylan yield (g/ 100g biomass)		Reference
	NaOH	KOH	
Corn stover	24.6	23.0	Wu et al. (2020)
Banana peel	12.2	8.8	Pereira et al. (2020)
Sugarcane bagasse	20.5	17.0	Kaur et al. (2019)
Sweet sorghum bagasse	33.3	21.4	Wei et al. (2018)
Sugarcane bagasse	18.8	15.6	Choojit et al. (2017)
Corn husk	33.0	26.0	Samanta et al. (2016)
Pigeon pea stalk	17.8	16.2	Samanta et al. (2013)
<i>Sehima nervosum</i> grass	27.3	23.4	Samanta et al. (2012)

Sodium hydroxide extracts xylan from lignocellulosic biomasses by hydrolysis of ester linkages which release it from the lignocellulosic matrix into the alkaline solution. Moreover, xylan extracted by sodium hydroxide has exhibited a greater degree of enzymatic hydrolysis than other alkaline pretreatments (Samanta et al., 2012; Modenbach and Nokes, 2014). Therefore, sodium hydroxide extraction method is considered as the more feasible method for xylan extraction from lignocellulosic biomasses.

2.2.3 Xylan viscosity

One interesting property of long chain polysaccharides including xylans is their viscosity. Certain polysaccharides with distinct viscosity can be differently applied in industrial applications (Table 3). For applications, xylans with higher viscosity can form films or gel-like compounds that have been used as packaging films, coatings, cellular immobilization materials, acoustic insulation materials and drug carriers (Ebringerová and Hromádková, 1999; Pääkkönen et al., 2016). For xylans with low viscosity, they can be applied as food hydrocolloids which are used as thickening and gelling agents to improve the structure and texture of food products (Sedlmeyer, 2011).

Xylan chain length can be shortened by digesting the beta linkages in the main chain which can be done via enzymatic and acid hydrolyses. However, acid hydrolysis is non-specific and can generate undesirable byproducts, such as furfural, and/or high amounts of unwanted monosaccharides and/or oligosaccharides. Therefore, enzymatic hydrolysis is considered as a more feasible method to generate xylans with different chain length and study viscosity property since it reacts more specifically and does not generate toxic compounds and harsh, eroding condition to the equipment (Sorensen et al., 2006).

Table 3 Viscosities of various xylans and their applications

Xylan source	Viscosity (Pa.s)*	Application	Reference
Beechwood	3	hydrogel for carrier and releasing of vitamin B ₁₂ in vitro conditions	Kundu and Banerjee (2019)
Wheat straw	1.5	nanofibers from xylan and polyethylene oxide for wound dressings	Duan et al. (2019)
<i>Caesalpinia pulcherrima</i> seed	0.4	hydrocolloid	Sousa et al. (2017)
Beechwood	0.05	xylan-grafted-polyacrylamide for improvement of waste pulp	Xu et al. (2017)
Sugarcane bagasse	0.02	Cationic xylan grafted guanidine polymer for antimicrobial paper product	Xu et al. (2019)
Beechwood	0.004	Carboxymethyl xylan for improvement of paper dry strengthening	Cheng et al. (2018)

* Viscosity values were measured at a shear rate of 100 s⁻¹.

2.3 Xylanolytic enzymes

For complete breakdown of plant xylans, it requires the action of several hydrolytic enzymes including endoxylanase, β -xylosidase and debranching enzymes.

2.3.1 Endoxylanase (endo-1,4- β -xylanase, E.C.3.2.1.8)

Endoxylanase cleaves β -1,4-linked-backbone xylan randomly to release XOs (Michelin et al., 2012). Endoxylanase is classified in the glycoside hydrolases (GH) including GH10 and GH11. GH10 endoxylanase has higher molecular mass and lower isoelectric point (pI) than those of GH11 endoxylanase. Moreover, GH10 endoxylanase cleaves xylan backbone at non-reducing side of xylose with side chains such as arabinofuranosyl or 4-O-methyl-D-glucuronic acid. On the other hand, GH11 endoxylanase cleaves xylan backbone specifically in the area without side chain (Heinze et al., 2017). Endoxylanase can be produced by many organisms including fungi and bacteria (Table 4). Fungal endoxylanases have been reported with enzyme activity in the range between 3 and 815 U/mL at the temperature range between 40 and 60°C and pH range from 4 to 7. For bacterial endoxylanases, they have been reported with an activity between 2 and 1,007 U/mL at the temperature range from 37 to 60°C and pH range from 5 to 9.

Table 4 Previously reported microbial endoxylanases and their activities

Microorganisms	Condition for hydrolysis	Enzyme activity (U/mL)	References
<u>Fungi</u>			
<i>Alternaria alternata</i>	0.02 M acetate buffer pH 5, 50 °C, 30 min	3.0	Wipusaree et al. (2011)
<i>Aspergillus fumigatus</i>	0.25 M acetate buffer pH 5, 50 °C, 15 min	36.0	Carvalho et al. (2015)
<i>A. ustus</i>	0.05 M citrate buffer pH 5, 50 °C, 30 min	318.0	Ja'afaru (2013)
<i>A. niger</i>	0.05 M acetate buffer pH 5, 40 °C, 15 min	624.0	Mardawati et al. (2018)
<i>A. terreus</i>	0.05 M phosphate buffer pH 7, 55 °C, 5 min	474.0	Bakri et al. (2020)
<i>Cladosporium oxysporum</i>	0.05 M citrate buffer pH 4, 50 °C, 30 min	55.9	Guan et al. (2016)
<i>Cochliobolus sativus</i>	0.05 M phosphate buffer pH 7, 55 °C, 5 min	52.8	Bakri et al. (2020)
<i>Cryptococcus laurentii</i>	0.05 M phosphate buffer pH 6.5, 30 °C, 15 min	14.0	Otero et al. (2021)
<i>Humicola</i> sp. Ly01	0.1 M McIlvaine buffer pH 6, 60 °C, 10 min	41.8	Zhou et al. (2013)
<i>Hypocrea lixii</i>	0.05 M phosphate buffer pH 7, 45 °C, 15 min	38.9	Sakthiselvan et al. (2014)
<i>Penicillium</i> sp.	0.05 M acetate buffer pH 5, 40 °C, 15 min	789.0	Mardawati et al. (2018)
<i>P. canescens</i>	0.05 M phosphate buffer pH 6, 55 °C, 5 min	54.0	Bakri et al. (2020)
<i>Pyrenophora graminea</i>	0.05 M phosphate buffer pH 6, 55 °C, 5 min	14.3	Bakri et al. (2020)
<i>Trichoderma atroviride</i>	0.05 M citrate buffer pH 5.3, 50 °C, 10 min	205.9	Oliveira et al. (2014)
<i>T. viride</i>	0.05 M acetate buffer pH 5, 40 °C, 15 min	815.0	Mardawati et al. (2018)

Table 4 Previously reported microbial endoxylanases and their activities (continue)

Microorganisms	Condition for hydrolysis	Enzyme activity (U/mL)	References
<u>Bacteria</u>			
<i>Arthrobacter</i> sp.MTCC6915	0.05 M glycine-NaOH buffer pH 9, 60°C, 10 min	819.0	Sevanan et al. (2011)
<i>Bacillus</i> sp.GA2(1)	0.01 M phosphate buffer pH 7, 37 °C, 15 min	1.8	Chantorn et al. (2016)
<i>B. amyloliquefaciens</i>	0.05 M phosphate buffer pH 7, 50 °C, 10 min	9.0	Govender et al. (2009)
<i>B. circulans</i> D1	0.1 M acetate buffer pH 5, 60 °C, 10 min	8.0	Martins et al. (2005)
<i>B. safensis</i> XPS7	0.55 M citrate buffer pH 5, 45 °C, 15 min	141.3	Devi et al. (2022)
<i>B. stearothermophilus</i>	0.1 M phosphate buffer pH 7, 55 °C, 15 min	2.0	Khasin et al. (1993)
<i>Cellvibrio mixtus</i>	0.05 M citrate buffer pH 6, 50 °C, 10 min	10.1	Wu and He (2015)
<i>Micrococcus luteus</i>	0.05 M phosphate buffer pH 7, 40 °C, 30 min	1,007.0	Mmango-Kaseke et al. (2016)
<i>Nesterenkonia</i> sp.	0.05 M phosphate buffer pH 7, 50 °C, 10 min	2.5	Govender et al. (2009)
<i>Paenibacillus</i> sp. N1	0.1 M citric buffer pH 4, 45 °C, 10 min	24.6	Pathania (2012)
<i>Paenibacillus</i> sp. XJ18	0.2 M citrate phosphate buffer pH 9, 27°C, 15 min	2.5	Kurrataa'Yun et al. (2015)
<i>Providencia</i> sp. XI	0.1 M phosphate buffer pH 8, 60 °C, 15 min	36.3	Raj et al. (2013)
<i>Stenotrophomonas maltophilia</i>	0.1 M phosphate buffer pH 8, 50 °C, 15 min	26.4	Raj et al. (2013)
<i>Streptomyces</i> sp. P12-137	0.2 M acetate buffer pH 5, 50 °C, 20 min	28.0	Coman and Bahrim (2011)
<i>S. malaysiensis</i> AMT-3	0.05 M citrate buffer pH 5.3, 50 °C, 6 min	45.8	Nascimento et al. (2020)

2.3.2 β -xylosidase (EC 3.2.1.37)

β -xylosidase cleaves non-reducing end of short-chained XOs to release xylose monomers. This enzyme is classified in GH families 3, 39, 43, 52 and 54 according to the GH classification system, CAZy (Carbohydrate-Active Enzymes Database). The enzymes in this group are either extracellular or intracellular enzymes depending on microorganisms and their culture conditions (Li et al., 2018; Shao et al., 2011; Ohta et al., 2010). β -xylosidases have been studied mostly in bacteria and fungi (Table 5) with an activity in the range between 0.1 and 133 U/mg at the temperature range from 37 to 75°C and pH from 4.5 to 10.

Table 5 Previously reported microbial β -xylosidases and their activities

Microorganisms	Condition for hydrolysis	Enzyme activity	References
<u>Fungi</u>			
<i>Aspergillus niger</i>	0.1 M succinate buffer pH 5, 60 °C, 5 min	0.7 U/mL	Benassi et al. (2014)
<i>Colletotrichum graminicola</i>	0.05 M acetate buffer pH 5, 65 °C, 10 min	128 U/g	Zimbardi et al. (2013)
<i>Humicola insolens</i>	0.1 M McIlvaine buffer pH 6, 60 °C, 10 min	11.6 U/mg	Xia et al. (2015)
<i>Penicillium sclerotiorum</i>	0.05 M glycine-HCl pH 2.5, 60 °C, 5 min	31.1 U/mg	Knob and Carmona (2012)
<i>Pseudozyma hubeiensis</i>	0.05 M citrate buffer pH 4.5, 60 °C, 30 min	5.4 U/mL	Mhetras et al. (2016)
<i>Thermomyces lanuginosus</i>	0.05 M phosphate buffer pH 6, 50 °C, 10 min	210 U/mL	Corrêa et al. (2016)
<u>Bacteria</u>			
<i>Clostridium clariflavum</i>	0.2 M phosphate buffer pH 6, 60 °C, 5 min	4.4 U/mg	Geng et al. (2017)
<i>Dictyoglomus thermophilum</i>	0.05 M phosphate buffer pH 6, 75 °C, 10 min	78.5 U/mg	Li et al. (2018)
<i>Geobacillus</i> sp. WSUCF1	0.1 M phosphate buffer pH 7, 70 °C, 10 min	133 U/mg	Bhalla et al. (2014)
<i>G. thermodenitrificans</i>	0.05 M bicarbonate buffer pH 10, 70 °C, 30 min	4.2 U/mg	Anand et al. (2012)
<i>Leuconostoc lactis</i>	0.05 M phosphate buffer pH 5, 60 °C, 5 min	1.2 U/mL	Jang and Kim (2011)
<i>Paenibacillus curdlanolyticus</i>	0.05 M phosphate buffer, pH 7, 50 °C, 10 min	0.7 U/mg	Teeravivattanakit et al. (2016)
<i>Weissella</i> sp. Strain 92	0.05 M phosphate buffer pH 7, 37 °C, 1 min	11.2 U/mg	Falck et al. (2015)

2.3.3 Debranching enzymes

Debranching enzymes are necessary for removal of the side chains from the xylan backbone. Depending on the linked sugar molecules, side chains can be hydrolyzed by α -L-arabinofuranosidases (EC 3.2.1.55), α -D-glucuronidases (EC 3.2.1.139), acetylxylan esterases (EC 3.1.1.72), ferulic acid esterases (EC 3.1.1.73) and *p*-coumaric acid esterases (EC 3.1.1.-). Therefore, synergistic action of these enzymes (Figure 6) is important to achieve complete xylan degradation (Collins et al., 2005).

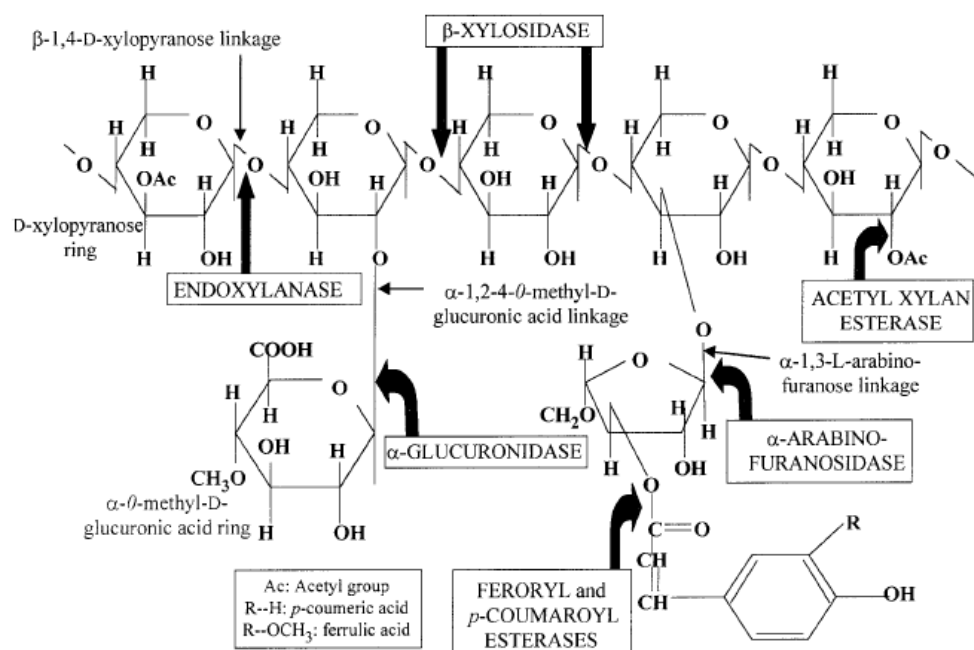


Figure 6 Degradation of xylan backbone and different side chains by xylanolytic enzymes. Certain enzyme groups are framed and cleavage positions are arrowed (Beg et al., 2001)

2.3.4 Xylanases from *A. pullulans*

Xylanases have been reportedly produced by fungi, bacteria or yeasts (Nasr et al., 2013; Chakdar et al., 2016). For decades, a yeast-like genus, *Aureobasidium*, has gained continuous interest based on many reports as good xylanase producers, especially the species *A. pullulans* (Leathers, 1986; Karni et al., 1993; Christov et al., 1997; Manitchotpisit et al., 2009; Ohta et al., 2010; Peterson et al., 2013; Bankeeree et al., 2014). Xylanolytic enzymes from *A. pullulans* have been

reported as cellulase-free which is advantageous since it would selectively digest xylan without affecting cellulose integrity and subsequent contamination of glucose (Leathers et al., 1984; Bankeeree et al., 2014; Bankeeree et al., 2016). Moreover, *A. pullulans* has been demonstrated to efficiently produce the enzymes from the low cost substrates including agricultural wastes such as corn cobs, wheat bran, rice bran, rice straw and sugarcane bagasse (Nasr et al., 2013; Bankeeree et al., 2014; Patipong et al., 2019).

2.3.4.1 Taxonomy and morphology of *A. pullulans*

Taxonomically, *A. pullulans* is classified in Phylum Ascomycota based on DNA sequence analyses even though ascospore formation has not been detected (de Hoog, 1993). Currently the genus *Aureobasidium* is classified in the Class Dothideomycetes, Order Dothideales, and Family Aureobasidiaceae, respectively, according to the molecular systematic analyses (Yurlova and de Hoog, 1997; Schoch et al., 2006). *Aureobasidium* yeasts are polymorphic and several morphologically different cells have been observed in different phases of their life cycle (Figure 7). In culture, it starts from yeast-like cells or blastospores in early stage and develops to short hyphae or pseudohyphae with budding conidia and/or thick-walled, dark-colored chlamydospores. Sometime, swollen cells can also be formed from either blastospores or chlamydospores depending on the environmental conditions. They also form new budding blastospores as well as becoming septate swollen cells (Ramos and García Acha, 1975; Pechak and Crang, 1977). *Aureobasidium pullulans* can be grown at room temperature on potato dextrose and yeast malt agar and form a colony with a diameter of 35-45 mm after 7 days. Young colony is light in color (creamy or pale pink) with flat, smooth and slimy surface. When reaching mature stage, the colony color becomes dark (olivaceous, dark brown, or black) with velvety texture with grayish fringe (Cooke, 1959). *Aureobasidium pullulans* can be found in a variety of habitats worldwide including plant leaves, painted wall, and bathroom surfaces and from inland to coastal areas (Liu et al., 2009; Kim et al., 2015; Singh et al., 2015; Vacher et al., 2016). In Thailand, several strains of *A. pullulans* with distinct phenotypes have been isolated, some of which show color variation from typical dark olivaceous and black to bright pink, yellow and purple (Punnapayak et al., 2003; Lotrakul et al., 2009; Manitchotpisit et al., 2009; Yanwisetpakdee et al., 2016).

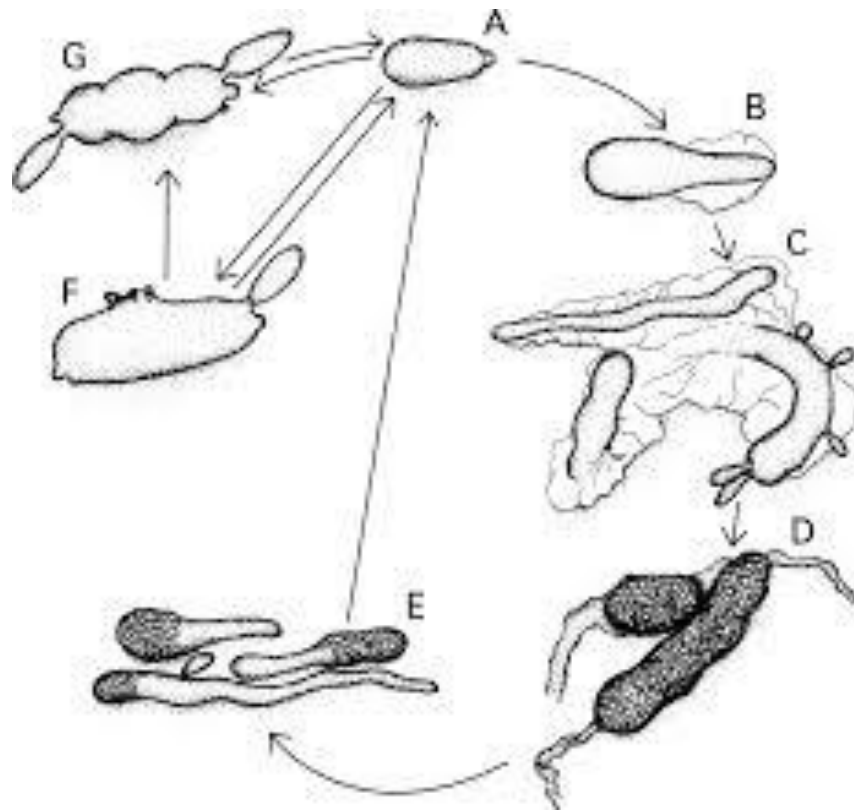


Figure 7 Morphological characteristic forms of *A. pullulans* with the development stage including (A) blastospore, (B) germinating blastospore, (C) initial hyphae, (D) chlamydospores, (E) germinating chlamydospores, (F) swollen cell and (G) septate swollen cell (Pechak and Crang, 1977)

2.3.4.2 Previous reports on xylanases from *A. pullulans*

2.3.4.2.1 Endoxylanase

Aureobasidium pullulans isolated from tropical vegetation, leaves, painted wall surfaces and wood surfaces (Leathers, 1986) has been reported to produce endoxylanase as extracellular enzyme without cellulase (Leathers, 1986). Endoxylanases from *A. pullulans* exhibited the activity in the range between 0.2 and 373 U/mL at optimal temperature from 30 to 70°C and pH from 4 to 6 (Leathers, 1986; Karni et al., 1993; Manitchotpisit et al., 2009; Nasr et al., 2013; Bankeeree et al., 2014; Patipong et al., 2019). *A. pullulans* endoxylanase can be produced by using agricultural

wastes such as corncob, sugarcane bagasse, wheat bran, rice straw and paddy husk that had lower cost than commercial xylan as carbon source at temperature between 27 and 30°C and 48-72 h-incubation time (Karni et al., 1993; Nasr et al., 2013; Bankeeree et al., 2014; Patipong et al., 2019).

2.3.4.2.2 β -xylosidase

Aureobasidium pullulans β -xylosidases are reported as intracellular enzyme locating in the periplasmic space of the cell (Ohta et al., 2010) with an activity in the range between 2 and 5 U/mg at optimal temperature (70 °C) and pH from 3.5 to 6 (Ohta et al., 2010; Bankeeree et al., 2016). This enzyme could be produced by using oat spelt xylan and corncob as the carbon source at temperature between 28 and 30°C and 72-120 h-incubation time (Ohta et al., 2010; Bankeeree et al., 2016).

2.4 Enzymatic hydrolysis of xylan

Xylans can be hydrolyzed by xylanolytic enzymes including endoxylanase (endo-1,4- β -xylanase) and β -xylosidase. Partial hydrolysis releases various xylooligosaccharides (XOs). Whereas completed hydrolysis releases xylose (Ohta et al., 2010; Michelin et al., 2012).

2.4.1 Partial xylan hydrolysis using endoxylanase

Several reports have shown that XOs can be produced from agricultural biomasses by partial enzymatic hydrolysis (Table 6). Various XOs yields (0.09-0.43 g/g initial xylan) were achieved at enzyme loading between 6 and 129 U/g substrate with substrate concentration ranging from 2 to 15% (w/v), pH 4.6-7.0 and 8-96 h-incubation time.

Table 6 XO_s production from lignocellulosic biomasses by endoxylanase

Hemicellulose sources	Endoxylanase dosage and hydrolysis condition	XO _s product yield (g/g initial xylan)	Reference
Birchwood	- enzyme 50 U/g xylan - 2 %(w/v) substrate - 50 °C, pH 4.6, 96 h	0.29	Nieto Domínguez et al. (2017)
Corn cob	- enzyme 129.4 U/g xylan - 15 %(w/v) substrate - 54 °C, pH 6, 12 h	0.16	Boonchuay et al. (2014)
Dissolving pulp	- enzyme 120 U/g xylan - 2 %(w/v) substrate - 50 °C, pH 5, 8 h	0.43	Wang et al. (2018)
Oil palm fronds	- enzyme 10 U/g xylan - 2 %(w/v) substrate - 40 °C, pH 4.6, 48 h	0.33	Siti-Normah et al. (2012)
<i>Sehima nervosum</i> grass	- enzyme 17.4 U/g xylan - 2 %(w/v) substrate - 50 °C, pH 5, 45 h	0.18	Samanta et al. (2012)
Sugarcane bagasse	- enzyme 60 U/g xylan - 2.6 %(w/v) substrate - 50 °C, pH 5, 96 h	0.37	Brienzo et al. (2010)
Sugarcane bagasse	- enzyme 30 U/g xylan - 2 %(w/v) substrate - 60 °C, pH 7, 10 h	0.24	Yang et al. (2007)
Tobacco stalk	- enzyme 5.9 U/g xylan - 2 % substrate - 28 °C, pH 5.5, 24 h	0.09	Kholis et al. (2015)
Vetiver grass	- enzyme 27.9 U/g xylan - 4 %(w/v) substrate - room temperature, pH 7, 92 h	0.24	Patipong et al. (2019)

2.4.2 Complete xylan hydrolysis using endoxylanase and β -xylosidase

Complete hydrolysis of xylan from agricultural biomasses have been shown in a number of reports (Table 7). Xylose yields ranging from 0.09 to 0.43 g/g initial xylan were achieved at endoxylanase loading between 1.5 and 3,000 U/g substrate, β -xylosidase loading between 1.5 and 100 U/g substrate, substrate concentration from 0.2 to 10% (w/v), pH 4.5-7.0 and 1-72 h-incubation time.

Table 7 Xylose production from lignocellulosic biomasses via enzyme hydrolysis

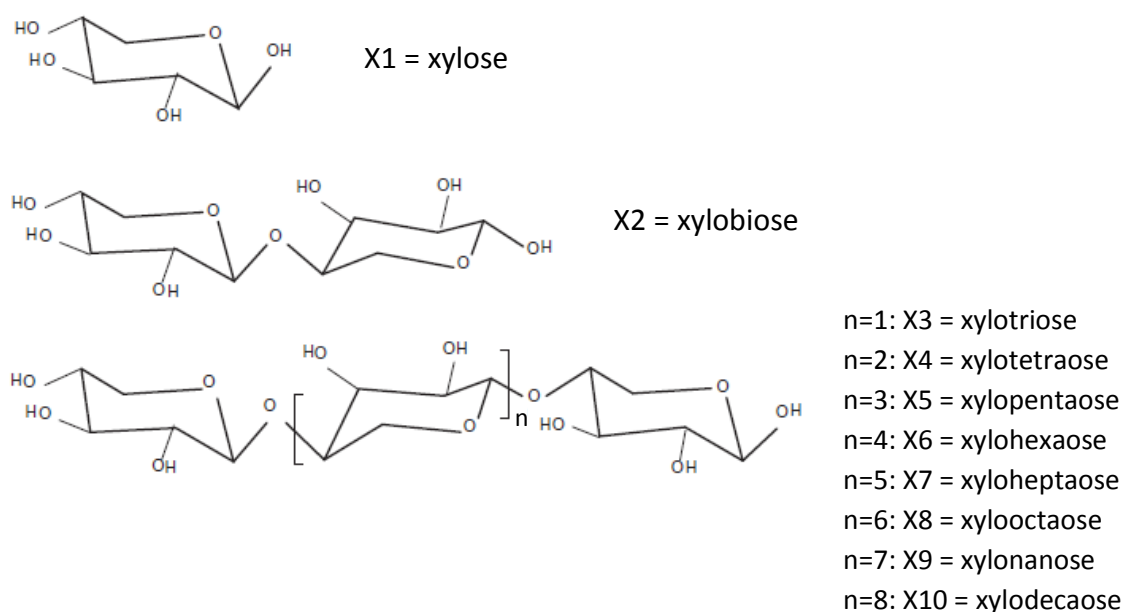
Hemicellulose sources	Enzyme dosage and hydrolysis condition	Xylose product yield (g/g initial xylan)	Reference
Black liquor	- Endoxylanase + β -xylosidase (16 + 6 U/g xylan) - 10 %(w/v) substrate, 70 °C, pH 6, 4 h	0.81	Bankeeree et al. (2018)
Oat spelts	- Endoxylanase + β -xylosidase (1.5 + 1.5 U/g xylan) - 1 %(w/v) substrate, 30 °C, pH 4.5, 1 h	0.01	Christov et al. (1997)
Oat spelts	- Endoxylanase + β -xylosidase (49 + 4.2 U/mg xylan) - 1 %(w/v) substrate, 55 °C, pH 7, 3 h	0.56	Tuncer and Ball (2003)
Pistachio shell	- Endoxylanase + β -xylosidase (3,000 + 33 U/g xylan) - 4 %(w/v) substrate, 40 °C, pH 6, 72 h	0.36	Cho et al. (2002)
Poplar sawdust	- Endoxylanase + β -xylosidase (500 + 100 U/g xylan) - 0.2 %(w/v) substrate, 50 °C, pH 6, 18 h	0.22	Li et al. (2020)

Table 7 Xylose production from lignocellulosic biomasses via enzyme hydrolysis (continue)

Hemicellulose sources	Enzyme dosage and hydrolysis condition	Xylose product yield (g/g initial xylan)	Reference
Sugarcane bagasse	- Endoxylanase + β -xylosidase (200 + 50 U/g xylan) - 1 %(w/v) substrate, 50 °C, pH 7, 24 h	0.31	Ye et al. (2017)
Sugarcane bagasse	- Endoxylanase + β -xylosidase (10 + 16 U/g xylan) - 8 %(w/v) substrate, 50 °C, pH 5, 72 h	0.46	Martins et al. (2018)

2.5 Xylooligosaccharides

XOs are oligosaccharides containing two to ten xylose molecules linked by β -(1 \rightarrow 4)-linked (Figure 8). Several reports have regarded XOs as prebiotics which are defined as non-digestible food ingredients that stimulate the growth of health-promoting probiotic bacteria in the colon (Veenashri and Muralikrishna, 2011; Carvalho et al., 2013; Kholis et al., 2015). Moreover, they have been reported to scavenge free radicals as antioxidant (Gowdhaman and Ponnusami, 2015; Rashad et al., 2016).

**Figure 8** Structure of XOs (Carvalho et al., 2013)

2.5.1 Probiotic bacteria

Under in vitro condition, XOs have been reported to stimulate the growth of probiotic bacteria while at the same time suppress harmful bacteria which consequently reduce concentration of toxic fermentation products and pathogenesis in the gastrointestinal tract (Figure 9) (Vlasova et al., 2016). Moreover, XOs reportedly increase bacterial production of short chain fatty acids (SCFA) that helps in improvement of bowel health and reduces the gut pH which enhance mineral absorption and reduce risks of colon cancer (Jain et al., 2015). For the recent reports, lactobacilli and bifidobacteria are an important intestinal microbiota of mammalian species and have been reported to be widely commercialized probiotics (Faryar et al., 2015; Samanta et al., 2015; Vlasova et al., 2016).

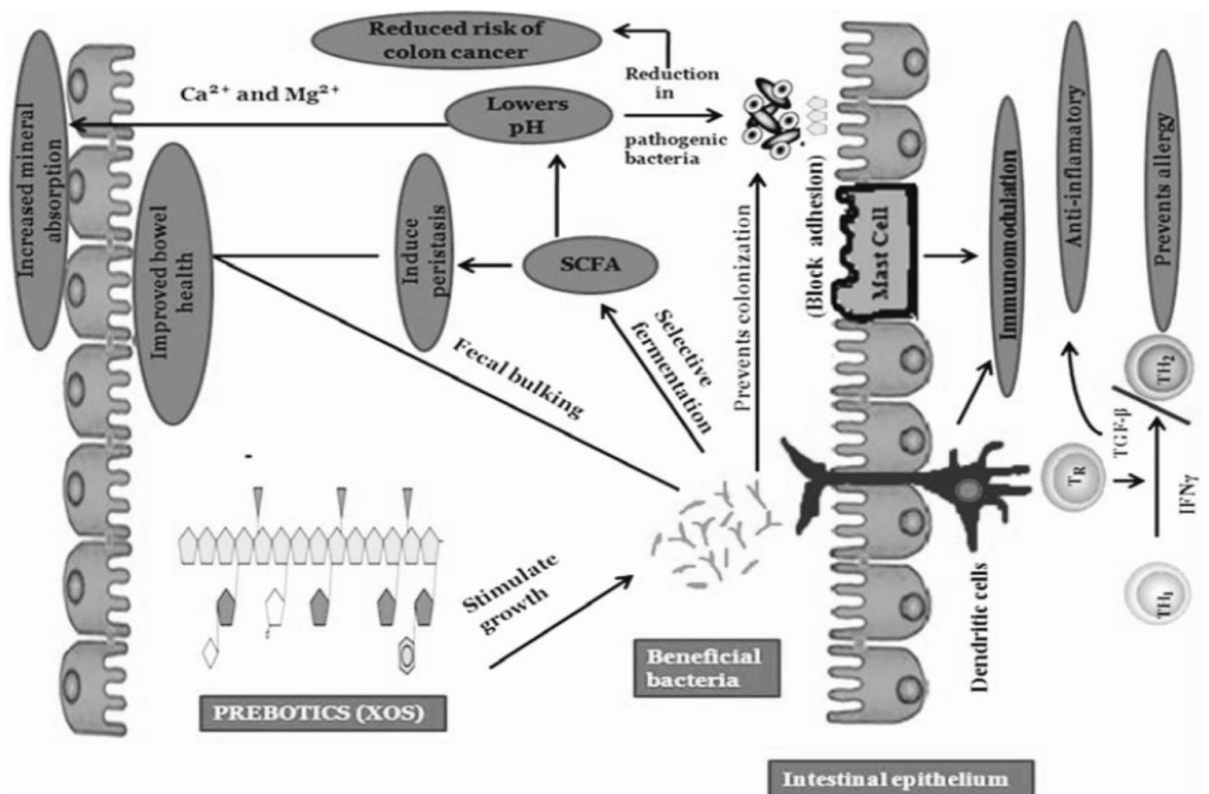


Figure 9 Benefits occurrence of prebiotic (XOs) in the colon (Jain et al., 2015)

2.5.1.1 Lactobacilli

Members of the genus *Lactobacillus* are gram-positive, immobile, non-spore producing, facultative anaerobic and acid-tolerant bacteria. This genus is classified in Phylum Firmicutes, Class Bacilli, Order Lactobacillales and Family Lactobacillaceae (Mesquita et al., 2017). The most well-known members of this genus are probiotic bacteria including *Lactobacillus casei*, *L. casei* subsp. *Rhombose*, *L. salivarius*, *L. gasseri*, *L. cellobiosus*, *L. plantarum*, *L. rhamnosus*, *L. helveticus*, *L. fermentum* and *L. brevis* (Song et al., 2015).

2.5.1.2 Bifidobacteria

Members of *Bifidobacteria* are gram-positive, non-motile, non-spore-forming and branched anaerobic bacteria. This genus is classified Phylum Actinobacteria, Class Actinobacteria, Order Bifidobacteriales and Family Bifidobacteriaceae (Mahmoudi et al., 2013). The most well-known members of this genus are probiotic bacteria including *Bifidobacterium longum*, *B. breve*, *B. adolescentis*, *B. animalis* and *B. bifidum* (Samanta et al., 2015).

2.5.2 Prebiotic activity of XOs

Several reports have shown that growth of many lactobacilli can be enhanced when XOs were added to the medium as the sole carbon source, including *Lactobacillus plantarum* S2 (XOs from corncob) (Yu et al., 2015), *L. casei* TISTR 390 and *L. brevis* TISTR 868 (XOs from vetiver grass) (Patipong et al., 2019), *L. viridiscens* NCIM 167 (XOs from corncob) (Samanta et al., 2012) and *L. acidophilus* ATCC 4356 (commercial XOs) (Mumcu and Temiz, 2014). However, the growth stimulation by XOs seems to be strain dependent since XOs failed to enhance the bacterial growth in some reports including *L. delbrueckii* YF-L811, *L. plantarum* S1 and *L. brevis* S27 (Maria et al., 2014; Pensza et al., 2018). *Lactobacillus* growth can also be inhibited if the XOs used was contaminated with toxic compounds such as furfural (Akobi et al., 2017).

For the enhancement of bifidobacterium growth, several reports have shown that XOs could stimulate the growth of this probiotic bacteria including *B. adolescentis* CIFL N0037 and *B. infantis* CIFL N0050 (XOs from birchwood) (Okazaki et al., 1990), *B. longum* NCIMB 8809 (XOs from rice husk) (Gullón Estévez et al., 2008) and *B. adolescentis* ATCC 15703 (XOs form corn fiber) (Aditya et al., 2015). However, XOs

showed the enhancement of bifidobacterium to be strain dependent since XOs failed to enhance the bacterial growth in some reports including *B. breve* Bb 03, *B. longum* KC 1 and *B. adolescentis* NCDC 236 (Mäkeläinen et al., 2010; Thakuria and Sheth, 2019).

2.5.3 Antioxidant property

Free radicals have been known to adversely affect human health leading to several diseases including cancer. These free radicals are produced by metabolic processes in the cells as well as enhancement from extracellular factors such as ionizing radiation, vehicle emission, industrial emissions, cigarette smoke, alcohol and high fat diet. Cellular free radical or oxidant level can be controlled by endogenous antioxidant. However, under some circumstances, these antioxidants cannot to suppress the rise of free radicals and the antioxidant impact is required. XOs produced from agricultural waste xylan have been reported to have antioxidant properties (Gowdhaman and Ponnusami, 2015; Yamani et al., 2016). Antioxidant activity can be determined using various protocols. The most method used for scavenging capacity assays using 2,2-di-phenyl-1-picrylhydrazyl (DPPH) as the substrate for stable free radical formation (Olszowy and Dawidowicz, 2017; Natividad et al., 2020). A number of reports have shown that XOs from different agricultural wastes exhibited antioxidant activities through both DPPH assay (Table 8).

Table 8 Radical scavenging activity of XOs from xylan through DPPH assay

XOs xylan sources	XOs concentration (mg/mL)	Radical scavenging activity (%)	Reference
Wheat bran	40	95	Huang et al. (2020)
Wheat bran	0.1	55	Ruthes et al. (2017)
Riceberry bran	20	73	Srinorasing et al. (2016)
Corn cobs	4	65	Yu et al. (2015)
Foxtail millet bran	1	73	Amadou et al. (2011)

2.6 Bioconversion of xylose to xylitol

2.6.1 Xylitol applications

Xylose derivatives have various applications in food industry. Xylose can be converted to be xylitol which is a natural polyol or sweetener with health benefits including dental decay prevention and diabetics relief (Morthensen et al., 2015; Wen et al., 2016). Xylitol market has value about \$340 million with applications in mouthwashes, toothpastes, chewing gums and food ingredients for special dietary uses (Prakash et al., 2011). Moreover, xylitol has a cooling effect because it has high endothermic heat of solution (34.8 cal/g). It is also applied as an antioxidant, moisturize, stabilizer, cryoprotectant and freezing point reducer. With its chemical and biological stabilities, it is used as a food preservative agent to extend the shelf life of food products, and there is no impact on amino acids that cause browning effects which can reduce the nutritional value of protein (Mohamad et al., 2015).

2.6.2 Xylitol bioconversion

Xylitol can be produced through the chemical and microbial processes. For the chemical process, xylitol is manufactured by chemical hydrogenation of xylose in the presence of a nickel catalyst at elevated temperature and pressure. The resultant product is very expensive because of the extensive separation and purification procedures. On the contrary, microbial process is highly attractive alternatives that produce a high-quality and cost-effective product. The microbial process uses bacteria, fungi and yeast for xylitol production from xylose. The best xylitol producers among the microorganisms yeasts which have been studied extensively in the recent decades (Rafiqul and Sakinah, 2013).

2.6.2.1 Xylose metabolic pathway for xylitol production

In the conversion of xylose to xylitol, yeasts naturally produce xylitol as an intermediate during the xylose metabolism. First, xylose is reduced to xylitol by a xylose reductase (EC 1.1.1.21) (XR). The resulting xylitol is either secreted or further oxidized to xylulose by xylitol dehydrogenase (EC 1.1.1.9) (XDH) in following step. Then, xylulose is converted to xylulose-5-phosphate by xylulokinase (EC 2.7.1.17) (XK) to enter the pentose phosphate pathway (also called hexose monophosphate (HMP) pathway)

for generating cell mass and maintenance energy (Figure 10). Therefore, XR and XDH are two key enzymes in xylose fermentation and xylitol production. The cofactors including nicotinamide adenine dinucleotide phosphate (NADPH) and nicotinamide adenine dinucleotide (NAD^+) are important to XR and XDH, respectively (Chen et al., 2010; Mohamad et al., 2015). Glucose reacts as a co-substrate to contribute glucose-6-phosphate (Glu-6-P) in HMP pathway and to regenerate NADPH (Tochampa et al., 2005).

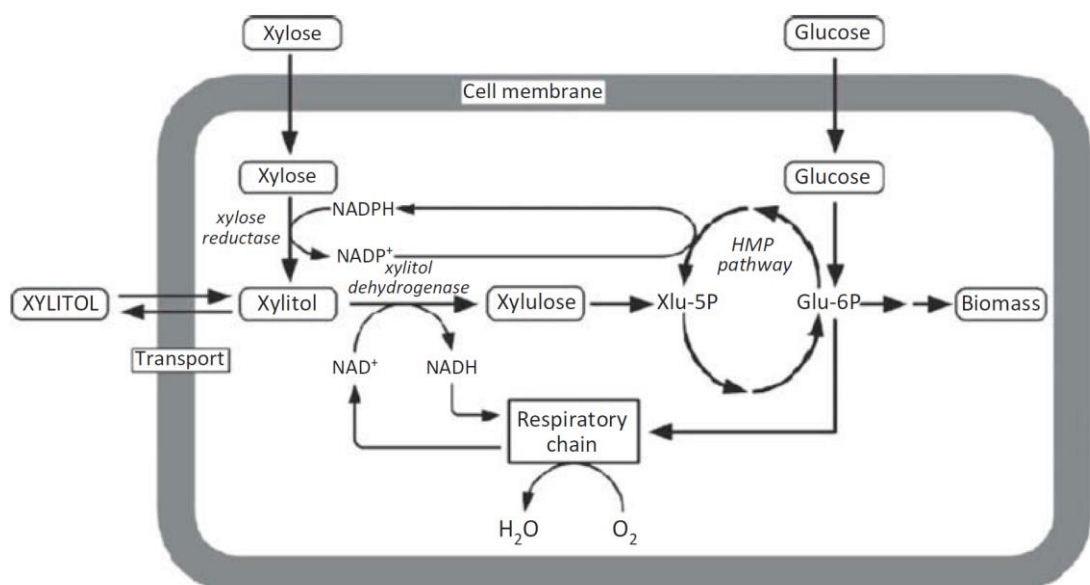


Figure 10 Metabolic pathways for xylitol production by yeast (Mohamad et al., 2015)

2.6.2.2 Yeast production of xylitol from lignocellulosic hydrolysate

There are limitations of industrial xylitol production including high production costs associated with relatively expensive purified substrate (xylose) and low conversion rate in low product (xylitol) yield (Ko et al., 2006). One possible solution to those problems is to use alternative materials such as lignocellulosic wastes because they are abundantly available, renewable and inexpensive. Some of the lignocellulosic raw materials used for the production of xylitol include corncobs, wheat straw, corn stover, wheat bran and etc (Rao et al., 2016). Grasses represent a possible plant biomass that could be used as substrate for xylitol production. These grasses grow rapidly and produce high hemicellulose-content biomass yield with minimal fertilizer input, and they contain a high level of hemicellulose (West, 2009).

Among xylitol-producing yeast, the genus *Candida* has been demonstrated to be the best xylitol producer (Rafiqul and Sakinah, 2013). Table 9 summarizes the studies on xylitol production on the conversion efficiency in the range between 0.24 and 0.82 g/g initial xylose by *Candida* spp. using lignocellulosic hydrolysate.

Table 9 Xylitol production by *Candida* spp. using lignocellulosic hydrolysate

<i>Candida</i> strains	Raw material	Fermentation condition	Xylitol yield (g/g initial xylose)	Reference
<i>C. guilliermondii</i> FTI 20037	Corn cob	- 200 g/L substrate - 30 °C, 64 h, 200 rpm - pH (not control)	0.24	Arifan and Nuswantari (2020)
<i>C. boidinii</i> XM 02G	Cocoa pod husk	- 24 g/L substrate - 384 h, 110 rpm - pH (not control)	0.52	Santana et al. (2018)
<i>C. tropicalis</i> KS 10-3	Sugarcane bagasse	- 32.3 g/L substrate - 30 °C, 96 h, 150 rpm - pH (not control)	0.47	Thancharoen et al. (2016)
<i>C. magnolia</i> TISTR 5663	Sugarcane bagasse	- 30 g/L substrate - 30 °C, 288 h, 250 rpm - pH 4	0.29	Wannawilai and Sirisansaneeya kul (2015)
<i>C. tropicalis</i> CCTCC M2012462	Corn cob	- 50 g/L substrate - 35 °C, 84 h, 150 rpm - pH 6	0.7	Ping et al. (2013)
<i>C. tropicalis</i> ATCC 96745	Sago bark	- 23 g/L substrate - 34 °C, 48 h, 200 rpm - pH 4	0.82	Mohamad et al. (2013)

Table 9 Xylitol production by *Candida* spp. using lignocellulosic hydrolysate (continue)

<i>Candida</i> strains	Raw material	Fermentation condition	Xylitol yield (g/g initial xylose)	Reference
<i>C. magnolia</i> FERM P-16522	Corn cob	25 g/L substrate - 30 °C, 36 h, 100 rpm - pH (not control)	0.75	Tada et al. (2012)
<i>C. athensensis</i> SB 18	Horticultural waste	123 g/L substrate - 30 °C, 102 h, 250 rpm - pH 7	0.81	Zhang et al. (2012)
<i>C. guilliermondii</i> ATCC 20216	Big bluestem grass	35 g/L substrate - 30 °C, 120 h, 150 rpm - pH 5	0.46	West (2009)
<i>C. guilliermondii</i> FTI 20037	Wheat straw	25 g/L substrate - 30 °C, 72 h, 250 rpm - pH (not control)	0.59	Canilha et al. (2008)

Chapter III

Materials and Methods

3.1 Equipments

<u>Equipments</u>	<u>Company/country</u>
Autoclave	Ta Chang Medical Instrument Factory/ Taiwan
BL 610 standard laboratory balance	Sartorius/Germany
Brookfield Synchro-Lectric Viscometer	Brookfield/ USA
Fourier Transform Infrared Spectrophotometer	Thermo Electron Corporation/ USA
Freeze dryer LL3000	Thermo Fisher Scientific/ USA
Haemacytometer	Boeco/ Germany
Hettich Rotofix 32 Centrifuge	Hettich/ Germany
High performance liquid chromatography (HPLC)	Shimadzu/ Japan
Hot air oven	Memmert/ Germany
Incubator shaker	Vision scientific/ South Korea
Laminar flow BV123	ISSOC/ Thailand
Light microscope CH30 RF200	Olympus/ Japan
Muffle furnance	Fisher Scientific/UK
pH meter PP-50	Sartorius/ Germany
Shaker SPL15	Labcon/ The Republic of South Africa
Shodex sugar sp0810 column	Showa Denko/ Japan
TC-205 precision balance	Denver Instrument Company/ USA
UV/VIS spectrophotometer HP8453	Agilent/ USA
Vacuum sealer	Yangzi/ China
Vortex Mixer	Scientific Industries/ USA

3.2 Chemicals

<u>Chemicals</u>	<u>Company/country</u>
3,5-dinitrosalicylic acid	Sigma-aldrich / USA
Glacial acetic acid, glacial	Merck/ Germany
Acetone	Qrec/ New Zealand
Activated carbon powder	Pure Sorb/ Thailand
Ammonium sulfate	Ajax Finechem/ Australia

<u>Chemicals</u>	<u>Company/country</u>
Arabinose	Hi-Media/ India
Ascorbic acid	Cosmeplus/ Thailand
L-Asparagine	Hi-Media/ India
Beechwood xylan	Hi-Media/ India
Beef extract	Hi-Media/ India
Cetyl trimethylammonium bromide (CTAB)	Ajax Finechem/ Australia
Citric acid	Ajax Finechem/ Australia
Decahydronaphthalene	Fluka/ Switzerland
2,2-diphenyl-1-picrylhydrazyl (DPPH)	Sigma-aldrich / USA
Disodium ethylenediamine tetraacetate (EDTA)	Vivantis/ Malaysia
Disodium hydrogen phosphate	Ajax Finechem/ Australia
Ethanol, 95%	Excise department/ Thailand
2-Ethoxyethanol	Merck/ Germany
Ferric nitrate nanohydrate	Loba Chemie/ India
Fructooligosaccharide	Vista Café/ Thailand
Galacturonic acid	Sigma-aldrich / USA
Gallic acid	Fluka/ Switzerland
Glucose	Ajax Finechem/ Australia
Glucuronic acid	Sigma-aldrich / USA
Hydrochloric acid	Ajax Finechem/ Australia
Inulin	Krungthepchemi/ Thailand
Magnesium sulfate	Ajax Finechem/ Australia
Manganese sulphate monohydrate	Merck/ Germany
Oxalic acid dihydrate	Carlo Erba/ Italy
<i>p</i> -nitrophenyl- β -D-xylopyranoside	Sigma-aldrich / USA
Peptone	Hi-Media/ India
Potassium acetate	Ajax Finechem/ Australia
Potassium bromide	Loba Chemie/ India
Potassium dihydrogen phosphate	Ajax Finechem/ Australia
Potassium permanganate	Merck/ Germany
Silver nitrate	Poch/ Poland

<u>Chemicals</u>	<u>Company/country</u>
Silver sulphate	Carlo Erba/ Italy
Skim milk	Hi-Media/ India
Sodium acetate trihydrate	Ajax Finechem/ Australia
Sodium borate dcahydrate	Ajax Finechem/ Australia
Sodium dihydrogen phosphate	Ajax Finechem/ Australia
Sodium hydroxide	Ajax Finechem/ Australia
Sulfuric acid	J.T.Baker/ USA
Tertiary butyl alcohol	Panreac/ Spain
Trisodium citrate	Ajax Finechem/ Australia
Tris (Hydroxymethyl) Methylamine	Ajax Finechem/ Australia
Xylitol	Sigma-aldrich/ USA
Xylobiose	Megazyme/ Ireland
Xylose	Sigma-aldrich/ USA
Xylotriose	Megazyme/ Ireland
Yeast extract	Hi-Media/ India
Yeast nitrogen base	Hi-Media/ India

3.3 Microorganisms

Thirty-six strains of *Aureobasidium* spp. (Table 10) were obtained from Plant Biomass Utilization Research Unit (PBURU), Department of Botany, Faculty of Science, Chulalongkorn University, Bangkok, Thailand (Manitchotpisit et al., 2009; Peterson et al., 2013; Yanwisetpakdee et al., 2016). The strains were cultured on yeast malt agar medium (YMA) at room temperature ($28\pm 2^\circ\text{C}$) (Lotrakul et al., 2009). For the probiotic bacteria, *L. brevis* TISTR 868, *L. casei* TISTR 390, *L. casei* subsp. *rhamnosus* TISTR 047, *B. longum* subsp. *longum* TISTR 2195, *B. breve* TISTR 2130 and *B. animalis* subsp. *animalis* TISTR 2194 were purchased from the Thailand Institute of Scientific and Technological Research, Pathum Thani, Thailand. They were maintained on de Man Rogosa Sharpe (MRS) agar at 4°C (De Man et al., 2008). The compositions of culture mediums used in this study were shown in Appendix A.

Table 10 36 strains of *Aureobasidium* spp.

Isolate	Source	Reference
<i>A. pullulans</i>	Plant Biomass Utilization	Manitchotpisit et al. (2009)
NRRL 58515	Research Unit (PBURU),	
NRRL 58516	Department of Botany,	
NRRL 58519	Faculty of Science,	
NRRL 58522	Chulalongkorn University,	
NRRL 58523	Bangkok, Thailand	
NRRL 58525		
NRRL 58526		
NRRL 58527		
NRRL 58528		
NRRL 58529		
NRRL 58536		
NRRL 58538		
NRRL 58540		
NRRL 58541		
NRRL 58542		
NRRL 58544		
NRRL 58547		
NRRL 58549		
NRRL 58550		
NRRL 58551		
NRRL 58552		
NRRL 58554		
NRRL 58557		
NRRL 58558		
NRRL 58559		
<i>A. thailandense</i>		Peterson et al. (2013)
NRRL 58539		
NRRL 58543		
<i>A. melanogenum</i>		Yanwisetpakdee et al. (2016)
PBUAP 13		
PBUAP 37		
PBUAP 44		
PBUAP 55		
PBUAP 58		
PBUAP 67		
PBUAP 71		
PBUAP 73		
PBUAP 75		



3.4 Optimization of xylan extraction from grasses

3.4.1 Grass samples collection

Ten grass samples were collected at Nakhon Ratchasima Animal Nutrition Research and Development Center, Pakchong Technology Research and Training Center and Department of Agronomy, Kasetsart University (Table 11). Figures of samples collection were shown in Appendix B.

Table 11 Grass samples in this study

Grass samples	Scientific name	Source
- Purple guinea grass	- <i>Panicum maximum</i> TD58	- Phetburi Animal Nutrition
- Barnyard grass	- <i>Hymenachne pseudointerrupta</i>	Research and
- Rhodes grass	- <i>Chloris gayana</i>	Development Center, Cha-am, Phetburi
- Sabi grass	- <i>Urochloa mosambicensis</i>	- Nakhon Ratchasima Animal
- Ruzi grass	- <i>Brachiaria ruziziensis</i>	Nutrition Research and
- Napier (Pakchong 1 hybrid) grass	- <i>Pennisetum purpureum</i> x <i>P. glaucum</i> Pakchong1	Development Center, Pak Chong, Nakhon
- Pangola grass	- <i>Digitaria eriantha</i>	Ratchasima
- Para grass	- <i>Brachiaria mutica</i>	
- Vetiver grass	- <i>Vetiveria zizanioides</i> Nash	- Pak Chong Technology Research and Training Center, Pak Chong, Nakhon Ratchasima
- Sugarcane leaf	- <i>Saccharum officinarum</i>	- Department of Agronomy, Kasetsart University, Kamphaeng Saen, Nakhon Pathom

3.4.2 Grass sample preparation and composition analysis

All samples were chopped and dried at 60 °C until constant weight was reached. The chopped samples were ground and sieved to particle size of 1 mm (Samanta et al., 2012). Biomass composition including cellulose, hemicellulose and lignin was determined according to Goering and Van Soest (1970). Chemicals preparation and procedure were shown in Appendix C.

3.4.3 Xylan extraction, structural analysis and optimization

The grass samples were extracted for xylan by using 12 % (w/v) of NaOH with liquid-to-solid ratio at 10:1 mL/g. The mixture was subjected to the autoclave steam treatment (121 °C, 15 lb/in²) for 45 min. After alkaline treatment, the supernatant was collected by centrifugation at 6,000xg for 10 minutes and was neutralized with glacial acetic acid for delignification. The pellets were removed by centrifugation. Then, the supernatant was added with 3 volume of 95% ethanol for xylan precipitation. After centrifugation, the xylan pellets were dried in hot air oven at 60 °C for 3 days (Samanta et al., 2012). Xylan yield and the relative xylan recovery were calculated using the following equations:

$$\text{Xylan yield (\% w/w)} = \frac{\text{Dry weight of extracted xylan (g)}}{\text{Dry weight of sample (g)}} \times 100$$

$$\text{The relative xylan recovery (\%)} = \frac{\text{Xylan yield (\%)}}{\text{Hemicellulose content in original grass (\%)}} \times 100$$

Five grass samples with the highest relative xylan recovery were selected for sugar composition and structural characterization. For analysis of sugar composition, five extracted xylans and commercial beechwood xylan as the control were hydrolyzed with 4%(v/v) H₂SO₄ with the liquid-to-solid ratio of 10:1 mL/g in autoclave for 1 h. Then, hydrolysates were neutralized by Ca₂CO₃. The neutral sugar contents were determined

by HPLC using refractive index detector and Varian hydrogen ion-exchange column at 40 °C with 5 mM H₂SO₄ as the mobile phase at a flow rate of 0.6 mL/min. Each sugar was quantified by comparing with regarding standard sugars including xylose, glucose, arabinose, galacturonic acid and glucuronic acid (Peng et al., 2009). For the analysis of structural characterization, extracted xylan samples were analyzed by a Fourier Transform Infrared Spectrophotometer (FT-IR) in the range of 4000-400 cm⁻¹ using a KBr disc containing 1%(w/w) ground xylan samples (Haqiqi et al., 2021).

For xylan extraction optimization, Response Surface Methodology (RSM) and Box-Behnken design (BBD) were applied to achieve the highest relative xylan recovery by using Design Expert, version 7.0 (Stat-Ease Inc., USA). NaOH concentration (12, 15, 18 %(w/v)), steaming time (30, 45, 60 min) and different liquid-to-solid ratio (5:1, 10:1, 15:1 mL/g) were selected as variable factors (Table 12). The predicted condition was tested in an independent experiment for validation. The experiment was conducted in triplicate. After optimization, three grass samples with the highest relative xylan recovery were selected for the investigation of viscosity property, hydrolysis and fermentation.

Table 12 Code and actual levels of three variables

Variables	Actual levels		
	-1	0	1
NaOH concentration (%(w/v); X ₁)	12	15	18
Steaming time (min; X ₂)	30	45	60
Liquid-to-solid ratio (mL/g; X ₃)	1:5	1:10	1:15

3.4 Production of endoxylanase and β -xylosidase from *A. pullulans*

3.4.1 Screening of endoxylanase and β -xylosidase

The strains of *A. pullulans* were cultivated in yeast malt broth (YMB) at room temperature (28±2°C) with 150 rpm agitation for 3 days as the seed cultures. The inocula were adjusted to 2.5x10⁷ cells/mL, and 100 μ L of each inoculum was transferred into a 250-mL Erlenmeyer flask with 100 mL of xylanase production medium (Bankeeree et al., 2014) containing corncob as the sole carbon source (Appendix A). The cultures

were incubated at room temperature with 150 rpm agitation for 3 days. After incubation, the culture supernatant was collected by centrifugation (6,000xg, 10 min) and used as crude endoxylanases (Bankeeree et al., 2014). The cell pellets were washed with deionized water, and ground in liquid nitrogen by mortar and pestle. The cell lysates were centrifuged, and the supernatants were used as crude β -xylosidase (Ohta et al., 2010; Bankeeree et al., 2018).

For endoxylanase assay, the enzyme activity was assayed using beechwood xylan as the substrate (Bankeeree et al., 2014). The released reducing sugars were determined by 3,5-dinitrosalicylic acid (DNS) method. The reaction mixtures containing 125 μ L of 5% (w/v) beechwood xylan solution, 50 μ L enzyme solution, 75 μ L distilled water and 250 μ L 50 mM sodium phosphate buffer (pH 5) were incubated at 50 °C for 15 min. Then, 750 μ L DNS was added and the mixtures boiled for 5 min. Distilled water (1.5 mL) was then added and the absorbance was measured at 540 nm. The xylose equivalent sugars were calculated using xylose standard curve (Miller, 1959; Bailey et al., 1992). Chemical preparation and standard curve were shown in Appendix D. One unit (U) of endoxylanase activity was defined as the amount of enzyme that catalyzes the release of 1 μ mole xylose equivalent per minute (Leathers, 1986; Christov et al., 1997).

For β -xylosidase assay, the enzyme activity was determined using *p*-nitrophenyl- β -D-xylopyranoside (pNPX) as the substrate. The reaction mixtures containing 10 μ L 2.5 mM pNPX, 25 μ L enzyme solution, 65 μ L distilled water and 100 μ L 100 mM sodium phosphate buffer (pH 5) were incubated at 50 °C for 10 min. Then, 200 μ L 0.1 M Na_2CO_3 was added and the absorbance was measured at 405 nm. The *p*-nitrophenol standard curve was used for activity calculation (Jang and Kim, 2011; Bankeeree et al., 2018). Chemical preparation and standard curve were shown in Appendix C. One unit of β -xylosidase activity was defined as the amount of enzyme that catalyzes the release of 1 μ mole *p*-nitrophenol per minute (Ohta et al., 2010).

The strains with high endoxylanase and/or β -xylosidase activity were selected to determine for optimum pH, optimum temperature and thermal stability.

3.4.3 Determination of optimal pH, optimal temperature and thermostability

For optimal pH determination, the selected endoxylanase and β -xylosidase were incubated in reaction mixtures containing each of 5 different buffers (50 mM):

sodium citrate buffer (pH 3 to 4), sodium acetate buffer (pH 4 to 5), sodium phosphate buffer (pH 5 to 8), tris-HCl buffer (pH 8 to 9) and Na₂HPO₄-NaOH buffer (pH 9 to 11) (Appendix D). For optimal temperature, the reactions were incubated at a temperature range of 40 to 80 °C. The relative activity was calculated as the percentage of the maximum activity. In order to determine the thermostability, both enzymes were incubated in optimal pH at 40, 50, 60, 70 and 80 °C. Samples were taken at 1, 2, 4, 6, 8 and 12 h and assayed under optimal condition. The remaining activity was calculated as the percentage of enzyme activity before incubation (0 h) (Khasin et al., 1993; Ribeiro et al., 2014). Both enzymes with high thermostability were selected for xylan hydrolysis.

3.5 Determination of molecular weight, degree of polymerization and viscosity property

3.5.1 Determination of molecular weight

The molecular weight of xylans were determined by gel permeation chromatography (GPC) at Analytical and Testing Service Center, The Petroleum and Petrochemical College, Chulalongkorn University, by using Shodex OHpak SB-804 HQ column (300 mm x 8.0 mm I.D.), calibrated with pullulan polysaccharide standards (Sigma-aldrich). The samples were dissolved in distilled water at a concentration of 0.1% (w/v). The column was operated at 40 °C and eluted with distilled water at a flow rate of 0.5 mL/min (Bian et al., 2010; Bai et al., 2012).

3.5.2 Determination of viscosity and degree of polymerization (DP)

The three selected grass xylans were hydrolyzed its (5%(w/v)) by 4 different dosage (0, 25, 50, 100 U/g substrate) of selected endoxylanase under optimal condition for 24 h to generate partially digested xylan with various chain lengths. Viscosity of each chain length xylan was measured at 50°C by rotational rheometry using a Brookfield Synchro-Lectric Viscometer (model RVF, Brookfield, Middleboro, MA) according to Sorensen et al. (2006) and Bai et al. (2012). For the chain lengths, they were determined as the average DP according to Miyazaki et al. (2005). The procedure was shown in Appendix F.

3.6 Enzymatic hydrolysis of xylan

3.6.1 Partial hydrolysis for XOs production

3.6.1.1 Partial enzymatic hydrolysis of xylan

Hydrolysis condition for the three selected grass xylans and commercial beechwood xylans was preliminarily determined according to the optimum condition of the selected endoxylanase. The hydrolysis mixture (10 mL in 20 mL Erlenmeyer flask) contained the xylan substrate (1% (w/v)) and the crude enzyme (50 U/g xylan) in the optimal buffer. The reaction was incubated with 150 rpm agitation at optimum temperature for 24 h. After hydrolysis, the mixture was heated to 100 °C for 10 min to stop the enzyme function. The releasing of reducing sugars were measured by DNS method (Akpinar et al., 2009; Brienzo et al., 2010).

3.6.1.2 Optimization of XOs production by RSM

To enhance the XOs production, Central Composite Design (CCD) and RSM were applied to find the optimal endoxylanase dosage (14.64, 25, 50, 75, 85.36 U/g xylan) and incubation time (14.06, 24, 48, 72, 81.94 h) that give the maximal yield (Table 13). The validation of the predicted condition was conducted in an independent experiment. The experiment was conducted in triplicate. The reducing sugars were measured by DNS method, while the contents of xylobiose and xylotriose were analyzed by HPLC at 40 °C with 5 mM H₂SO₄ as mobile phase at a flow rate 0.6 mL/min (Khat-udomkiri et al., 2018; Patipong et al., 2019).

Table 13 Code and actual levels of two variables for optimization of XOs production

Variables	Actual levels				
	-1.414	-1	0	1	1.414
Endoxylanase dosage (U/g xylan; A ₁)	14.64	25	50	75	85.36
Time incubation (h; A ₂)	14.06	24	48	72	81.94

After hydrolysis, XOs in the hydrolysates were enriched via activated carbon adsorption. Three volumes of cold 95% ethanol were added to the

hydrolysates to remove the undigested xylan through precipitation. The xylan pellet was discarded after centrifugation at 6,000xg for 10 min. The remaining XOs in the supernatant was obtained by evaporation in an incubator at 60 °C, and then dissolved in distilled water at 2% (w/v). Activated carbon powder was added to the XOs solution at 20% (w/v). The mixture was incubated with 200-rpm agitation at room temperature for 2 h. Then the mixture was suctioned through a 50 mL filter crucible porous number 3 (Pyrex, USA) and washed with 1,000 mL distilled water. The XOs were eluted by 1,000 mL of 50% (v/v) ethanol, evaporated in the rotary evaporator for 30 min and dried by lyophilization (Wang and Lu, 2013; Patipong et al., 2019). The enriched XOs powder was stored at 4 °C for determination of prebiotic and antioxidant properties.

3.6.2 Xylose production

3.6.2.1 Complete enzymatic hydrolysis of xylan

The complete hydrolysis of three xylan samples and commercial beechwood xylan was conducted in 20 mL Erlenmeyer flask with the reaching mixture (10 mL) containing 1% (w/v) xylan in suitable buffer of selected endoxylanase and β -xylosidase. The enzymes were added as either stepwise or in combination with 150-rpm agitation. For stepwise hydrolysis, xylan was hydrolyzed by 50 U/g xylan endoxylanase at its optimal temperature for 6 h in the first step. Then, 50 U/g xylan β -xylosidase was added to the reaction mixture and incubated at the β -xylosidase optimal temperature for 6 h. For cocktail hydrolysis, xylan was hydrolyzed by 50 U/g xylan endoxylanase and 50 U/g xylan β -xylosidase at various temperature ranging from 50, 60 to 70 °C for 12 h. The reaction was stopped by boiling at 100 °C for 10 min. The xylose contents in the hydrolysates were analyzed by HPLC. The hydrolysis condition with the highest xylose yield was selected for the optimization.

3.6.2.2 Optimization of xylose production by RSM

To enhance xylose yield, BBD and RSM were applied with endoxylanase dosage (30, 50, 70 U/g xylan), β -xylosidase dosage (30, 50, 70 U/g) and incubation time (6, 12, 18 h) as three variable factors (Table 14). The validation of predicted condition was investigated. The experiment was conducted in triplicate.

Table 14 Code and actual levels of three variables for optimization of xylose production

Variables	Actual levels		
	-1	0	1
Endoxylanase dosage (U/g xylan; B ₁)	30	50	70
β -xylosidase dosage (U/g xylan; B ₂)	30	50	70
Time incubation (h; B ₃)	6	12	18

3.7 Prebiotic property of XOs

Six strains of probiotic bacteria were cultivated in MRS broth at 37 °C under a static condition in an anaerobic container flushing with nitrogen gas for 24 h for seed culture preparation. The seed cultures were adjusted to OD₆₀₀ 0.1 with sterile medium before transferred (1% (v/v)) into the MRS broth individually supplemented with glucose, XOs, commercial fructooligosaccharide and commercial inulin at 2 mg carbon/mL. Culture without carbon source was used as blank. The cultures were incubated under the same condition until the mid-log phase of each strain was reach (the growth curves of each strain in glucose-containing medium were shown in Appendix F): *L. brevis* (10 h), *L. casei* (11 h), *L. casei* subsp. *rhamnosus* (9 h), *B. longum* subsp. *longum* (15 h), *B. breve* (16 h) and *B. animalis* subsp. *animalis* (14 h). The probiotic bacteria growth was determined as log colony forming unit (CFU) using a standard plate count technique under anaerobic condition (Broeckx et al., 2019; Patipong et al., 2019).

3.8 Antioxidant activity of XOs

The antioxidant activity of the three XOs was analyzed by using DPPH comparing with gallic acid and ascorbic acid as the controls. The samples were solubilized in distilled water at various concentrations. Each sample solution (100 μ L) was added to 900 μ L of 0.1 mM DPPH in methanol. The mixture solution was incubated in the dark at room temperature for 30 min. The DPPH radical scavenging activity was measured at 517 nm and calculated following the equation (Gowdhaman and Ponnusami, 2015):

$$\text{DPPH radical scavenging activity (\%)} = \frac{\text{Abs}_{\text{blank}} - \text{Abs}_{\text{sample}}}{\text{Abs}_{\text{blank}}} \times 100$$

Where $\text{Abs}_{\text{blank}}$ was the absorbance value of DPPH, and $\text{Abs}_{\text{sample}}$ was the absorbance value of DPPH treated with the samples. The sample solution was analyzed at least five concentrations to calculate the half maximal inhibition concentration (IC_{50}).

3.9 Xylitol production

3.9.1 Screening of xylitol-producing yeast

Fourteen Thai strains of xylitol-producing yeasts isolated from fruit scraps were obtained from PBURU (Table 15). Each strain was cultivated in yeast peptone xylose (YPX) broth at 30°C with 150 rpm shaking for 2 days and used as seed culture. The inoculum was adjusted to 1.5×10^7 cells/mL, and 20 μL of inoculum was transferred into a 50-mL Erlenmeyer flask with 20 mL of xylitol production medium (Appendix A). After incubation at 30°C with 150 rpm agitation for 2 days (Wu et al., 2018), supernatant were harvested after centrifugation (6,000xg, 10 min) for xylitol measurement by HPLC. The strain with the highest xylitol conversion efficiency was selected for determination of optimal temperature (25, 30, 35 and 40 °C) and incubation time (24, 48, 72 and 98 h) using factorial design. Results obtained from this experiment were used for the following medium optimization.

Table 15 Fourteen strains of xylitol-producing yeasts

Isolate	Species identity	Percent similarity (%)*	GenBank accession number*
FS1	<i>Candida tropicalis</i>	100	KX664489.1
FS2	<i>Candida tropicalis</i>	99	MG373784.1
FS3	<i>Candida tropicalis</i>	99	KX664668.1
FS4	<i>Candida tropicalis</i>	99	KY102464.1
FS5	<i>Candida tropicalis</i>	100	KY102481.1
FS6	<i>Candida tropicalis</i>	99	KY102481.1
FS7	<i>Candida tropicalis</i>	99	MF767862.1

Table 15 14 strains of xylitol-producing yeasts (continue)^a

Isolate	Species identity	Percent similarity (%) ^a	GenBank accession number ^b
FS8	<i>Candida tropicalis</i>	100	MF767862.1
FS9	<i>Candida tropicalis</i>	99	KX664670.1
FS10	<i>Candida tropicalis</i>	99	KM361510.1
FS11	<i>Candida glabatra</i>	99	LC317498.1
FS12	<i>Candida glabatra</i>	99	JN391276.1
FS13	<i>Meyerozyma caribbica</i>	100	KY104225.1
FS14	<i>Meyerozyma caribbica</i>	100	KY104222.1

^a The percent similarity was received from sequence alignment and GenBank accession number.

^b The 14 isolates and species identity by the ribosomal DNA Internal Transcribe Spacer (ITS) sequencing, using ITS4 (5'-TCCTCCGCTTATTGATATGC-3') and ITS5 (5'-GGAAGTAAAA GTCGTAACAAGG-3').

3.9.2 Optimization of xylitol production

Condition for optimization of xylitol production was performed using optimum temperature and incubation time of selected strain of xylitol-producing yeast obtained in 3.9.1. BBD and RSM were applied with xylose, glucose and yeast extract concentrations as three variable factors (Table 16) to predict the optimal medium concentration that yield the highest xylitol conversion efficiency. The validation of the predicted response was conducted in an independent experiment. The experiment was conducted in triplicate.

Table 16 Code and actual levels of three variables for optimization of xylitol production

Variables	Actual levels		
	-1	0	1
Xylose concentrations (g/L; C ₁)	10	60	110
Glucose concentrations (g/L; C ₂)	0	5	10
Yeast extract concentrations (g/L; C ₃)	0	3.5	7

3.10 Statistical analysis

The results were expressed as mean values with one standard deviation derived from three replications. The SPSS statistical computer package (SPSS Inc., USA) was used to analyze the experimental data using One-Way ANOVA and Duncan's multiple range test (DMRT) or Independent-Samples t-test when appropriated. Significant difference was determined at $p \leq 0.05$.



Chapter IV

Results

4.1 Biomass composition of grass samples

From biomass composition of ten grass samples (Table 17), they consisted of cellulose (22.33-34.81 %), hemicellulose (26.07-33.67 %), lignin (6.03-9.67 %), ash (1.35-5.67 %) and other (23.33-36.33 %). The highest amounts of hemicellulose content (>30%) were detected in vetiver grass, napier grass, sugarcane leaf, rhodes grass and barnyard grass. The lowest lignin contents at $6.03 \pm 0.82\%$ and $6.20 \pm 0.23\%$ were detected in purple guinea grass and sabi grass, respectively.

Table 17 Biomass composition of the grass samples

Samples	Biomass composition (%)*				
	Cellulose	Hemicellulose	Lignin	Ash	Other
Vetiver grass	31.33 ± 1.15^b	31.67 ± 0.58^b	7.67 ± 1.53^b	3.33 ± 0.58^{cd}	26.00 ± 1.00^{de}
Napier grass	31.33 ± 1.51^b	33.67 ± 0.58^a	8.67 ± 0.58^{ab}	3.00 ± 0.58^{cd}	23.33 ± 1.16^f
Sugarcane leaf	32.79 ± 0.45^{ab}	32.69 ± 1.03^{ab}	8.29 ± 0.11^{ab}	1.71 ± 0.02^{ef}	24.52 ± 0.69^{ef}
Purple guinea grass	33.82 ± 0.64^{ab}	27.70 ± 0.58^e	6.03 ± 0.82^c	2.73 ± 0.48^{cde}	29.71 ± 0.41^{bc}
Para grass	22.67 ± 1.53^c	32.33 ± 0.58^b	9.33 ± 0.58^a	4.67 ± 0.58^{ab}	31.00 ± 1.00^b
Ruzi grass	22.33 ± 1.15^c	29.33 ± 1.15^{cd}	8.33 ± 0.58^{ab}	3.67 ± 0.58^{bc}	36.33 ± 0.58^a
Pangola grass	25.33 ± 0.58^c	28.67 ± 1.15^{de}	9.00 ± 1.00^a	5.67 ± 1.15^a	31.33 ± 0.58^b
Sabi grass	34.81 ± 0.52^a	26.07 ± 0.60^f	6.20 ± 0.23^c	3.15 ± 0.21^{cd}	29.77 ± 0.61^{bc}
Rhodes grass	30.54 ± 0.67^b	30.09 ± 0.57^c	9.09 ± 0.39^a	2.35 ± 0.83^{def}	27.93 ± 0.32^{cd}
Barnyard grass	30.58 ± 1.44^b	30.08 ± 0.53^c	8.40 ± 0.61^{ab}	1.35 ± 0.40^f	29.59 ± 0.32^{bc}

* Data were presented as the average value \pm standard deviation. Different superscript letters in the same column indicated significant difference at $p \leq 0.05$ in DMRT.

4.2 Optimization of xylan extraction from grasses

4.2.1 Xylan extraction efficiency

Using 12%(w/v) NaOH, the relative xylan recovery from the grass samples ranged from 42.76±3.33 to 77.51±1.89 % (Figure 11). Five grass samples with the highest xylan recovery were sabi grass (59.62±1.46 %), vetiver grass (63.49±1.23 %), napier grass (68.58±0.94 %), purple guinea grass (76.76±3.15 %) and sugarcane leaf (77.51±1.89 %). These five samples were selected for structural characterization and optimization.

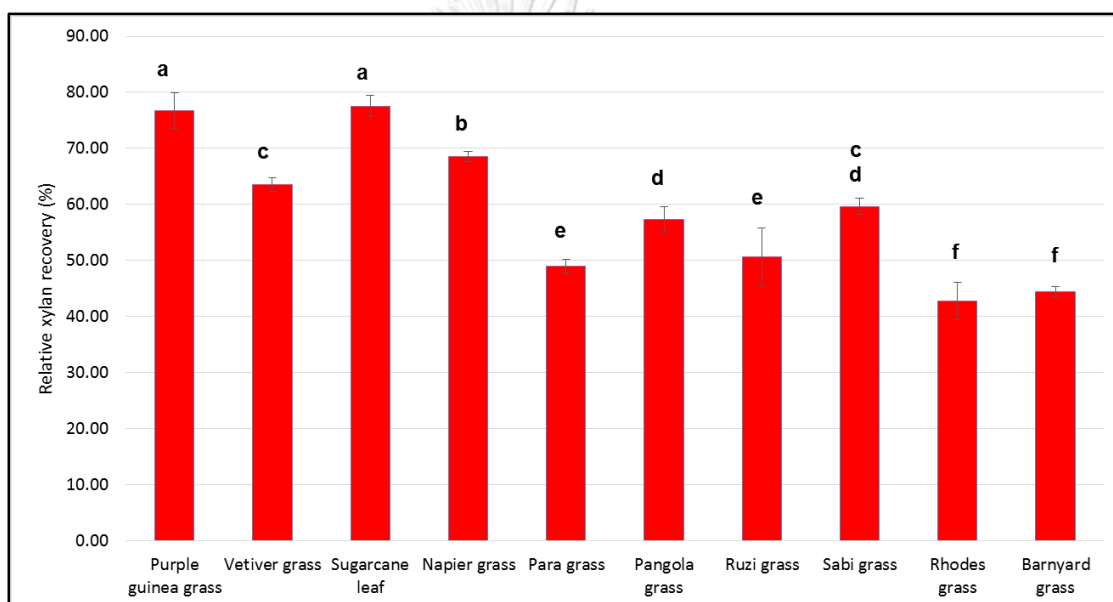


Figure 11 Relative xylan recovery (%) of ten grass samples after alkali extraction.

Different letters above the bar graphs indicate significant differences according to DMRT at $p \leq 0.05$. Bar indicated standard deviation derived from three replicates

4.2.2 Sugar composition

According to Table 18, xylose (75.58-77.22%) was the dominant component sugar from 4 grass xylan samples and there were small amount of arabinose (20.59-21.95%) and trace amount of glucuronic acid (2.19-3.06%) indicating that they were (glucurono)arabinoxylan. On the contrary, sugarcane leaf xylan consisted of only xylose (81.50%) and arabinose (18.50%) indicating that it was arabinoxylan. Only xylose

(84.72%) and glucuronic acid (15.28%) were found in glucuronoxylan from commercial beechwood xylan.

Table 18 Sugar composition of xylan samples

Xylan samples	Sugar composition (%) [*]		
	Xylose	Arabinose	Glucuronic acid
Beechwood	84.72±0.36 ^a	ND ^{**}	15.28±0.38 ^a
Napier grass	77.22±0.71 ^c	20.59±0.42 ^a	2.19±0.83 ^c
Sugarcane leaf	81.50±0.45 ^b	18.50±0.42 ^b	ND ^{**}
Vetiver grass	75.58±0.12 ^d	21.36±1.49 ^a	3.06±0.08 ^b
Sabi grass	75.81±0.28 ^d	21.95±0.93 ^a	2.24±0.14 ^c
Purple guinea grass	76.73±0.34 ^c	20.86±0.38 ^a	2.41±0.10 ^{bc}

^{*} Data were presented as the average value ± standard deviation. Different superscript letters in the same column indicated significant difference at $p \leq 0.05$ in DMRT.

^{**} ND = Not detected

4.2.3 FT-IR spectra

The FT-IR spectra of the extracted xylans and commercial beechwood xylan were shown in Figure 12. All samples showed typical peaks of xylans at 3437, 2920, 1407, 1046, 897, 639 and 530 cm^{-1} . The xylan samples exhibited a peak at 989 and 1550 cm^{-1} . At 1415 cm^{-1} was detected in commercial beechwood xylan and 4 grass xylans. The peak spectra at 3437 and 2920 cm^{-1} corresponded to the stretching of H-bond in OH group and C-H stretching (Peng et al., 2013). The peak at 1407 cm^{-1} was the stretching of C-H; moreover, the peak at 1046 cm^{-1} revealed the C-O, C-C stretching and C-OH bending of xylose pyran ring (Xie et al., 2020). The spectra band at 897 cm^{-1} corresponded to the stretching vibration in C-O-C to indicate β -1,4-xylosidic linkage of xylan structure (Sun et al., 2004). Moreover, absorption bands at 639 and 530 cm^{-1} revealed the result of stretching or bending of C-C-H or C-O-C (Kačuráková et al., 1999). The peaks appearance of xylan samples, the peak at 989 cm^{-1} was due to the presence of arabinose side chain (Peng et al., 2009) and the peak at 1550 cm^{-1} was originated from the phenolic ring absorbance of lignin (Vena et al., 2013). The peak appearance at 1415 cm^{-1} of commercial beechwood xylan and 4 grass xylan samples revealed the carboxyl group stretching of the glucuronic acid (Sharma et al., 2020).

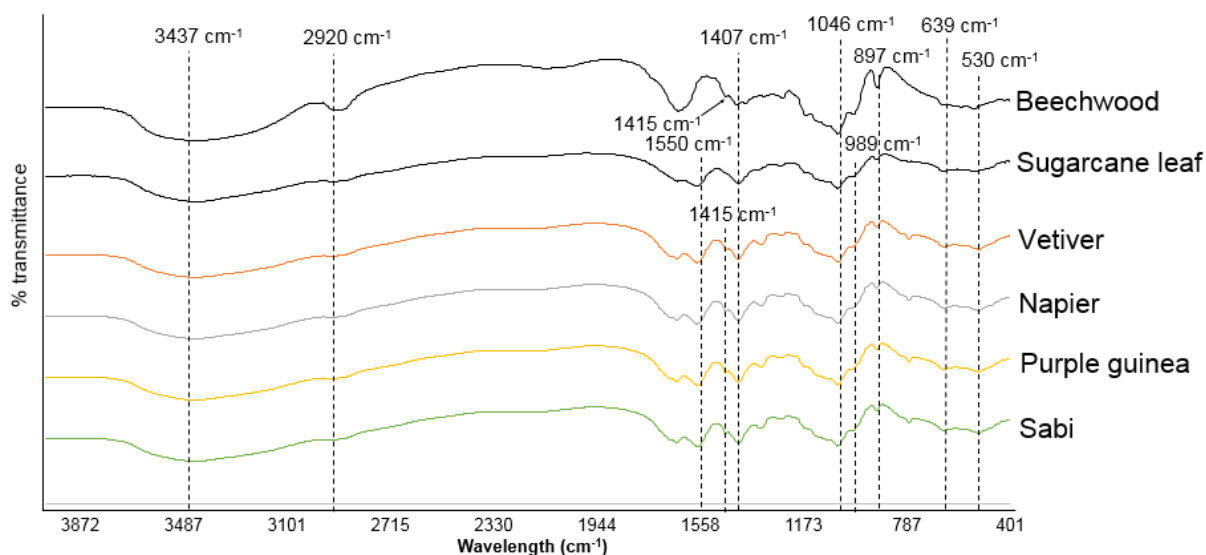


Figure 12 The FT-IR spectra pattern of the xylan samples

4.2.4 Optimization of xylan extraction

4.2.4.1 Sugarcane leaf

The response surface plots for xylan extraction from sugarcane leaf were shown in Figure 13. BBD with 3 levels of 3 variable factors was used and the response values were presented in Table 19. The data based on a second order polynomial could be expressed by following equation:

$$Y_1 = -364.20 + 29.39X_1 + 3.01X_2 + 130.85X_3 - 0.05X_1X_2 + 1.99X_1X_3 - 0.71X_2X_3 - 0.98X_1^2 - 0.01X_2^2 - 26.44X_3^2$$

Where Y_1 was the relative xylan recovery of sugarcane leaf (%), X_1 was NaOH concentration (%w/v), X_2 was steaming time (min) and X_3 was liquid-to-solid ratio (mL/g). According to ANOVA analysis (Appendix G), R^2 value was 0.99 indicating that the equation could explain 99% of the observed response. The model was significant with $p = 0.0001$ whereas lack of fit was not significant ($p = 0.07$), suggesting that the regression model could accurately predict the response. Moreover, a low coefficient of variation (CV = 2.85%) indicated the precision and reliability of the experiments. The RSM assessment showed that the optimum condition could be

achieved when adjusting 14.32% (w/v) of NaOH for 32.36 min and the liquid-to-solid ratio of 13.25:1 with the relative xylan recovery at 99.61%. Extraction of sugarcane leaf xylan was performed under the suggested condition to confirm the prediction. The result showed that the relative xylan recovery at $99.42 \pm 4.05\%$ was not significantly different from the predicted value ($p=0.95$), indicating that the equations were accurate. Using this optimized condition, the xylan extraction from sugarcane leaf was 1.28-fold higher than that with the unoptimized condition.

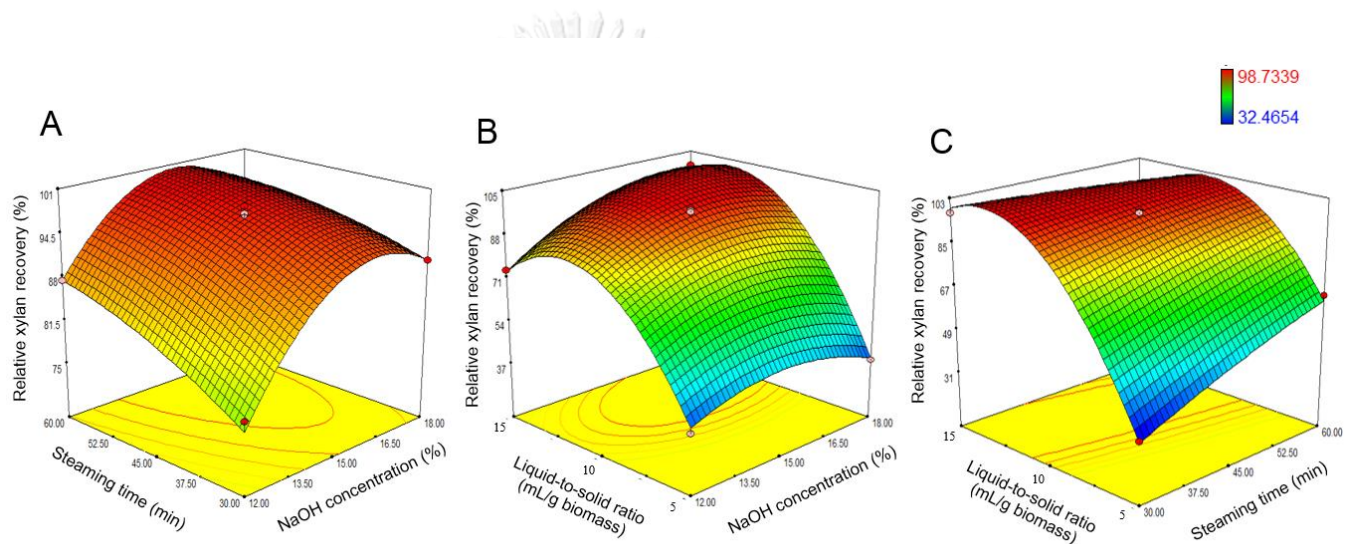


Figure 13 Response surface plots of optimal condition for xylan extraction from sugarcane leaf. (A) Effects of NaOH concentration and steaming time, (B) Effects of NaOH concentration and solid to liquid ratio and (C) Effect of steaming time and solid to liquid ratio

Table 19 BBD matrix with experimental and RSM predicted values of relative xylan recovery from sugarcane leaf

Run	Code level			Actual level			Relative xylan recovery (%)	
	X ₁	X ₂	X ₃	NaOH concentration (%w/v)	Steaming Time (min)	Ratio of solid to NaOH solution (g : mL)	Predicted	Observed*
1	-1	-1	0	12.00	30.00	1:10	75.51	76.99±0.88
2	+1	-1	0	18.00	30.00	1:10	90.56	90.60±1.04
3	-1	+1	0	12.00	60.00	1:10	87.59	87.55±3.66
4	+1	+1	0	18.00	60.00	1:10	94.62	93.15±2.79
5	-1	0	-1	12.00	45.00	1:5	39.80	37.73±2.34
6	+1	0	-1	18.00	45.00	1:5	38.88	38.24±4.59
7	-1	0	+1	12.00	45.00	1:15	73.67	74.31±1.09
8	+1	0	+1	18.00	45.00	1:15	96.66	98.73±5.90
9	0	-1	-1	15.00	30.00	1:5	31.86	32.47±0.74
10	0	+1	-1	15.00	60.00	1:5	61.29	63.40±2.86
11	0	-1	+1	15.00	30.00	1:15	99.05	96.93±9.51
12	0	+1	+1	15.00	60.00	1:15	85.75	85.14±0.88
13	0	0	0	15.00	45.00	1:10	97.66	98.42±3.09
14	0	0	0	15.00	45.00	1:10	97.66	97.38±0.88
15	0	0	0	15.00	45.00	1:10	97.66	96.87±5.79

* Mean ± SD derived from three replicates

4.2.4.2 Napier grass

For xylan extraction from napier grass, the response surface plots were presented in Figure 14. The levels of factors and the response values including the relative xylan recovery were shown in Table 20. The data based on a second order polynomial was expressed by following equation:

$$Y_2 = -282.69 + 20.15X_1 + 1.80X_2 + 125.26X_3 - 0.08X_1X_2 + 1.07X_1X_3 - 0.14X_2X_3 - 0.60X_1^2 - 0.01X_2^2 - 24.23X_3^2$$

Where Y_2 was the relative xylan recovery of napier grass (%), X_1 was NaOH concentration (%w/v), X_2 was steaming time (min) and X_3 was liquid-to-solid ratio (mL/g). According to ANOVA analysis (Appendix G), the equation could explain 99% of the observed response at R^2 value (0.99). The model was significant with $p = 0.0001$ whereas lack of fit was not significant ($p = 0.30$), suggesting that the regression model could accurately predict the response. Moreover, a low coefficient of variation (CV = 3.70%) indicated the precision and reliability of the experiments. The RSM assessment showed that the optimum condition could be achieved when adjusting 16.80% (w/v) of NaOH for 30.08 min and the liquid-to-solid ratio of 14.75:1 with the relative xylan recovery at 96.97%. Extraction of napier grass xylan was performed under the suggested condition to confirm the prediction. The result showed that the relative xylan recovery at $93.49 \pm 3.91\%$ was not significantly different from the predicted value ($p=0.25$), suggesting that the equations were accurate. Using this optimized condition, the xylan extraction from napier grass was 1.36-fold higher than that with the unoptimized condition.

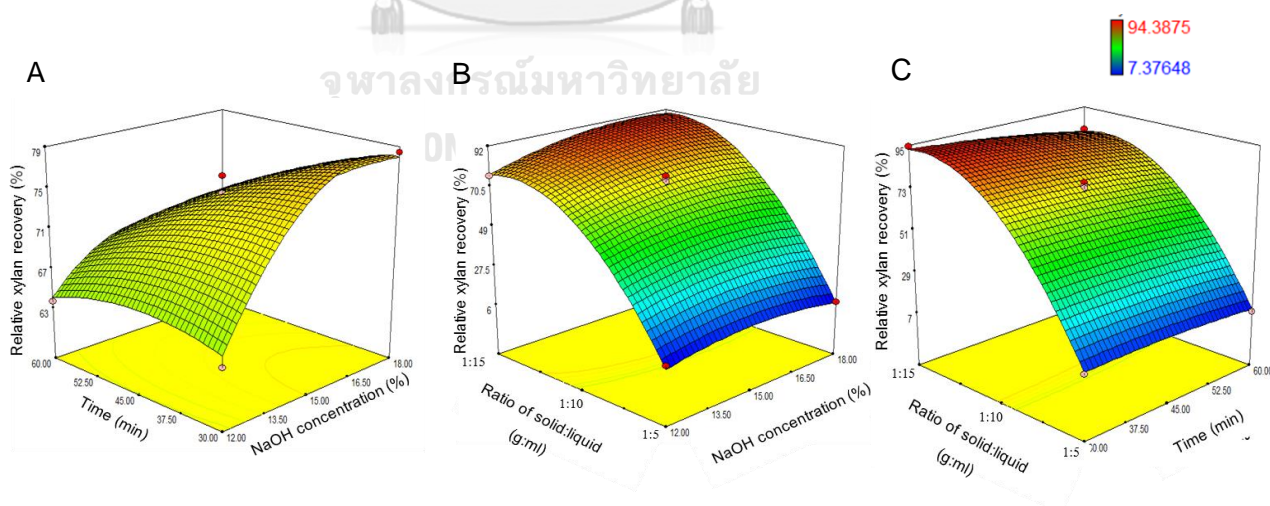


Figure 14 Response surface plots of optimal condition for xylan extraction from napier grass. (A) Effects of NaOH concentration and steaming time, (B) Effects of NaOH concentration and solid to liquid ratio and (C) Effect of steaming time and solid to liquid ratio

Table 20 BBD matrix with experimental and RSM predicted values of relative xylan recovery from napier grass

Run	Code level			Actual level			Relative xylan recovery (%)	
	X ₁	X ₂	X ₃	NaOH concentration (%w/v)	Steaming Time (min)	Ratio of solid to NaOH solution (g : mL)	Predicted	Observed*
1	-1	-1	0	12.00	30.00	1:10	64.82	63.74±4.29
2	+1	-1	0	18.00	30.00	1:10	78.01	78.43±9.04
3	-1	+1	0	12.00	60.00	1:10	64.05	63.64±1.18
4	+1	+1	0	18.00	60.00	1:10	64.05	64.85±3.09
5	-1	0	-1	12.00	45.00	1:5	6.94	8.90±0.94
6	+1	0	-1	18.00	45.00	1:5	7.60	7.43±0.49
7	-1	0	+1	12.00	45.00	1:15	76.82	76.23±2.27
8	+1	0	+1	18.00	45.00	1:15	89.88	87.62±2.97
9	0	-1	-1	15.00	30.00	1:5	12.43	11.37±2.26
10	0	+1	-1	15.00	60.00	1:5	9.02	7.38±0.49
11	0	-1	+1	15.00	30.00	1:15	93.41	94.39±3.72
12	0	+1	+1	15.00	60.00	1:15	82.49	82.03±2.04
13	0	0	0	15.00	45.00	1:10	76.02	74.50±3.81
14	0	0	0	15.00	45.00	1:10	76.02	76.23±9.66
15	0	0	0	15.00	45.00	1:10	76.02	73.14±2.32

* Mean ± SD derived from three replicates

4.2.4.3 Purple guinea grass

The response surface plots for xylan extraction from purple guinea grass were shown in Figure 15. BBD with 3 levels of 3 variable factors was used and the response values were presented in Table 21. The data based on a second order polynomial could be expressed by following equation:

$$Y_3 = -264.79 + 11.07X_1 + 2.27X_2 + 174.52X_3 - 0.01X_1X_2 - 1.87X_1X_3 - 0.17X_2X_3 - 0.17X_1^2 - 0.02X_2^2 - 26.89X_3^2$$

Where Y_3 was the relative xylan recovery of purple guinea grass (%), X_1 was NaOH concentration (%w/v), X_2 was steaming time (min) and X_3 was liquid-to-solid ratio (mL/g). According to ANOVA analysis (Appendix G), R^2 value was 0.96 indicating that the equation could explain 96% of the observed response. The model was significant with $p = 0.0044$ whereas lack of fit was not significant ($p = 0.06$), suggesting that the regression model could accurately predict the response. Moreover, a low coefficient of variation ($CV = 12.22\%$) indicated the precision and reliability of the experiments. The RSM assessment showed that the optimum condition could be achieved when adjusting 13.30% (w/v) of NaOH for 43.50 min and the liquid-to-solid ratio of 13.30:1 with the relative xylan recovery at 99.94%. Extraction of purple guinea grass xylan was performed under the suggested condition to confirm the prediction. The result showed that the relative xylan recovery at $95.85 \pm 7.55\%$ was not significantly different from the predicted value ($p=0.58$), indicating that the equations were accurate. Using this optimized condition, the xylan extraction from purple guinea grass was 1.25-fold higher than that with the unoptimized condition.

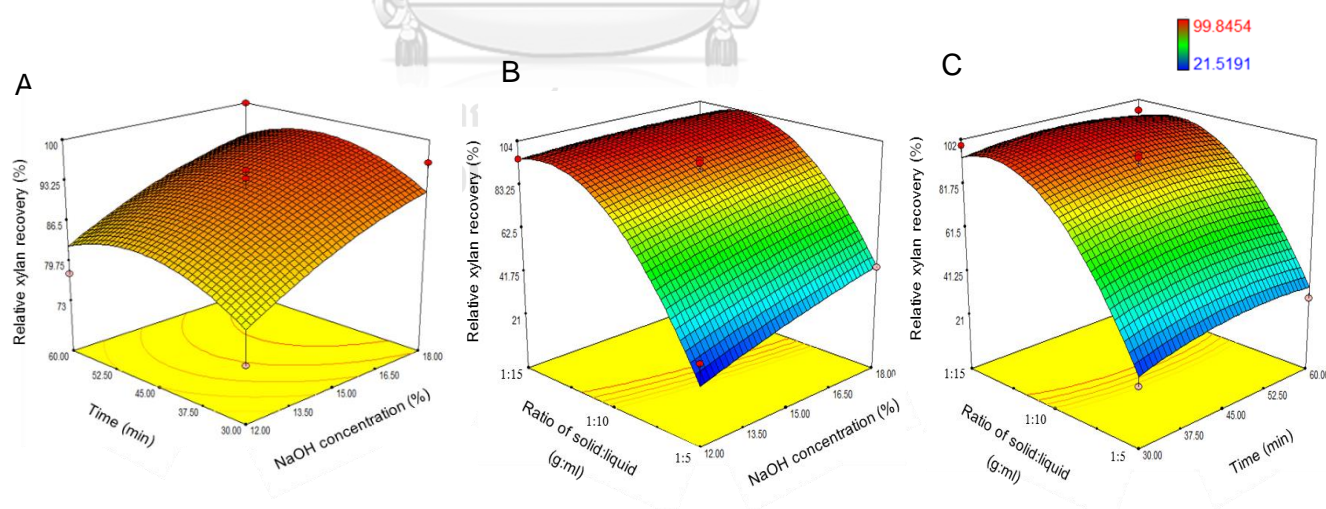


Figure 15 Response surface plots of optimal condition for xylan extraction from purple guinea grass. (A) Effects of NaOH concentration and steaming time, (B) Effects of NaOH concentration and solid to liquid ratio and (C) Effect of steaming time and solid to liquid ratio

Table 21 BBD matrix with experimental and RSM predicted values of relative xylan recovery from purple guinea grass

Run	Code level			Actual level			Relative xylan recovery (%)	
	X ₁	X ₂	X ₃	NaOH concentration (%w/v)	Steaming Time (min)	Ratio of solid to NaOH solution (g : mL)	Predicted	Observed*
1	-1	-1	0	12.00	30.00	1:10	79.27	73.41±2.76
2	+1	-1	0	18.00	30.00	1:10	91.40	96.27±3.31
3	-1	+1	0	12.00	60.00	1:10	82.41	77.62±6.51
4	+1	+1	0	18.00	60.00	1:10	94.23	99.85±6.19
5	-1	0	-1	12.00	45.00	1:5	21.11	31.29±1.04
6	+1	0	-1	18.00	45.00	1:5	44.25	44.25±3.21
7	-1	0	+1	12.00	45.00	1:15	96.27	95.67±3.21
8	+1	0	+1	18.00	45.00	1:15	97.72	86.20±2.97
9	0	-1	-1	15.00	30.00	1:5	25.33	21.52±1.82
10	0	+1	-1	15.00	60.00	1:5	33.39	28.75±2.01
11	0	-1	+1	15.00	30.00	1:15	93.80	99.11±7.23
12	0	+1	+1	15.00	60.00	1:15	91.91	96.38±4.26
13	0	0	0	15.00	45.00	1:10	92.78	89.65±1.04
14	0	0	0	15.00	45.00	1:10	92.78	95.07±7.30
15	0	0	0	15.00	45.00	1:10	92.78	93.64±4.40

* Mean ± SD derived from three replicates

4.2.4.4 Vetiver grass

For xylan extraction from vetiver grass, the response surface plots were presented in Figure 16. The levels of factors and the response values including the relative xylan recovery were shown in Table 22. The data based on a second order polynomial was expressed by following equation:

$$Y_4 = 142.76 - 20.45X_1 - 1.38X_2 + 100.95X_3 + 0.02X_1X_2 + 2.50X_1X_3 + 0.11X_2X_3 + 0.44X_1^2 + 0.01X_2^2 - 27.73X_3^2$$

Where Y_4 was the relative xylan recovery of vetiver (%), X_1 was NaOH concentration (%w/v), X_2 was steaming time (min) and X_3 was liquid-to-solid ratio (mL/g). According to ANOVA analysis (Appendix G), R^2 value was 0.98 indicating that the equation could explain 98% of the observed response. The model was significant with $p = 0.0004$ whereas lack of fit was not significant ($p = 0.27$), suggesting that the regression model could accurately predict the response. Moreover, a low coefficient of variation ($CV = 8.06\%$) indicated the precision and reliability of the experiments. The RSM assessment showed that the optimum condition could be achieved when adjusting 16.70% (w/v) of NaOH for 45.97 min and the liquid-to-solid ratio of 13.55:1 with the relative xylan recovery at 93.89%. Extraction of vetiver grass xylan was performed under the suggested condition to confirm the prediction. The result showed that the relative xylan recovery at $87.89 \pm 0.70\%$ was not significantly different from the predicted value ($p=0.15$), suggesting that the equations were accurate. Using this optimized condition, the xylan extraction from vetiver grass was 1.38-fold higher than that with the unoptimized condition.

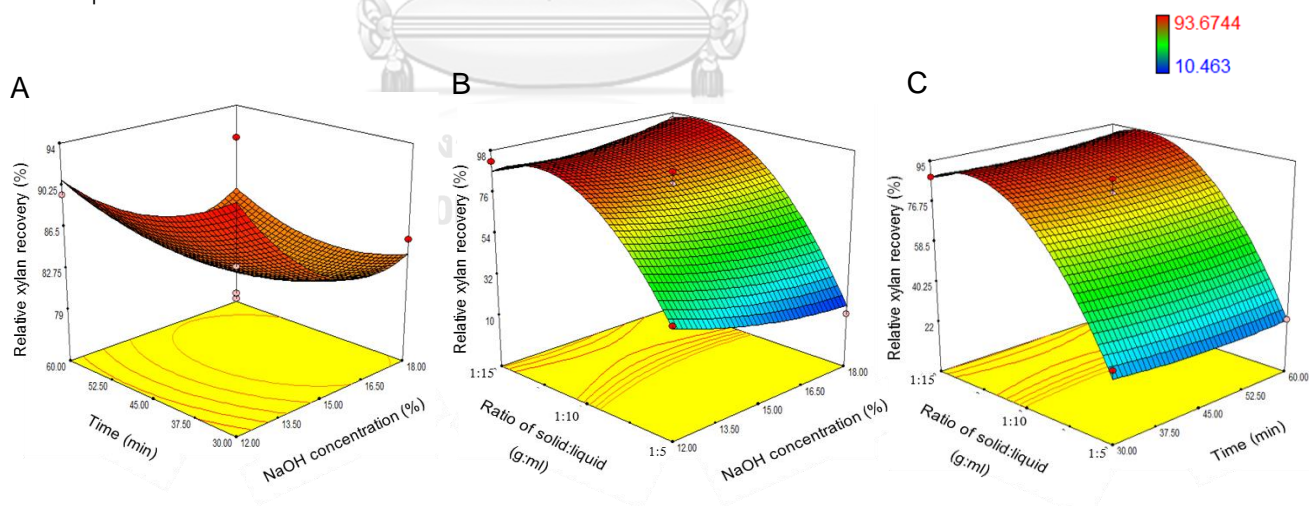


Figure 16 Response surface plots of optimal condition for xylan extraction from vetiver grass. (A) Effects of NaOH concentration and steaming time, (B) Effects of NaOH concentration and solid to liquid ratio and (C) Effect of steaming time and solid to liquid ratio

Table 22 BBD matrix with experimental and RSM predicted values of relative xylan recovery from vetiver grass

Run	Code level			Actual level			Relative xylan recovery (%)	
	X ₁	X ₂	X ₃	NaOH concentration (%w/v)	Steaming Time (min)	Ratio of solid to NaOH solution (g : mL)	Predicted	Observed*
1	-1	-1	0	12.00	30.00	1:10	93.28	88.28±8.58
2	+1	-1	0	18.00	30.00	1:10	84.12	85.43±7.87
3	-1	+1	0	12.00	60.00	1:10	90.78	89.46±8.51
4	+1	+1	0	18.00	60.00	1:10	85.81	90.81±5.12
5	-1	0	-1	12.00	45.00	1:5	37.48	38.86±2.37
6	+1	0	-1	18.00	45.00	1:5	15.40	10.46±1.33
7	-1	0	+1	12.00	45.00	1:15	87.11	92.05±8.34
8	+1	0	+1	18.00	45.00	1:15	95.05	93.67±5.98
9	0	-1	-1	15.00	30.00	1:5	26.27	29.89±2.65
10	0	+1	-1	15.00	60.00	1:5	22.69	22.63±1.58
11	0	-1	+1	15.00	30.00	1:15	87.75	87.81±6.91
12	0	+1	+1	15.00	60.00	1:15	90.50	86.88±8.43
13	0	0	0	15.00	45.00	1:10	82.52	87.06±5.67
14	0	0	0	15.00	45.00	1:10	82.52	79.99±1.82
15	0	0	0	15.00	45.00	1:10	82.52	80.52±5.47

* Mean ± SD derived from three replicates

4.2.4.5 Sabi

The response surface plots for xylan extraction from sabi grass were shown in Figure 17. BBD with 3 levels of 3 variable factors was used and the response values were presented in Table 23. The data based on a second order polynomial could be expressed by following equation:

$$Y_5 = -244.57 + 17.83X_1 + 2.13X_2 + 106.77X_3 + 0.01X_1X_2 - 0.52X_1X_3 - 0.11X_2X_3 - 0.54X_1^2 - 0.02X_2^2 - 16.83X_3^2$$

Where Y_5 was the relative xylan recovery of sabi (%), X_1 was NaOH concentration (%w/v), X_2 was steaming time (min) and X_3 was liquid-to-solid ratio (mL/g). Based on the ANOVA statistical significant model (Appendix G), the equation exhibited 98% of the observed response at R^2 value (0.98). The model was significant with $p = 0.0008$ whereas lack of fit was not significant ($p = 0.07$), suggesting that the regression model could accurately predict the response. Moreover, a low coefficient of variation ($CV = 7.25\%$) indicated the precision and reliability of the experiments. The RSM assessment showed that the optimum condition could be achieved when adjusting 12.87% (w/v) of NaOH for 42.97 min and the liquid-to-solid ratio of 13.10:1 with the relative xylan recovery at 89.99%. Extraction of sabi grass xylan was performed under the suggested condition to confirm the prediction. The result showed that the relative xylan recovery at $88.89 \pm 0.54\%$ was not significantly different from the predicted value ($p=0.73$), indicating that the equations were accurate. Using this optimized condition, the xylan extraction from sabi grass was 1.49-fold higher than that with the unoptimized condition.

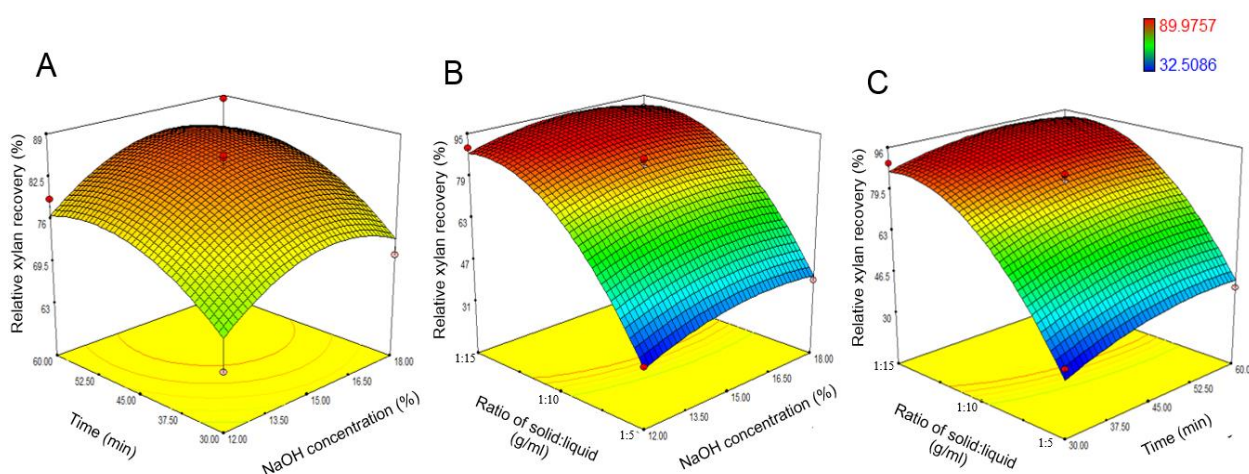


Figure 17 Response surface plots of optimal condition for xylan extraction from sabi grass. (A) Effects of NaOH concentration and steaming time, (B) Effects of NaOH concentration and solid to liquid ratio and (C) Effect of steaming time and solid to liquid ratio

Table 23 BBD matrix with experimental and RSM predicted values of relative xylan recovery from sabi grass

Run	Code level			Actual level			Relative xylan recovery (%)	
	X ₁	X ₂	X ₃	NaOH concentration (%w/v)	Steaming Time (min)	Ratio of solid to NaOH solution (g : mL)	Predicted	Observed*
1	-1	-1	0	12.00	30.00	1:10	68.13	63.23±0.96
2	+1	-1	0	18.00	30.00	1:10	73.17	70.61±0.58
3	-1	+1	0	12.00	60.00	1:10	76.67	79.23±3.86
4	+1	+1	0	18.00	60.00	1:10	83.42	88.32±3.49
5	-1	0	-1	12.00	45.00	1:5	31.92	32.51±1.64
6	+1	0	-1	18.00	45.00	1:5	40.94	39.20±1.12
7	-1	0	+1	12.00	45.00	1:15	87.78	89.53±0.79
8	+1	0	+1	18.00	45.00	1:15	90.56	89.98±0.58
9	0	-1	-1	15.00	30.00	1:5	30.57	34.88±3.90
10	0	+1	-1	15.00	60.00	1:5	43.39	40.24±1.93
11	0	-1	+1	15.00	30.00	1:15	86.74	89.89±0.50
12	0	+1	+1	15.00	60.00	1:15	92.71	88.40±0.38
13	0	0	0	15.00	45.00	1:10	84.53	85.41±1.04
14	0	0	0	15.00	45.00	1:10	84.53	85.74±1.16
15	0	0	0	15.00	45.00	1:10	84.53	82.46±0.42

* Mean ± SD derived from three replicates

When relative xylan recovery of five grasses were compared (Table 24). The value varied in the range between 87.89±0.70 and 99.42±4.05%. The highest relative xylan recovery was detected in sugarcane leaf (99.42%), napier grass (93.49%) and purple guinea grass (95.85%). Therefore, the xylan samples from these grasses were selected for investigations of viscosity property and enzymatic hydrolysis for xylooligosaccharides (XOs) and xylose production.

Table 24 Comparison of five grasses xylan extraction under optimize condition

Grass samples	Actual optimize conditions	Actual relative xylan recovery (%)*
Sugarcane leaf	- 14.32%(w/v) NaOH - 32.36 min in autoclave - 1g biomass:13.25 mL NaOH	99.42±4.05 ^a
Napier grass	- 16.80%(w/v) NaOH - 30.08 min in autoclave - 1g biomass:14.75 mL NaOH	93.49±3.91 ^{ab}
Purple guinea grass	- 13.30%(w/v) NaOH - 43.50 min in autoclave - 1g biomass:13.30 mL NaOH	95.85±7.55 ^{ab}
Vetiver grass	- 16.70%(w/v) NaOH - 45.97 min in autoclave - 1g biomass:13.55 mL NaOH	87.89±0.70 ^b
Sabi grass	- 12.87%(w/v) NaOH - 42.97 min in autoclave - 1g biomass:13.10 mL NaOH	88.89±0.54 ^b

* Data were presented as the average value ± standard deviation. Different superscript letters indicated significant difference at $p \leq 0.05$ in DMRT.

4.3 Endoxylanase and β -xylosidase production from *A. pullulans*

4.3.1 Screening of endoxylanase and β -xylosidase

All strains of *Aureobasidium* spp. could produce endoxylanase with activities in the range between 0.56 ± 0.17 and 22.43 ± 0.27 U/mL (Figure 18). The highest endoxylanase activity was detected in *A. pullulans* NRRL 58523 (22.43 ± 0.27 U/mL), *A. pullulans* NRRL 58536 (21.84 ± 0.44 U/mL) and *A. pullulans* NRRL 58519 (21.64 ± 0.55 U/mL), and. Therefore, these strains were selected for determination of optimal pH, optimal temperature and thermostability.

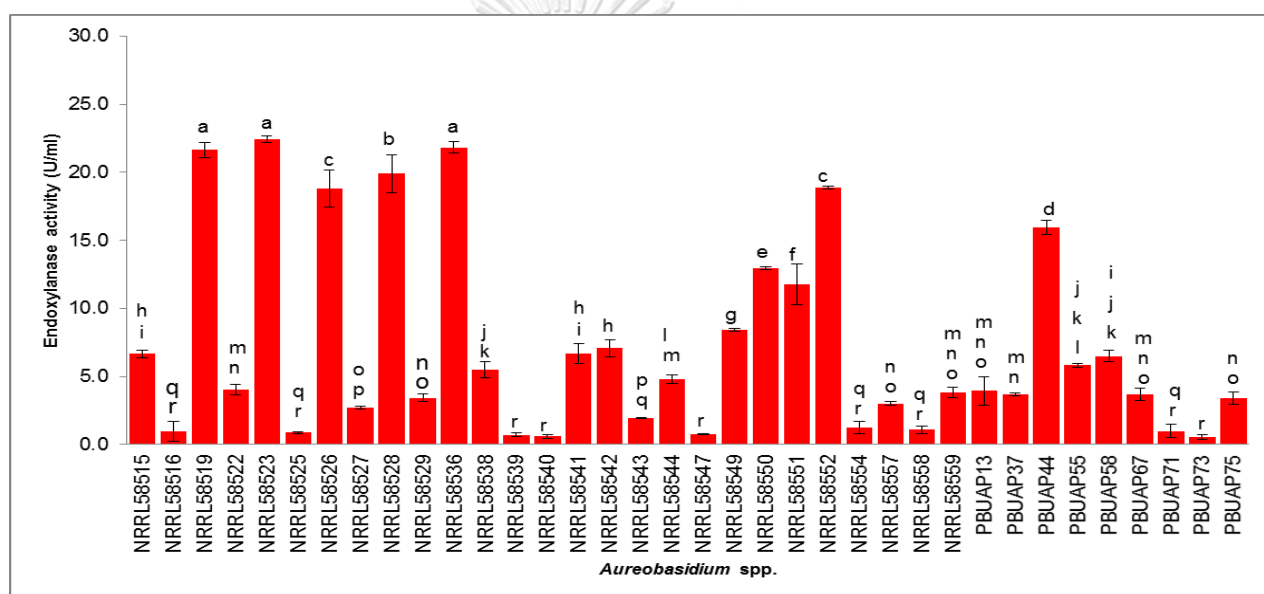


Figure 18 Endoxylanase activity of *Aureobasidium* spp. Different letters above the bar graphs indicate significant differences according to DMRT at $p \leq 0.05$. Bar indicated standard deviation derived from three replicates.

For intracellular β -xylosidase (Figure 19), every *Aureobasidium* strains produced the enzyme with activities in the range between 4.63 ± 0.48 and 37.64 ± 3.71 U/g. The highest β -xylosidase activity (37.64 ± 3.71 U/g) was found in *A. pullulans* NRRL58559. For *A. melanogenum*, the highest activity were from PBUAP37 and PBUAP13 at 28.35 ± 2.12 U/g and 26.66 ± 2.05 U/g, respectively. Therefore, these strains were selected for determination of optimal pH, optimal temperature and thermostability.

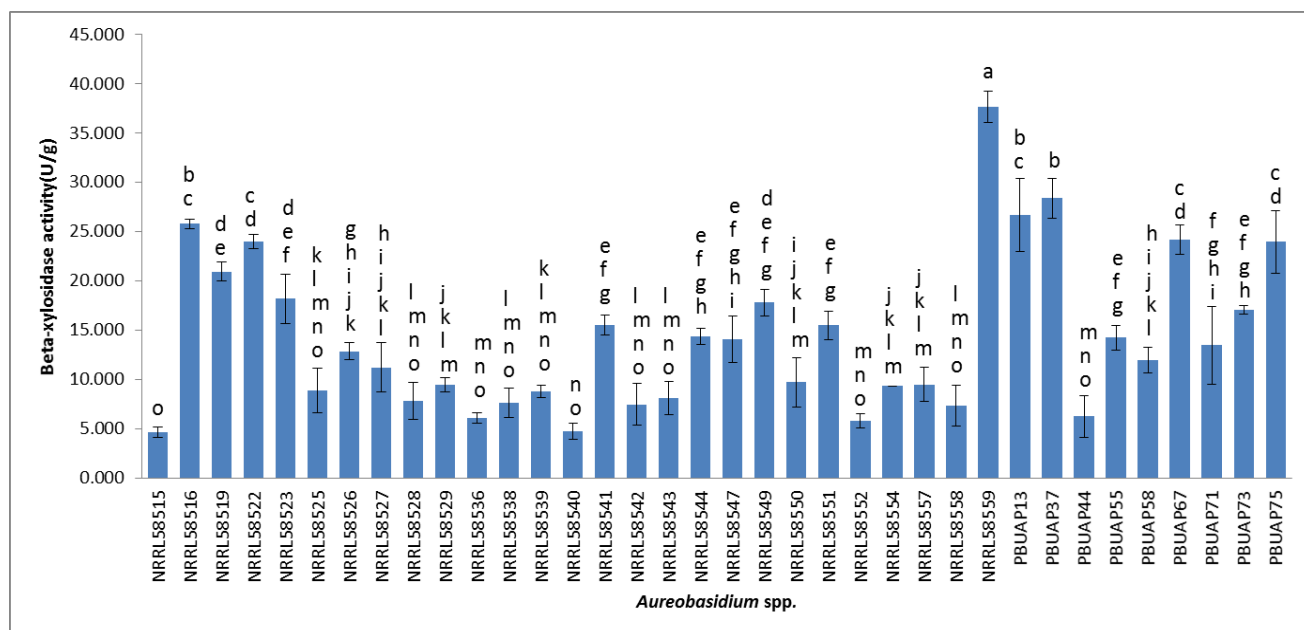


Figure 19 β -xylosidase activity of *Aureobasidium* spp. Different letters above the bar graphs indicate significant differences according to DMRT at $p \leq 0.05$. Bar indicated standard deviation derived from three replicates.

4.3.2 Determination of optimal pH and temperature

The optimal pH and temperature of the selected endoxylanases from *A. pullulans* NRRL58519, NRRL58523 and NRRL58536 were identical at pH 4 in 50 mM sodium citrate buffer and 50°C (Figure 20). The enzymes catalyzed relatively well from pH 3 to 5 at temperature between 40 and 60°C. The enzymes lost most of their activity at higher than pH 5 and temperature over 70°C.

For β -xylosidase from *A. pullulans* NRRL 58559 and *A. melanogenum* PBUAP 13 and PBUAP 37, all of them showed identical optimal pH and temperature at pH 4 in 50 mM sodium citrate buffer and 70°C (Figure 21). The enzymes worked relatively well from pH 3 to 5 at temperature between 50 and 70°C. At 40°C, the enzymes showed moderate activity (around 50 % of its maximum activity). The enzymes lost the most activity at pH higher than 5 and 80 °C. In addition to the three selected enzymes, β -xylosidase from *A. pullulans* CBS 156684 (Bankeeree et al., 2018) was also included in the experiment. This enzyme had identical optimal pH and temperature as the three enzymes and showed very similar response of ranging pH and temperature.

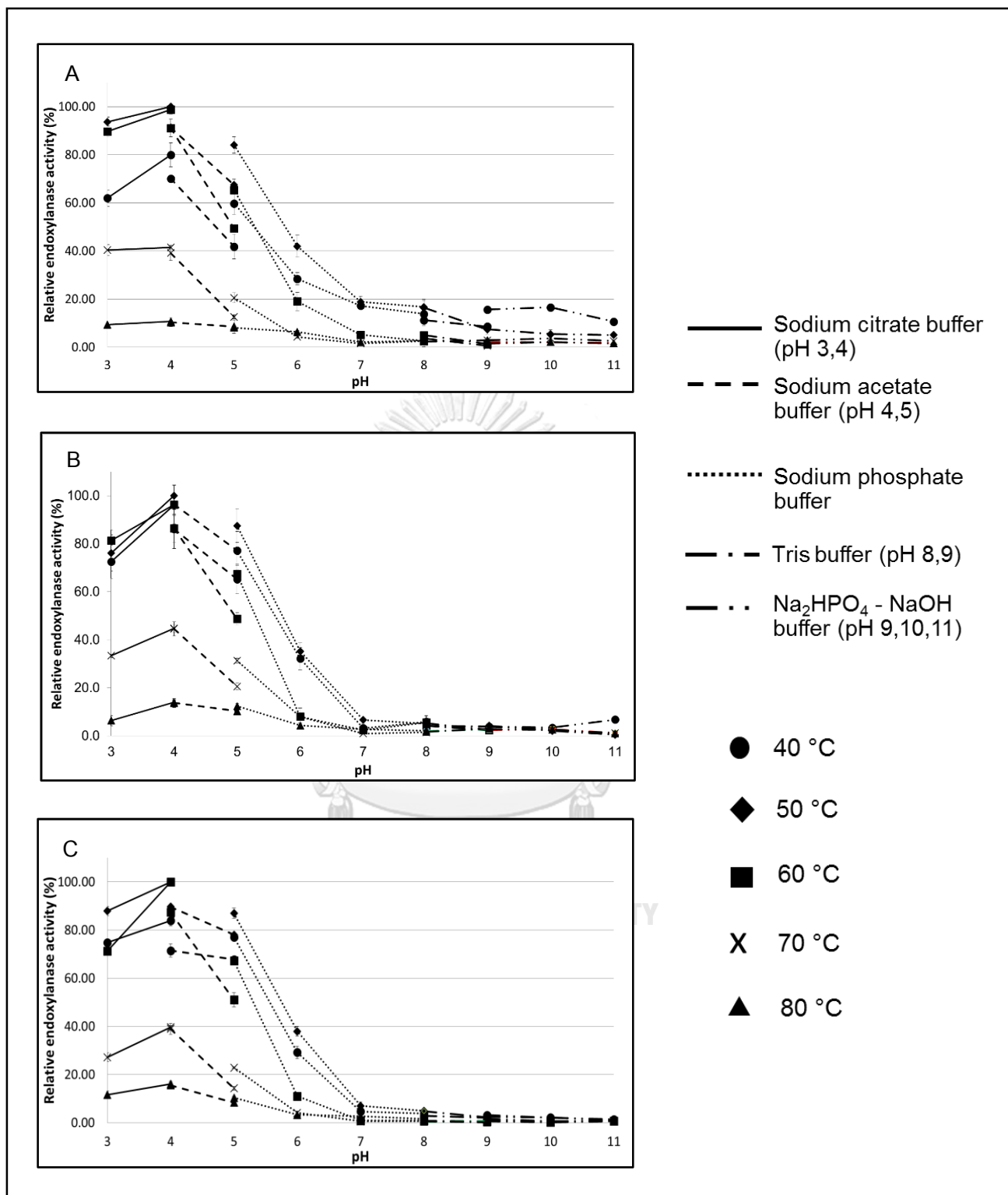


Figure 20 Optimum pH and temperature of endoxylanases from (A) *A. pullulans* NRRL 58519; (B) *A. pullulans* NRRL 58523 and (C) *A. pullulans* NRRL 58536

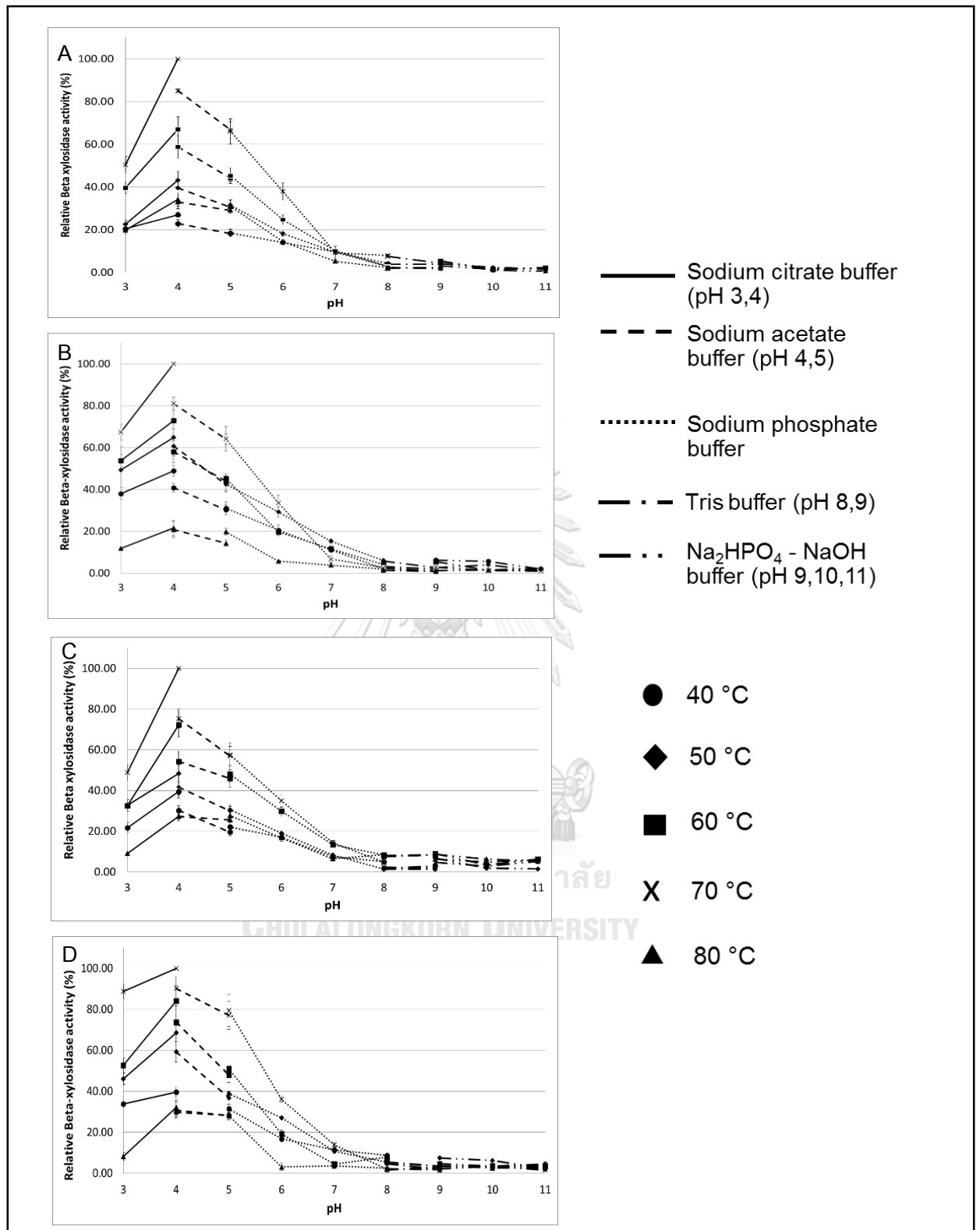


Figure 21 Optimum pH and temperature of β -xylosidase from (A) *A. pullulans* CBS135684; (B) *A. pullulans* NRRL 58559, (C) *A. melanogenum* PBUAP 37 and (D) *A. melanogenum* PBUAP 13

4.3.3 Thermostability of xylanases

For endoxylanase thermostability (Figure 22), incubation at 40 °C did not significantly affect the activity of the three selected crude enzymes with more than 90% of the activity remaining after 12h. The enzymes lost their activity after 1 h at a temperature range of 60 to 80 °C. At the optimum temperature (50 °C), the endoxylanase from *A. pullulans* NRRL 58523 and 58536 were relatively stable with half of their activity remaining after 12 h. However, endoxylanase strain NRRL 58536 lost its activity more rapidly at 4 h, with 65% remain compared to NRRL 58523 (over 80%). *A. pullulans* NRRL 58519 endoxylanase was relatively less stable with only 29.66±2.81% of activity remaining after 12 h. Therefore, endoxylanase from *A. pullulans* NRRL 58523 was selected for further hydrolysis studies.

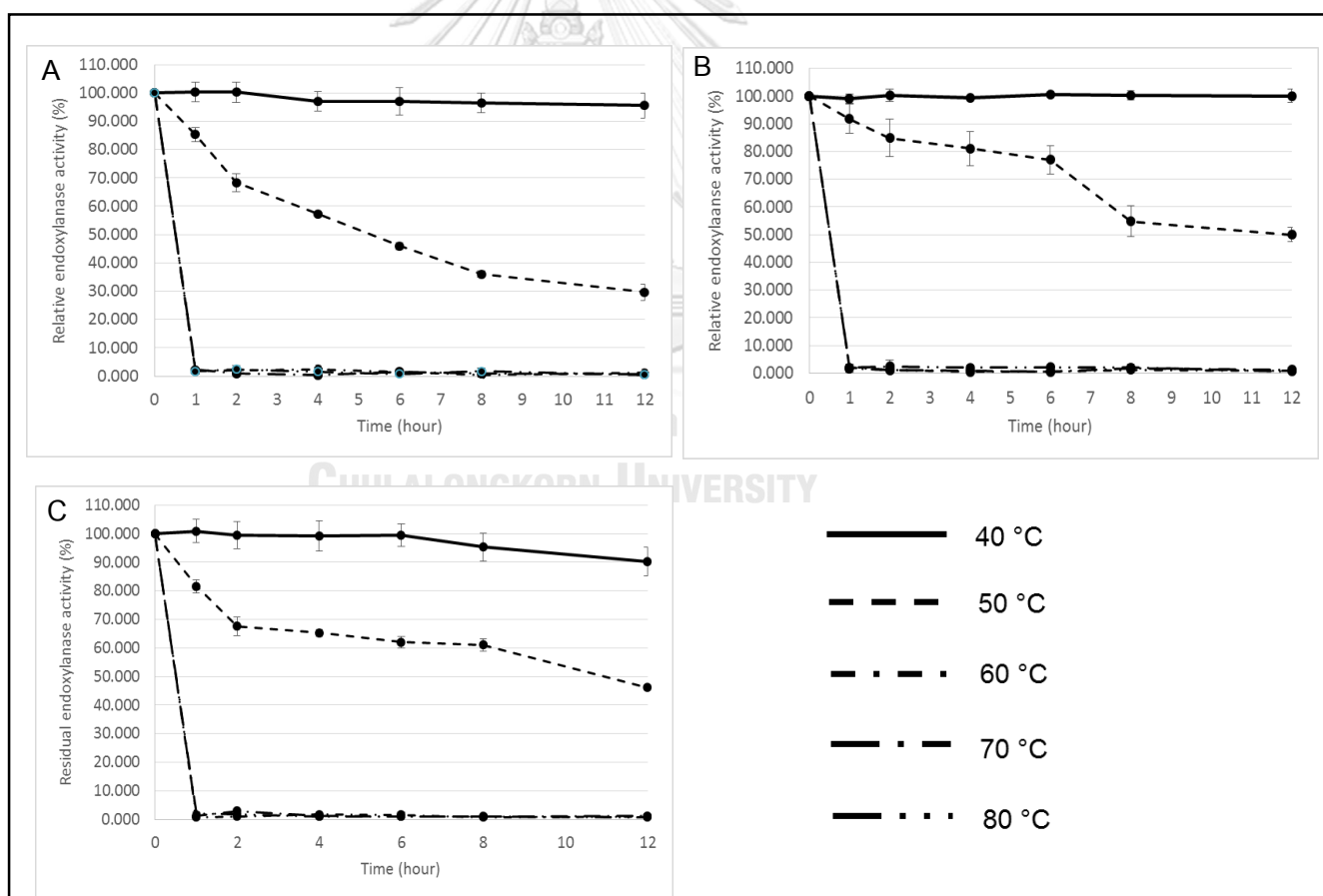


Figure 22 Thermostability of endoxylanase from: (A) *A. pullulans* NRRL58519, (B) *A. pullulans* NRRL58523, (C) *A. pullulans* NRRL58536

For β -xylosidase (Figure 23), all enzymes were highly stable at 40 and 50°C with no activity loss after 12 h. The enzymes lost their activity after 1 h at a temperature at 80 °C. At the optimum temperature (70 °C), β -xylosidase from *A. pullulans* CBS 135684 was relatively stable with more than 85% of the activity remaining after 12 h. Comparing to other enzymes, *A. melanogenum* PBUAP 37, *A. melanogenum* PBUAP 13 and *A. pullulans* NRRL 58559 exhibited to remain the activity at $78.72\pm 5.24\%$, $75.50\pm 4.40\%$ and $48.41\pm 3.98\%$, respectively after 12 h. Therefore, β -xylosidase from *A. pullulans* CBS 135684 was selected for xylose production.

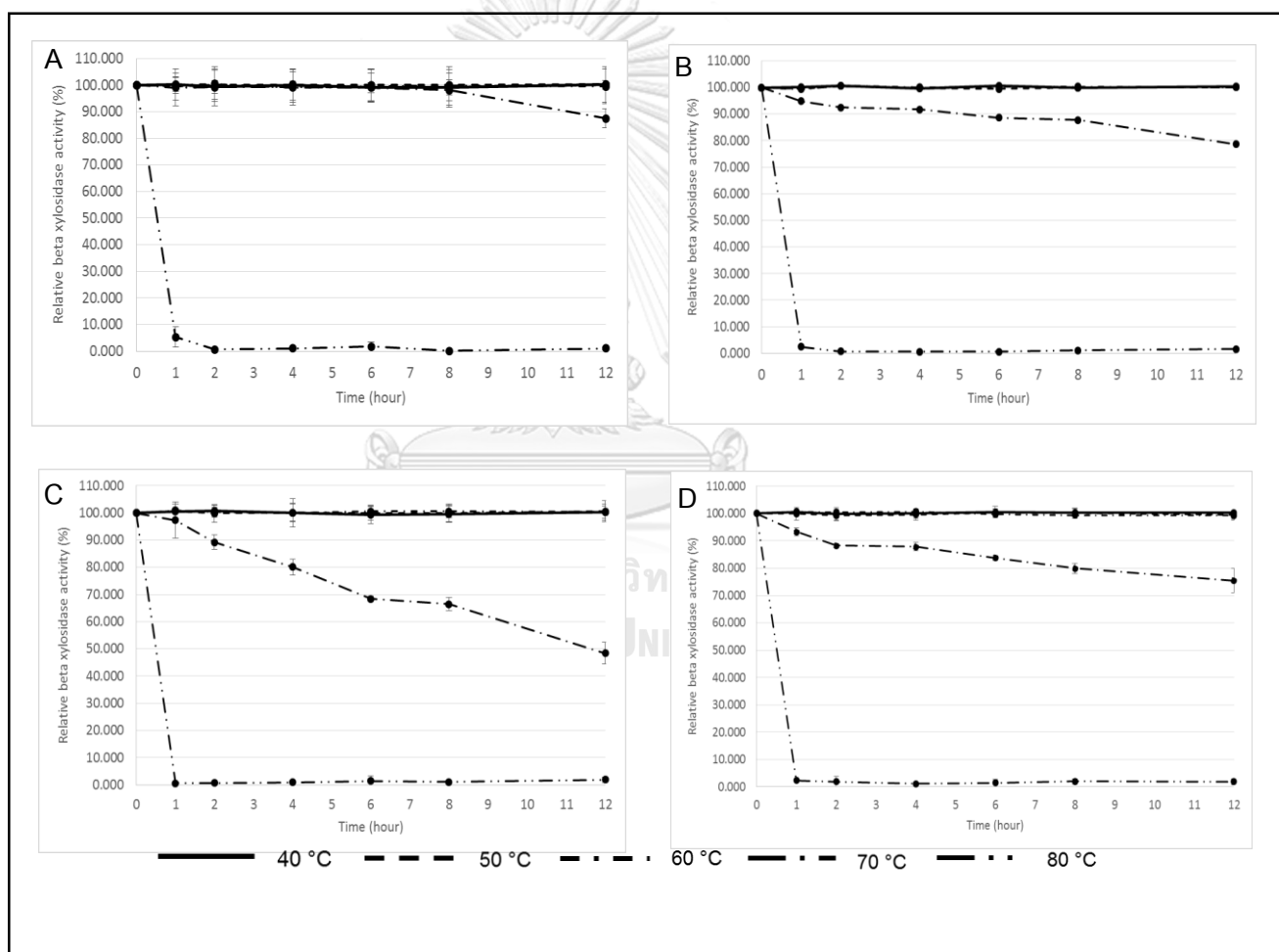


Figure 23 Thermostability of β -xylosidase: (A) *A. pullulans* CBS 135684, (B) *A. melanogenum* PBUAP 37, (C) *A. pullulans* NRRL 58559 and (D) *A. melanogenum* PBUAP 13

4.4 Determination of molecular weight, average DP and viscosity property

Molecular weight of sugarcane leaf, napier grass and purple guinea grass were 1,737 - 4,027,110, 1,237 - 2,945,100 and 1,584 - 3,432,840 g/mol, respectively. The average DP values were found to be related to their average molecular weights. The average DP of sugarcane leaf, napier grass and purple guinea grass xylans were 239.10 ± 17.98 , 159.17 ± 13.80 and 180.85 ± 5.30 , respectively.

The viscosity at shear rate 100 s^{-1} and the average DP of the xylans with the treatment of endoxylanase concentrations (0, 25, 50, 100 U/g xylan) were shown in Figure 24. Before enzyme disruption, the highest viscosity was detected in sugarcane leaf xylan. After enzyme disruption, the viscosity values of sugarcane leaf, purple guinea grass and napier grass decreased from 11.33 ± 0.58 to 6.83 ± 0.29 , 9.74 ± 0.22 to 6.50 ± 0.50 and 9.67 ± 0.58 to 6.17 ± 0.29 mPa.s, respectively. For the average DP after enzyme disruption of the xylans, they were found to be related to their viscosity. The average DP of sugarcane leaf, purple guinea grass and napier grass xylans decreased from 239.10 ± 17.98 to 8.71 ± 0.46 , 180.85 ± 5.30 to 9.34 ± 0.68 and 159.17 ± 13.80 to 8.15 ± 0.17 , respectively.

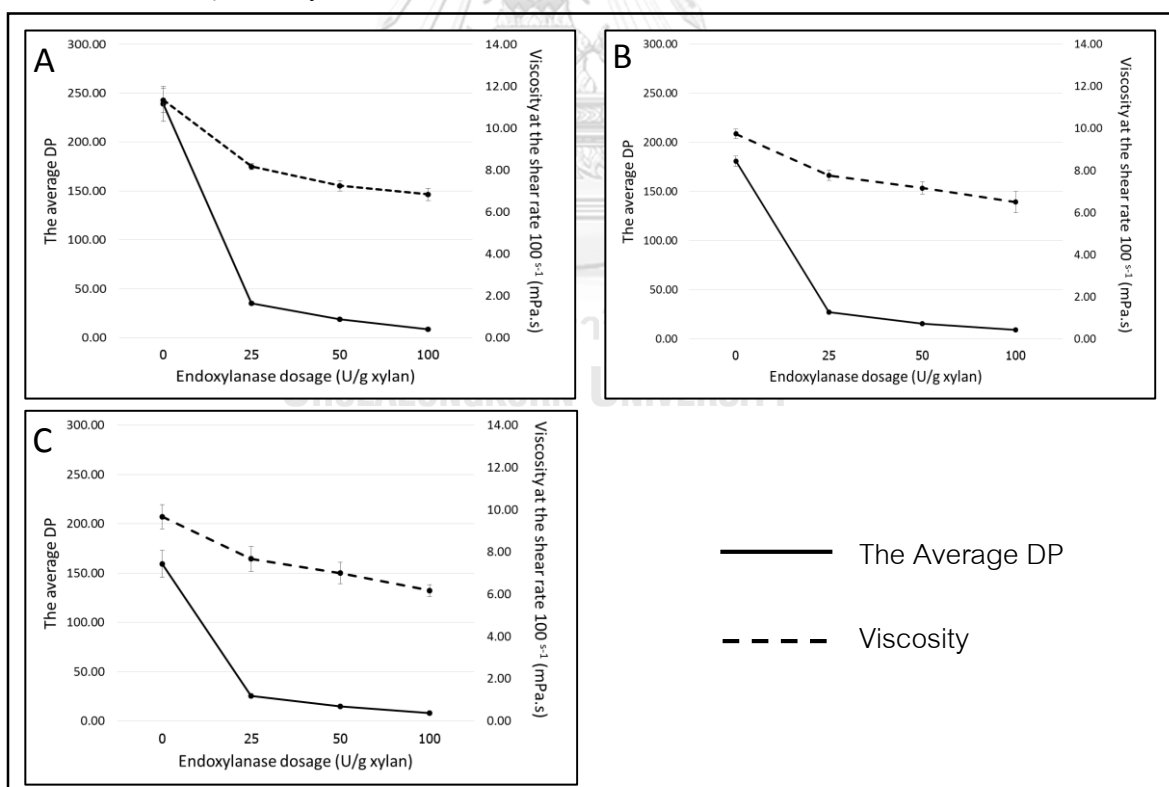


Figure 24 Viscosity at shear rate 100 s^{-1} and the average DP of (A) sugarcane leaf xylan, (B) purple guinea grass xylan and (C) napier grass xylan before and after endoxylanase disruption at different dosages treatment (0, 25, 50, 100 U/g substrate)

4.5 XO_s production

4.5.1 Partial enzymatic hydrolysis

The three extracted xylans and commercial beechwood xylan were partially digested to XO_s by the crude endoxylanase from *A. pullulans* NRRL58523 at 50 U/g xylan under the optimal condition for 24 h (Figure 25). The largest reducing sugar yield (0.36 ± 0.01 g/g xylan) was obtained from commercial beechwood xylan following by sugarcane leaf xylan (0.24 ± 0.01 g/g xylan), purple guinea grass (0.15 ± 0.01 g/g xylan) and napier grass xylan (0.14 ± 0.01 g/g xylan).

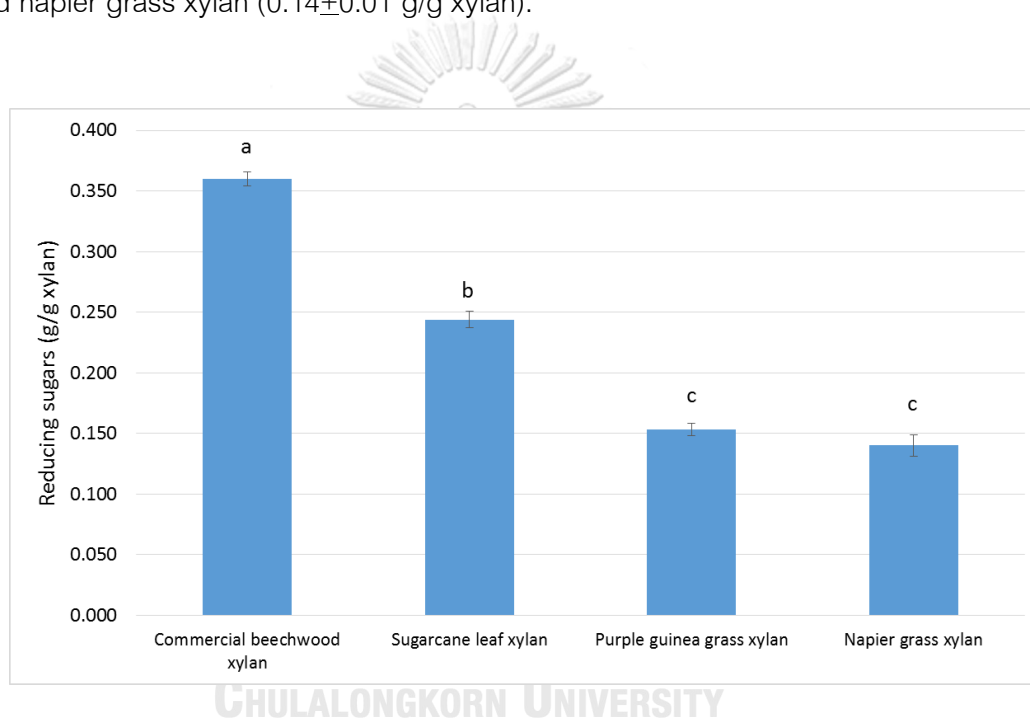


Figure 25 Amount of the reducing sugars obtained from the hydrolysis of three xylans.

Different letters above the bar graphs indicate significant differences according to DMRT at $p \leq 0.05$. Bar indicated standard deviation derived from three replicates.

4.5.2 Optimization of partial xylans hydrolysis

To enhance the XO_s yield, the optimal enzyme dosage and incubation time were predicted using CCD and RSM (Figure 26).

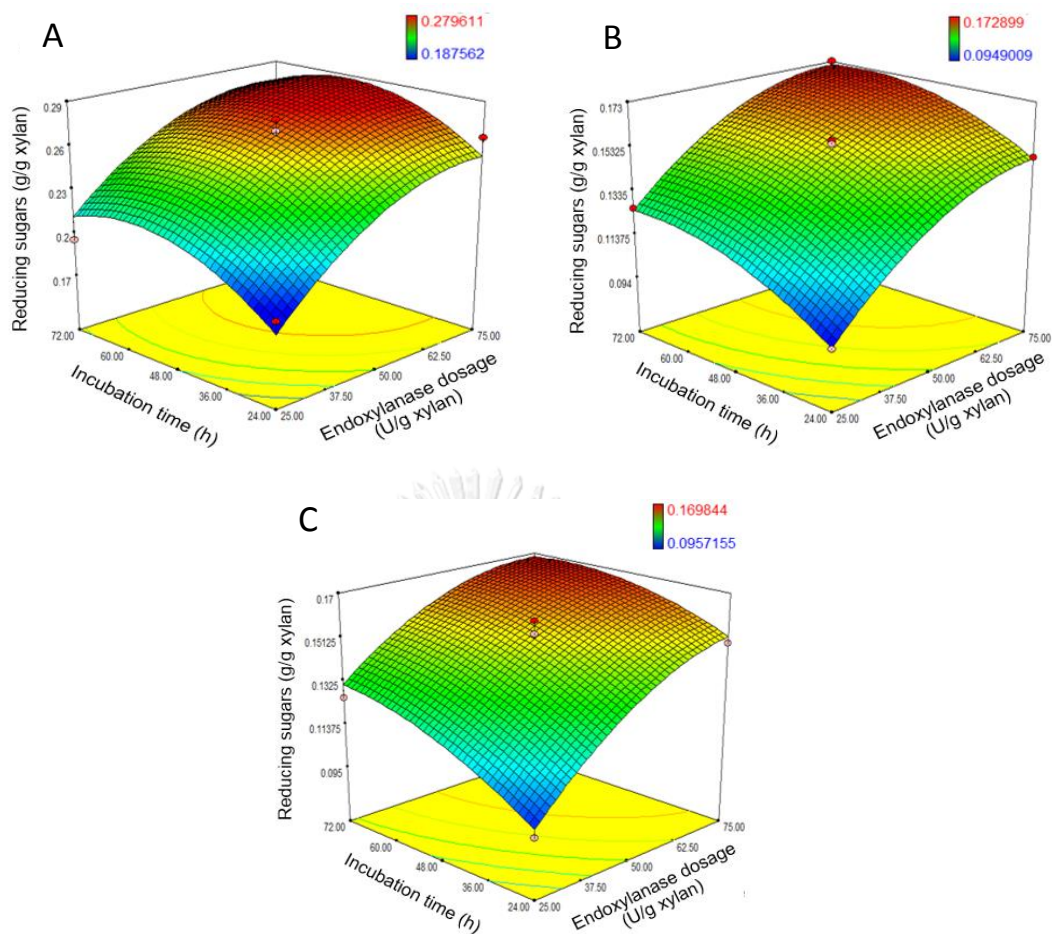


Figure 26 Response surface plots for optimal condition of partial xylan hydrolysis of (A) sugarcane leaf xylan, (B) Purple guinea grass xylan and (C) Napier grass xylan for determination of the releasing of reducing sugars

4.5.2.1 Sugarcane leaf xylan

The response surface plot for releasing of reducing sugars from sugarcane leaf xylan was shown in Figure 26 (A). CCD with 3 levels of 3 variable factors was used and the response values were presented in Table 25. The data based on a second order polynomial could be expressed by following equation:

$$XOS_7 = -1.44 \times 10^{-3} + 4.79 \times 10^{-3} A_1 + 4.37 \times 10^{-3} A_2 - 4.16 \times 10^{-6} A_1 A_2 - 3.21 \times 10^{-5} A_1^2 - 3.74 \times 10^{-5} A_2^2$$

Where XOS_7 was reducing sugars from partial hydrolysis of sugarcane leaf xylan (g/g xylan), A_1 was endoxylanase dosage (U/g xylan) and A_2 was

incubation time (h). Based on the ANOVA statistical significant model (Appendix H), the equation exhibited 91% of the observed response at R^2 value (0.91). The model was significant with $p = 0.0108$ whereas lack of fit was not significant ($p = 0.06$), suggesting that the regression model could accurately predict the response. Moreover, a low coefficient of variation (CV = 6.94%) indicated the precision and reliability of the experiments. The RSM assessment showed that the optimum condition could be achieved when adjusting 65.32 U/g xylan of endoxylanase dosage and 52.89 h of incubation time with the releasing of reducing sugars at 0.29 g/g xylan. Partial hydrolysis of sugarcane leaf xylan was performed under the suggested condition to confirm the prediction with the reducing sugar yield at 0.27 ± 0.01 g/g xylan ($p=0.13$), which was not significantly different from the predicted value, recommended that the equations were accurate. Using this optimized condition, the total amount of reducing sugars was 1.12-fold higher than the unoptimized condition. At this condition, xylobiose and xylotriose were determined at 0.16 ± 0.02 and 0.08 ± 0.01 g/g xylan, respectively.

Table 25 CCD and RSM predicted values of reducing sugars from partial hydrolysis of sugarcane leaf xylan

Run	Code level		Actual level		Reducing sugars (g/g xylan)	
	A ₁	A ₂	Endoxylanase dosage (U/g xylan)	Incubation time (h)	Predicted	Observed*
1	-1	-1	25	24	0.18	0.19±0.01
2	+1	-1	75	24	0.25	0.27±0.01
3	-1	+1	25	72	0.21	0.20±0.01
4	+1	+1	75	72	0.28	0.26±0.01
5	-1.414	0	14.64	48	0.18	0.19±0.01
6	+1.414	0	85.36	48	0.28	0.28±0.01
7	0	-1.414	50	14.06	0.20	0.19±0.01
8	0	+1.414	50	81.94	0.25	0.27±0.01
9	0	0	50	48	0.27	0.27±0.01
10	0	0	50	48	0.27	0.27±0.01
11	0	0	50	48	0.27	0.28±0.02

* Mean ± SD derived from three replicates

4.5.2.2 Purple guinea grass xylan

For partial hydrolysis of purple guinea grass xylan, the response surface plot was presented in Figure 26 (B). The levels of factors and the response values including the releasing of reducing sugars were shown in Table 26. The data based on a second order polynomial was expressed by following equation:

$$XOS_2 = -8.99 \times 10^{-3} + 3.03 \times 10^{-3} A_1 + 2.10 \times 10^{-3} A_2 - 2.80 \times 10^{-6} A_1 A_2 - 1.90 \times 10^{-5} A_1^2 - 1.47 \times 10^{-5} A_2^2$$

Where XOS_2 was reducing sugars from partial hydrolysis of purple guinea grass xylan (g/g xylan), A_1 was endoxylanase dosage (U/g xylan) and A_2 was incubation time (h). Based on the ANOVA statistical significant model (Appendix H), the equation exhibited 99% of the observed response at R^2 value (0.99). The model was significant with $p = 0.0001$ whereas lack of fit was not significant ($p = 0.17$), suggesting that the regression model could accurately predict the response. Moreover, a low coefficient of variation (CV = 0.94%) indicated the precision and reliability of the experiments. The RSM assessment showed that the optimum condition could be achieved when adjusting 74.86 U/g xylan of endoxylanase dosage and 64.31 h of incubation time with the releasing of reducing sugars at 0.17 g/g xylan. Partial hydrolysis of purple guinea grass was performed under the suggested condition to confirm the prediction with the releasing of reducing sugars at 0.17 ± 0.01 g/g xylan ($p=0.78$), which was not significantly different from the predicted value, recommended that the equations were accurate. Using this optimized condition, the total amount of reducing sugars was 1.13-fold higher than the unoptimized condition. At this condition, xylobiose and xylotriose were determined at 0.09 ± 0.01 and 0.04 ± 0.01 g/g xylan, respectively.

Table 26 CCD and RSM predicted values of reducing sugars from partial hydrolysis of purple guinea grass xylan

Run	Code level		Actual level		Reducing sugars (g/g xylan)	
	A ₁	A ₂	Endoxylanase dosage (U/g xylan)	Incubation time (h)	Predicted	Observed*
1	-1	-1	25	24	0.09	0.09±0.01
2	+1	-1	75	24	0.15	0.15±0.01
3	-1	+1	25	72	0.12	0.13±0.01
4	+1	+1	75	72	0.17	0.17±0.01
5	-1.414	0	14.64	48	0.10	0.10±0.01
6	+1.414	0	85.36	48	0.17	0.17±0.01
7	0	-1.414	50	14.06	0.12	0.12±0.01
8	0	+1.414	50	81.94	0.16	0.16±0.01
9	0	0	50	48	0.16	0.16±0.01
10	0	0	50	48	0.16	0.16±0.01
11	0	0	50	48	0.16	0.16±0.01

* Mean ± SD derived from three replicates

4.5.2.3 Napier grass xylan

The response surface plot for releasing of reducing sugars from napier grass xylan was shown in Figure 26 (C). CCD with 3 levels of 3 variable factors was used and the response values were presented in Table 27. The data based on a second order polynomial could be expressed by following equation:

$$XOS_3 = 4.86 \times 10^{-3} + 2.79 \times 10^{-3} A_1 + 1.85 \times 10^{-3} A_2 - 6.70 \times 10^{-6} A_1 A_2 - 1.58 \times 10^{-5} A_1^2 - 1.056 \times 10^{-5} A_2^2$$

Where XOS_3 was reducing sugars from partial hydrolysis of napier grass xylan (g/g xylan), A_1 was endoxylanase dosage (U/g xylan) and A_2 was incubation time (h). Based on the ANOVA statistical significant model (Appendix H), the equation exhibited 96% of the observed response at R^2 value (0.96). The model was significant with $p = 0.0013$ whereas lack of fit was not significant ($p = 0.26$), suggesting that the

regression model could accurately predict the response. Moreover, a low coefficient of variation (CV = 4.66%) indicated the precision and reliability of the experiments. The RSM assessment showed that the optimum condition could be achieved when adjusting 74.88 U/g xylan of endoxylanase dosage and 64.21 h of incubation time with reducing sugar yield at 0.17 g/g xylan. Partial hydrolysis of napier grass xylan was performed under the suggested condition to confirm the prediction. The result showed that the reducing sugar yield at 0.17 ± 0.01 g/g initial xylan was not significantly different from the predicted value ($p=0.62$), indicating that the equations were accurate. Using this optimized condition, the releasing of reducing sugars was 1.11-fold higher than that with the unoptimized condition. At this condition, xylobiose and xylotriose were determined at 0.08 ± 0.01 and 0.03 ± 0.01 g/g xylan, respectively.

Table 27 CCD and RSM predicted values of reducing sugars from partial hydrolysis of napier grass xylan

Run	Code level		Actual level		Reducing sugars (g/g xylan)	
	A ₁	A ₂	Endoxylanase dosage (U/g xylan)	Incubation time (h)	Predicted	Observed*
1	-1	-1	25	24	0.10	0.10±0.01
2	+1	-1	75	24	0.15	0.15±0.01
3	-1	+1	25	72	0.13	0.13±0.01
4	+1	+1	75	72	0.17	0.16±0.01
5	-1.414	0	14.64	48	0.10	0.11±0.02
6	+1.414	0	85.36	48	0.17	0.17±0.01
7	0	-1.414	50	14.06	0.12	0.13±0.02
8	0	+1.414	50	81.94	0.16	0.17±0.01
9	0	0	50	48	0.15	0.15±0.01
10	0	0	50	48	0.15	0.16±0.01
11	0	0	50	48	0.15	0.15±0.02

*Mean ± SD derived from three replicates

4.6 Xylose production

4.6.1 Complete enzymatic hydrolysis of xylan

To determine the most suitable protocol for complete hydrolysis, single step hydrolysis using mixture of endoxylanase and β -xylosidase (cocktail) and two-step hydrolysis using single enzyme for each step (stepwise) were compared (Figure 27). Each xylan released the highest xylose yield in the cocktail process at 50°C. The highest xylose yield was observed in commercial beechwood (0.49±0.01 g/g initial xylan) following by sugarcane leaf, purple guinea grass and napier grass xylans at 0.19±0.01, 0.13±0.01 and 0.12±0.001 g/g initial xylan, respectively. When incubation temperature was raised to 60 and 70°C, the xylose yields were reduced in all xylans digested. The stepwise process with incubation temperature at 50°C for endoxylanase following by 70 °C for β -xylosidase, lower xylose yields in the ranges between 0.10±0.01 and 0.40±0.01 g/g initial xylan were obtained. Therefore, the hydrolysis via the cocktail protocol at 50°C was selected for further optimization of xylose production.

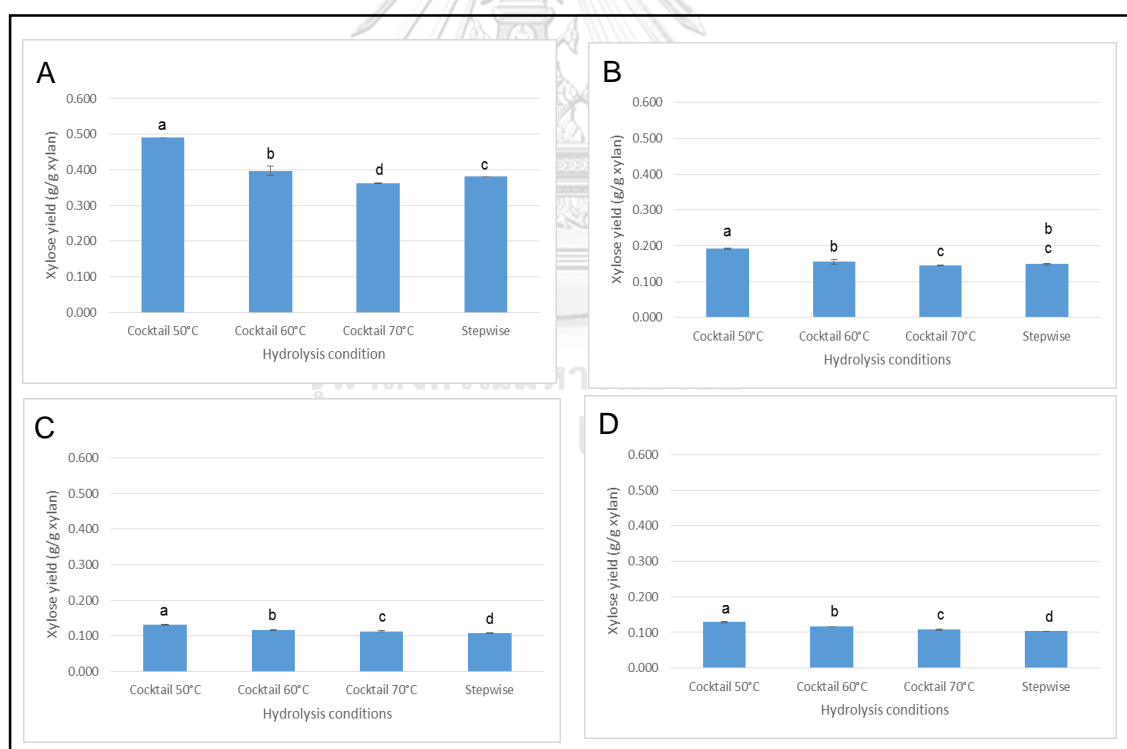


Figure 27 Comparison of different hydrolysis protocols for complete hydrolysis of xylans: (A) commercial beechwood xylan, (B) sugarcane leaf xylan, (C) purple guinea grass xylan and (D) napier grass xylan. Different letters above the bar graphs indicate significant differences according to DMRT at $p \leq 0.05$. Bar indicated standard deviation derived from three replicates.

4.6.2 Optimization of xylose production

4.6.2.1 Sugarcane leaf xylan

For optimization of complete sugarcane leaf xylan hydrolysis, the response surface plots and the levels of factors and the response values were presented in Figure 28 and Table 28, respectively. The data based on a second order polynomial was expressed by following equation:

$$X_1 = 0.03 + 1.30 \times 10^{-3} B_1 + 1.05 \times 10^{-3} B_2 + 0.01 B_3 - 3.32 \times 10^{-6} B_1 B_2 + 3.93 \times 10^{-6} B_1 B_3 - 2.19 \times 10^{-5} B_2 B_3 - 7.27 \times 10^{-6} B_1^2 - 1.37 \times 10^{-6} B_2^2 - 3.33 \times 10^{-4} B_3^2$$

Where X_1 was the xylose yield from complete hydrolysis of sugarcane leaf xylan (g/g initial xylan), B_1 was endoxylanase concentration (U/g substrate), B_2 was β -xylosidase concentration (U/g substrate) and B_3 was incubation time (h). Based on the ANOVA statistical significant model (Appendix I), the equation exhibited 94% of the observed response at R^2 value (0.94). The model was significant with $p = 0.0157$ whereas lack of fit was not significant ($p = 0.29$), suggesting that the regression model could accurately predict the response. Moreover, a low coefficient of variation (CV = 4.66%) indicated the precision and reliability of the experiments. The RSM assessment showed that the optimum condition could be achieved when adjusting 69.93 U/g substrate of endoxylanase dosage, 67.85 U/g substrate of β -xylosidase dosage and 17.71 h of incubation time with xylose yield at 0.21 g/g initial xylan. Complete hydrolysis of sugarcane leaf xylan was performed under the suggested condition to confirm the prediction. The result showed that the xylose yield at 0.20 ± 0.01 g/g initial xylan was not significantly different from the predicted value ($p=0.10$), indicating that the equations were accurate. Using this optimized condition, the xylose yield was 1.05-fold higher than that with the unoptimized condition.

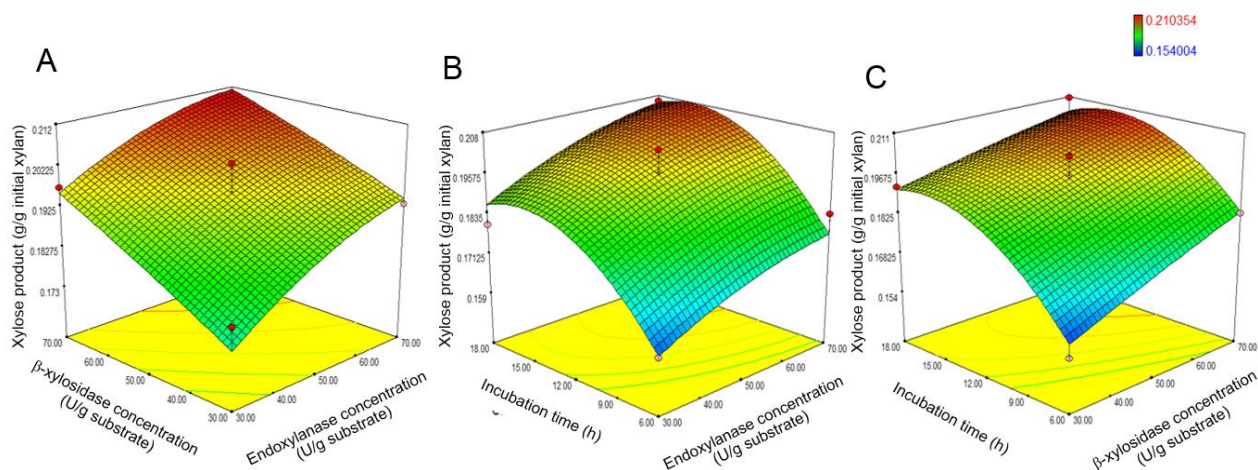


Figure 28 Response surface plots for optimal condition of xylose production from sugarcane leaf xylan. (A) Effect of β -xylosidase and endoxylanase dosages, (B) Effect of incubation time and endoxylanase dosage and (C) Effect of incubation time and β -xylosidase dosage

Table 28 BBD and RSM predicted values of xylose production from sugarcane leaf xylan

Run	Code level			Actual level			Xylose yield (g/g xylan)	
	B ₁	B ₂	B ₃	Endoxylanase dosage (U/g xylan)	β -xylosidase dosage (U/g xylan)	Incubation time (h)	Predicted	Observed*
1	-1	-1	0	30	30	12	0.17	0.18±0.01
2	+1	-1	0	70	30	12	0.19	0.19±0.01
3	-1	+1	0	30	70	12	0.20	0.20±0.02
4	+1	+1	0	70	70	12	0.21	0.21±0.01
5	-1	0	-1	30	50	6	0.16	0.16±0.01
6	+1	0	-1	70	50	6	0.18	0.18±0.01
7	-1	0	+1	30	50	18	0.19	0.18±0.02
8	+1	0	+1	70	50	18	0.21	0.21±0.02
9	0	-1	-1	50	30	6	0.16	0.15±0.01
10	0	+1	-1	50	70	6	0.18	0.18±0.01
11	0	-1	+1	50	30	18	0.19	0.19±0.00
12	0	+1	+1	50	70	18	0.21	0.21±0.01
13	0	0	0	50	50	12	0.20	0.20±0.01
14	0	0	0	50	50	12	0.20	0.19±0.02
15	0	0	0	50	50	12	0.20	0.20±0.01

*Mean ± SD derived from three replicates

4.6.2.2 Purple guinea grass xylan

The response surface plot for xylose production from purple guinea grass xylan was shown in Figure 29. BBD with 3 levels of 3 variable factors was used and the response values were presented in Table 29. The data based on a second order polynomial could be expressed by following equation:

$$X_2 = 0.18 - 4.05 \times 10^{-3} B_1 - 6.85 \times 10^{-4} B_2 + 5.89 \times 10^{-3} B_3 + 1.43 \times 10^{-5} B_1 B_2 + 1.52 \times 10^{-5} B_1 B_3 - 1.36 \times 10^{-5} B_2 B_3 + 3.71 \times 10^{-5} B_1^2 + 5.80 \times 10^{-6} B_2^2 - 1.59 \times 10^{-4} B_3^2$$

Where X_2 was the xylose product of purple guinea grass xylan (g/g initial xylan), B_1 was endoxylanase dosage (U/g substrate), B_2 was β -xylosidase dosage (U/g substrate) and B_3 was incubation time (h). Based on the ANOVA statistical significant model (Appendix I), the equation exhibited 91% of the observed response at R^2 value (0.91). The model was significant with $p = 0.0311$ whereas lack of fit was not significant ($p = 0.06$), suggesting that the regression model could accurately predict the response. Moreover, a low coefficient of variation (CV = 6.31%) indicated the precision and reliability of the experiments. The RSM assessment showed that the optimum condition could be achieved when adjusting 69.90 U/g xylan of endoxylanase dosage, 70.00 U/g substrate of β -xylosidase dosage and 17.71 h of incubation time with the xylose yield at 0.18 g/g xylan. Complete hydrolysis of purple guinea grass xylan was performed under the suggested condition to confirm the prediction with the xylose yield at 0.17 ± 0.01 g/g xylan ($p=0.66$), which was not significantly different from the predicted value, recommended that the equations were accurate. Using this optimized condition, the xylose yield was 1.36-fold higher than the unoptimized condition.

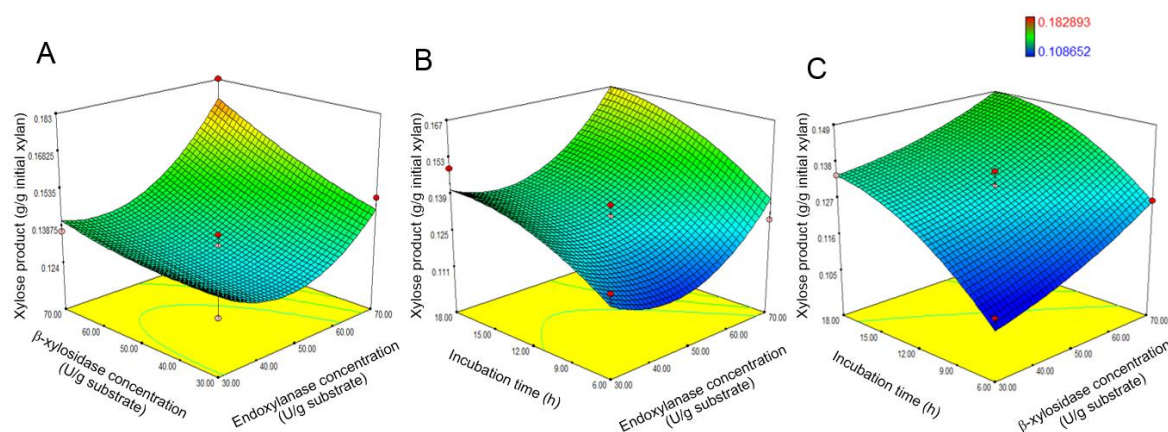


Figure 29 Response surface plots for optimal condition of xylose production from purple guinea grass xylan. (A) Effect of β -xylosidase and endoxylanase dosages, (B) Effect of incubation time and endoxylanase dosage and (C) Effect of incubation time and β -xylosidase dosage

Table 29 BBD and RSM predicted values of xylose production from purple guinea grass xylan

Run	Code level			Actual level			Xylose product (g/g xylan)	
	B ₁	B ₂	B ₃	Endoxylanase dosage (U/g xylan)	β -xylosidase dosage (U/g xylan)	Incubation time (h)	Predicted	Observed*
1	-1	-1	0	30	30	12	0.13	0.13±0.01
2	+1	-1	0	70	30	12	0.15	0.15±0.01
3	-1	+1	0	30	70	12	0.14	0.14±0.02
4	+1	+1	0	70	70	12	0.17	0.18±0.01
5	-1	0	-1	30	50	6	0.12	0.12±0.01
6	+1	0	-1	70	50	6	0.14	0.13±0.01
7	-1	0	+1	30	50	18	0.14	0.15±0.02
8	+1	0	+1	70	50	18	0.17	0.16±0.01
9	0	-1	-1	50	30	6	0.11	0.11±0.01
10	0	+1	-1	50	70	6	0.13	0.13±0.01
11	0	-1	+1	50	30	18	0.13	0.13±0.01
12	0	+1	+1	50	70	18	0.15	0.15±0.01
13	0	0	0	50	50	12	0.13	0.14±0.00
14	0	0	0	50	50	12	0.13	0.13±0.01
15	0	0	0	50	50	12	0.13	0.13±0.00

*Mean ± SD derived from three replicates

4.6.2.3 Napier grass xylan

For optimization of complete napier grass xylan hydrolysis, the response surface plots and the levels of factors and the response values were presented in Figure 30 and Table 30, respectively. The data based on a second order polynomial was expressed by following equation:

$$X_3 = 0.03 + 2.91 \times 10^{-4} B_1 + 7.45 \times 10^{-4} B_2 + 8.10 \times 10^{-3} B_3 - 1.78 \times 10^{-6} B_1 B_2 - 1.76 \times 10^{-5} B_1 B_3 - 2.63 \times 10^{-5} B_2 B_3 + 3.76 \times 10^{-6} B_1^2 - 5.97 \times 10^{-7} B_2^2 - 1.62 \times 10^{-4} B_3^2$$

Where X_3 was the xylose product from complete hydrolysis of napier grass xylan (g/g xylan), B_1 was endoxylanase dosage (U/g substrate), B_2 was β -xylosidase dosage (U/g substrate) and B_3 was incubation time (h). Based on the ANOVA statistical significant model (Appendix I), the equation exhibited 98% of the observed response at R^2 value (0.98). The model was significant with $p = 0.0010$ whereas lack of fit was not significant ($p = 0.31$), suggesting that the regression model could accurately predict the response. Moreover, a low coefficient of variation (CV = 2.24%) indicated the precision and reliability of the experiments. The RSM assessment showed that the optimum condition could be achieved when adjusting 68.05 U/g substrate of endoxylanase dosage, 63.10 U/g substrate of β -xylosidase dosage and 17.38 h of incubation time with xylose yield at 0.14 g/g xylan. Complete hydrolysis of napier grass xylan was performed under the suggested condition to confirm the prediction. The result showed that the xylose yield at 0.13 ± 0.01 g/g xylan was not significantly different from the predicted value ($p=0.16$), indicating that the equations were accurate. Using this optimized condition, the xylose yield was 1.08-fold higher than that with the unoptimized condition.

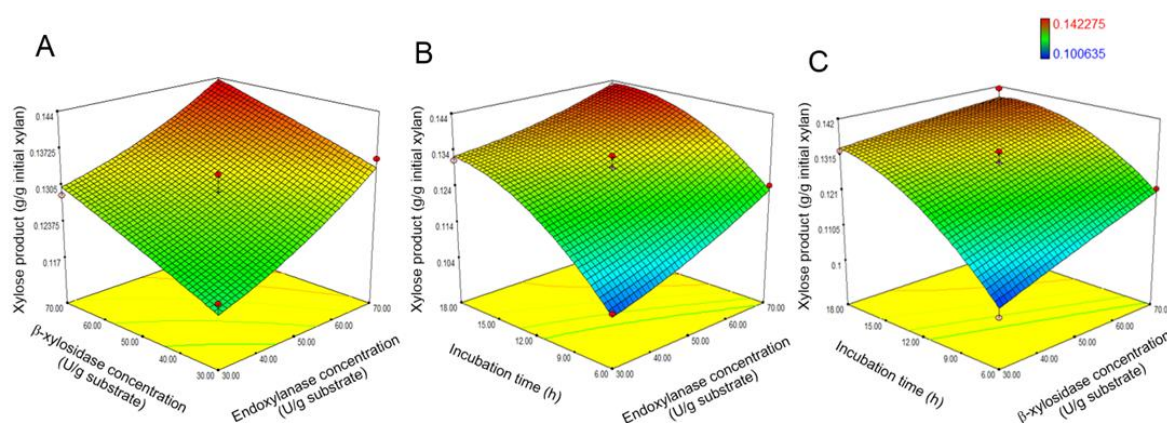


Figure 30 Response surface plots for optimal condition of xylose production from napier grass xylan. (A) Effect of β -xylosidase and endoxylanase dosages, (B) Effect of incubation time and endoxylanase dosage and (C) Effect of incubation time and β -xylosidase dosage

Table 30 BBD and RSM predicted values of xylose production from napier grass xylan

Run	Code level			Actual level			Xylose product (g/g xylan)	
	B ₁	B ₂	B ₃	Endoxylanase doage (U/g xylan)	β -xylosidase dosage (U/g xylan)	Incubation time (h)	Predicted	Observed*
1	-1	-1	0	30	30	12	0.12	0.12±0.01
2	+1	-1	0	70	30	12	0.13	0.14±0.01
3	-1	+1	0	30	70	12	0.13	0.13±0.02
4	+1	+1	0	70	70	12	0.14	0.14±0.01
5	-1	0	-1	30	50	6	0.10	0.11±0.01
6	+1	0	-1	70	50	6	0.12	0.12±0.01
7	-1	0	+1	30	50	18	0.13	0.13±0.02
8	+1	0	+1	70	50	18	0.14	0.14±0.01
9	0	-1	-1	50	30	6	0.10	0.10±0.01
10	0	+1	-1	50	70	6	0.12	0.12±0.01
11	0	-1	+1	50	30	18	0.13	0.13±0.01
12	0	+1	+1	50	70	18	0.14	0.14±0.00
13	0	0	0	50	50	12	0.13	0.13±0.01
14	0	0	0	50	50	12	0.13	0.13±0.01
15	0	0	0	50	50	12	0.13	0.13±0.00

* Mean ± SD derived from three replicates

4.7 Prebiotic property of XOs

Both positive controls, commercial inulin and fructooligosaccharide, exhibited prebiotic activities by significantly enhanced the growth of all probiotic bacteria (Table 31). The produced XOs from the selected xylans were able to significantly stimulate the growth of all *Lactobacillus* strains in ranges of 7.67 ± 0.19 to 7.90 ± 0.05 log CFU/mL for *L. casei* subsp. *rhamnosus*, 7.86 ± 0.03 to 7.94 ± 0.03 log CFU/mL for *L. brevis* and 7.74 ± 0.23 to 7.84 ± 0.06 log CFU/mL for *L. casei* which were not significantly different from fructooligosaccharide and significantly higher than that of the negative control, glucose. However, they failed to stimulate the growth of all *Bifidobacterium* strain when compared to glucose.

Table 31 Growth of *Lactobacillus* spp. and *Bifidobacterium* spp. in MRS medium with carbon sources including XOs and other compounds (2 mg carbon /mL)

Supplement	Bacterial growth (log CFU/mL)*					
	<i>B. animalis</i> subsp. <i>animalis</i> TISTR 2194	<i>B. longum</i> subsp. <i>longum</i> TISTR 2195	<i>B. breve</i> TISTR 2130	<i>L. casei</i> subsp. <i>rhamnosus</i> TISTR 047	<i>L. brevis</i> TISTR 868	<i>L. casei</i> TISTR 390
None	6.48 ± 0.03^e	6.42 ± 0.11^d	6.63 ± 0.06^d	6.51 ± 0.07^d	6.36 ± 0.02^d	6.52 ± 0.06^d
Glucose	8.38 ± 0.06^b	8.33 ± 0.07^b	8.44 ± 0.04^a	7.42 ± 0.03^c	7.46 ± 0.15^c	7.50 ± 0.06^c
Commercial inulin	8.65 ± 0.16^a	8.61 ± 0.02^a	8.49 ± 0.02^a	7.98 ± 0.07^a	8.10 ± 0.05^a	8.12 ± 0.08^a
Commercial fructooligosaccharide	8.63 ± 0.06^a	8.36 ± 0.09^b	8.54 ± 0.06^a	7.84 ± 0.06^{ab}	7.97 ± 0.03^b	7.89 ± 0.11^b
XOs-sugarcane leaf	7.68 ± 0.14^d	7.76 ± 0.14^c	7.93 ± 0.08^c	7.67 ± 0.19^b	7.86 ± 0.03^b	7.74 ± 0.23^b
XOs-purple guinea grass	7.83 ± 0.13^{cd}	7.84 ± 0.21^c	8.24 ± 0.06^b	7.90 ± 0.05^a	7.94 ± 0.03^b	7.84 ± 0.06^b
XOs-napier grass	7.92 ± 0.08^c	7.90 ± 0.05^c	7.88 ± 0.06^c	7.82 ± 0.11^{ab}	7.88 ± 0.06^b	7.78 ± 0.18^b

* Data were presented as the average value \pm standard deviation. Different superscript letters in the same column indicated significant difference at $p \leq 0.05$ in DMRT.

4.8 Antioxidant activity of XO

Antioxidant activity of XO from sugarcane leaf, purple guinea grass and napier grass, ascorbic acid and gallic acid were shown as DPPH radical scavenging activity in Figure 31. The scavenging effect raised proportionally to the increasing concentrations. The calculated IC_{50} of gallic acid and ascorbic acid were at 0.01 and 0.05 mg/mL, respectively, whereas much higher IC_{50} were obtained from XO from sugarcane leaf, napier grass and purple guinea grass were at 6.58, 15.61, and 14.11 mg/mL, respectively.

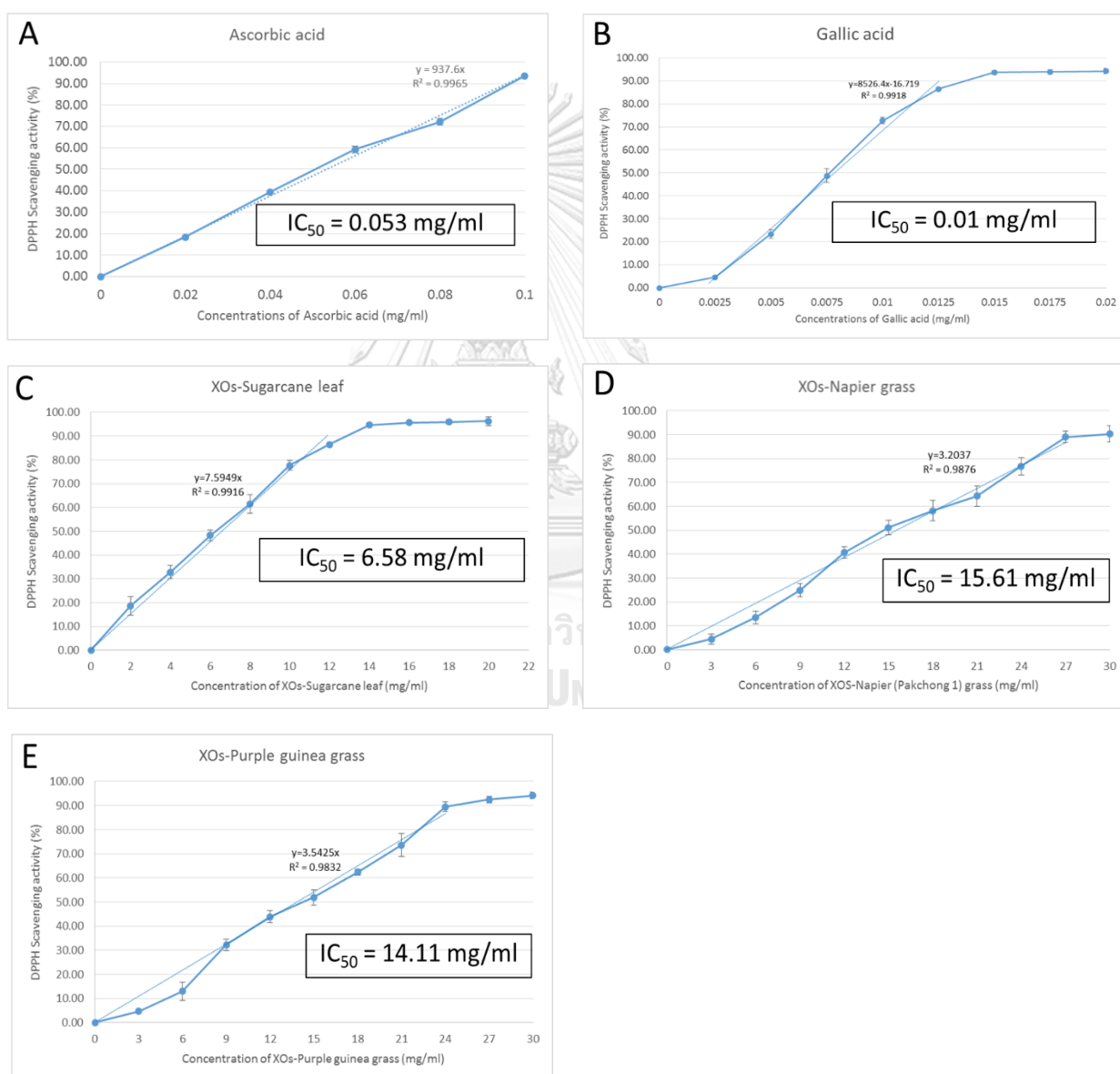


Figure 31 DPPH radical scavenging activity of: (A) gallic acid, (B) ascorbic acid, (C) XO-Sugarcane leaf, (D) XO-Napier grass and (E) XO-Purple guinea grass

4.9 Xylitol production

4.9.1 Screening of xylitol-producing yeasts

The xylitol conversion percentages of 14 *Candida* strains (Figure 32) were in the ranges from 13.67±3.17 to 52.53±3.51% for 10 *Candida tropicalis* strains, 6.42±0.47 to 6.44±0.35% for *C. glabatra* strains and 26±09 to 39±96 % for *Meyerozyma caribbica* strains. The maximal xylitol conversion percentage was detected in *C. tropicalis* FS10 at 52.53±3.51%.

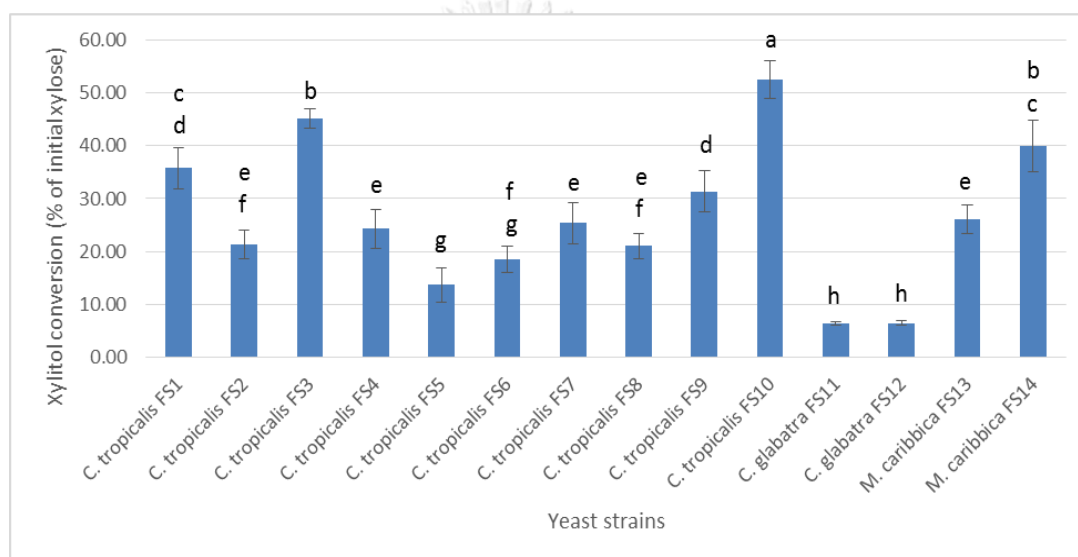


Figure 32 Xylitol conversion of 14 strains of *Candida* spp. using commercial xylose. Different letters above the bar graphs indicate significant differences according to DMRT at $p \leq 0.05$. Bar indicated standard deviation derived from three replicates

Candida tropicalis FS10 was selected for the optimization of xylitol production using factorial design with a focus on temperature and incubation time (Figure 33). The maximal conversion percentage was achieved at 35°C and 48-h incubation. Therefore, these conditions were applied for the following optimization.

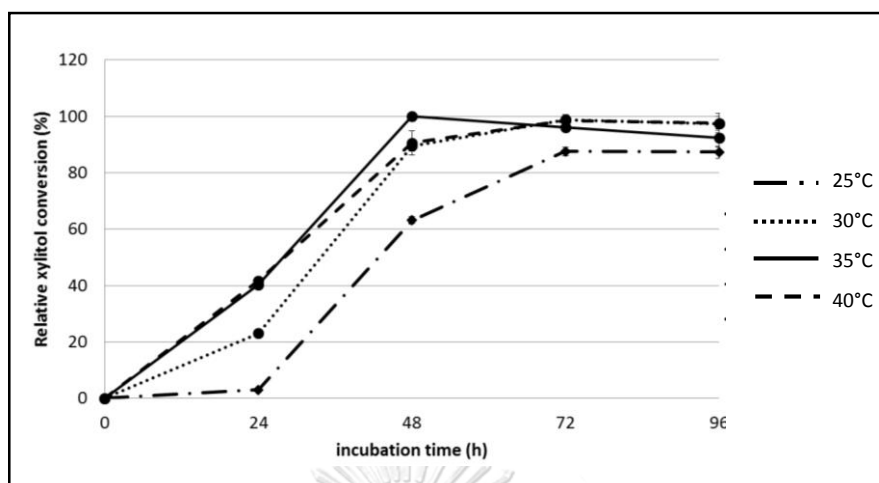


Figure 33 Effect on temperature and incubation time on xylitol production by *C. tropicalis* FS10 and The relative xylitol conversion was calculated as the percentage of the maximum xylitol conversion. Experiments were performed in triplicate and bars indicate standard deviations.

Moreover, the xylitol conversion using commercial xylose and xylose from sugarcane leaf, purple guinea grass and napier grass was produced by this selected yeast at 35°C for 48 h in medium containing 45 g/L xylose, 5 g/L glucose and 2 g/L yeast extract (Figure 34). The largest xylitol conversion ($58.75 \pm 0.80\%$) was obtained from commercial xylose following by xylose from sugarcane leaf xylan ($19.58 \pm 0.44\%$), purple guinea grass ($18.51 \pm 0.25\%$) and napier grass ($17.78 \pm 0.44\%$).

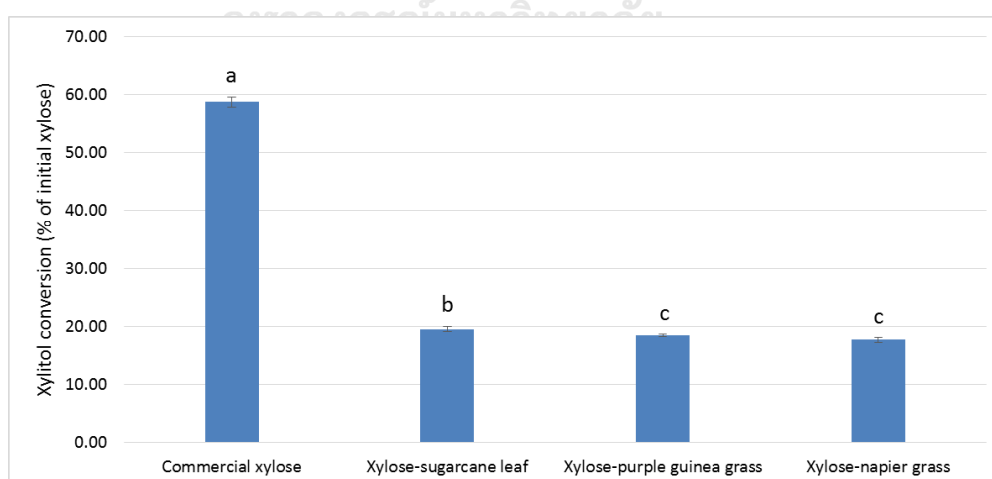


Figure 34 The percentage of xylitol conversion from commercial xylose and xylose from sugarcane leaf, purple guinea grass and napier grass. Different letters above the bar graphs indicate significant differences according to DMRT at $p \leq 0.05$. Bar indicated standard deviation derived from three replicates

4.9.2 Optimization of xylitol production

4.9.2.1 Commercial xylose

For optimization of xylitol production from commercial xylose, the response surface plots and the levels of factors and the response values were presented in Figure 35 and Table 32, respectively. The data based on a second order polynomial was expressed by following equation:

$$XL_1 = -22.05 + 0.95C_1 + 3.94C_2 + 22.24C_3 + 0.02C_1C_2 + 0.06C_1C_3 + 0.04C_2C_3 - 0.008C_1^2 - 0.50C_2^2 - 2.46C_3^2$$

Where XL_1 was xylitol conversion of commercial xylose (% of initial xylose), C_1 was xylose concentration (g/L), C_2 was glucose concentration (g/L) and C_3 was yeast extract concentration (g/L). Based on the ANOVA statistical significant model (Appendix J), the equation exhibited 97% of the observed response at R^2 value (0.97). The model was significant with $p = 0.0027$ whereas lack of fit was not significant ($p = 0.05$), suggesting that the regression model could accurately predict the response. Moreover, a low coefficient of variation (CV = 20.66%) indicated the precision and reliability of the experiments. The RSM assessment showed that the optimum condition could be achieved when adjusting 96.15 g/L xylose concentration, 6.01 g/L glucose concentration and 5.45 g/L yeast extract concentration with xylitol conversion at 89.42 % of initial xylose. Xylitol production from commercial xylose was performed under the suggested condition to confirm the prediction. The result showed that xylitol conversion at 89.15 ± 1.51 % of initial xylose ($p=0.96$) was not significantly different from the predicted value, recommended that the equations were accurate. Using this optimized condition, the xylitol conversion from commercial xylose was 1.57-fold higher than that with the unoptimized condition.

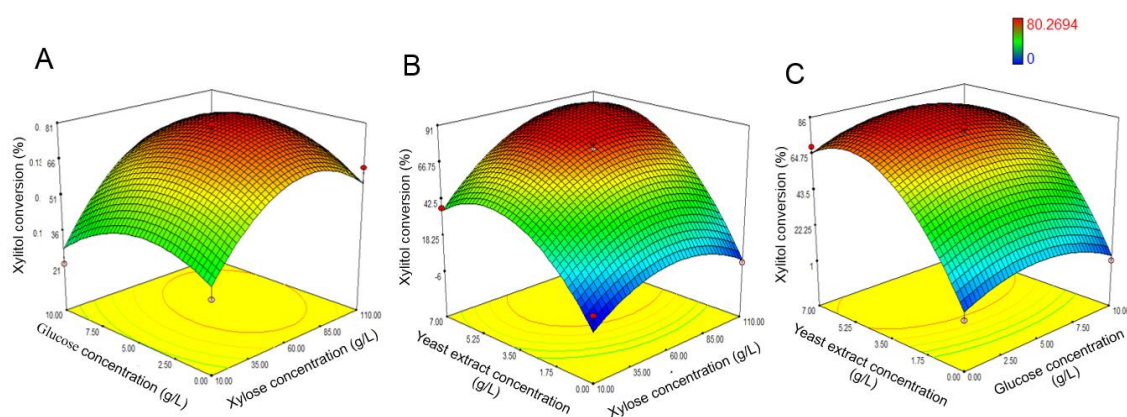


Figure 35 Response surface plots for optimal condition of xylitol conversion from commercial xylose. (A) Effect of xylose and glucose concentrations, (B) Effect of xylose and yeast extract concentrations and (C) Effect of glucose and yeast extract concentrations

Table 32 BBD and RSM predicted the percentages of xylitol conversion from commercial xylose

Run	Code level			Actual level			Xylitol conversion (%)	
	C ₁	C ₂	C ₃	Xylose concentration (g/L)	Glucose concentration (g/L)	Yeast extract concentration (g/L)	Predicted	Observed*
1	-1	-1	0	10	0	3.5	36.35	31.18±0.24
2	+1	-1	0	110	0	3.5	56.07	62.72±0.15
3	-1	+1	0	10	10	3.5	28.34	21.69±2.29
4	+1	+1	0	110	10	3.5	63.10	68.27±0.54
5	-1	0	-1	10	5	0	0.00	4.50±0.08
6	+1	0	-1	110	5	0	1.82	0.00±0.00
7	-1	0	+1	10	5	7	35.15	36.97±0.46
8	+1	0	+1	110	5	7	82.32	72.32±0.50
9	0	-1	-1	60	0	0	6.27	1.44±0.08
10	0	+1	-1	60	10	0	4.42	1.06±0.11
11	0	-1	+1	60	0	7	65.49	68.84±0.95
12	0	+1	+1	60	10	7	66.35	71.19±0.14
13	0	0	0	60	5	3.5	78.29	75.21±0.14
14	0	0	0	60	5	3.5	78.29	79.38±0.22
15	0	0	0	60	5	3.5	78.29	80.27±0.49

* Mean ± SD derived from three replicates

4.9.2.2 Xylose-sugarcane leaf

The response surface plots for xylitol production from xylose-sugarcane leaf were shown in Figure 36. BBD with 3 levels of 3 variable factors was used and the response values were presented in Table 33. The data based on a second order polynomial could be expressed by following equation:

$$XL_2 = -19.67 + 0.99C_1 + 2.73C_2 + 4.56C_3 - 0.01C_1C_2 - 0.04C_1C_3 - 0.08C_2C_3 - 0.006C_1^2 - 0.18C_2^2 - 0.16C_3^2$$

Where XL_2 was xylitol conversion of xylose-sugarcane leaf (% of initial xylose), C_1 was xylose concentration (g/L), C_2 was glucose concentration (g/L) and C_3 was yeast extract concentration (g/L). Based on the ANOVA statistical significant model (Appendix J), the equation exhibited 93% of the observed response at R^2 value (0.93). The model was significant with $p = 0.0174$ whereas lack of fit was not significant ($p = 0.12$), suggesting that the regression model could accurately predict the response. Moreover, a low coefficient of variation ($CV = 24.37\%$) indicated the precision and reliability of the experiments. The RSM assessment showed the optimum condition of a medium containing 56.69 g/L xylose concentration, 5.44 g/L glucose concentration and 4.71 g/L yeast extract concentration which could produce the xylitol with xylitol conversion efficiency at 29.28 % of initial xylose. Xylitol production from xylose-sugarcane leaf was performed under the suggested condition to confirm the prediction. The result showed that xylitol conversion at 28.78 ± 1.22 % of initial xylose ($p=0.88$) was not significantly different from the predicted value, recommended that the equations were accurate. Using this optimized condition, the xylitol conversion from xylose-sugarcane leaf was 1.47-fold higher than that with the unoptimized condition.

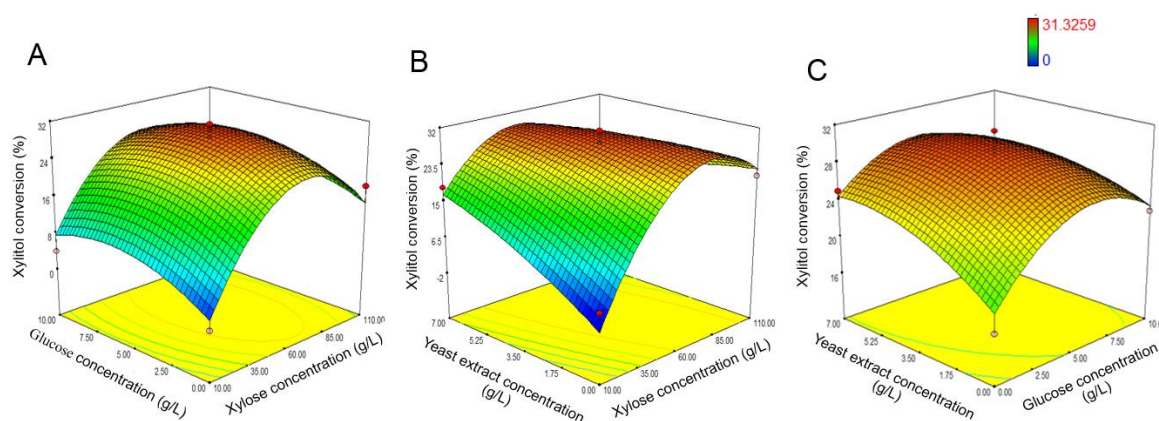


Figure 36 Response surface plots for optimal condition of xylitol conversion from xylose-sugarcane leaf. (A) Effect of xylose and glucose concentrations, (B) Effect of xylose and yeast extract concentrations and (C) Effect of glucose and yeast extract concentrations

Table 33 BBD and RSM predicted the percentages of xylitol conversion from xylose-sugarcane leaf

Run	Code level			Actual level			Xylitol conversion (%)	
	C ₁	C ₂	C ₃	Xylose concentration (g/L)	Glucose concentration (g/L)	Yeast extract concentration (g/L)	Predicted	Observed*
1	-1	-1	0	10	0	3.5	2.13	0.00±0.00
2	+1	-1	0	110	0	3.5	14.61	18.26±0.30
3	-1	+1	0	10	10	3.5	7.59	3.94±0.06
4	+1	+1	0	110	10	3.5	14.01	16.22±0.94
5	-1	0	-1	10	5	0	0.00	2.53±0.31
6	+1	0	-1	110	5	0	22.67	21.08±1.02
7	-1	0	+1	10	5	7	16.67	18.26±0.98
8	+1	0	+1	110	5	7	11.31	7.12±0.53
9	0	-1	-1	60	0	0	18.14	16.09±0.32
10	0	+1	-1	60	10	0	23.41	22.87±0.41
11	0	-1	+1	60	0	7	24.43	24.96±1.02
12	0	+1	+1	60	10	7	24.09	26.15±0.10
13	0	0	0	60	5	3.5	29.08	27.82±0.99
14	0	0	0	60	5	3.5	29.08	28.09±0.54
15	0	0	0	60	5	3.5	29.08	31.33±1.45

* Mean ± SD derived from three replicates

4.9.2.3 Xylose-purple guinea grass

For optimization of xylitol production from xylose-purple guinea grass, the response surface plots and the levels of factors and the response values were presented in Figure 37 and Table 34, respectively. The data based on a second order polynomial was expressed by following equation:

$$XL_3 = -20.27 + 0.90C_1 + 3.39C_2 + 5.68C_3 - 0.007C_1C_2 - 0.04C_1C_3 - 0.16C_2C_3 - 0.005C_1^2 - 0.22C_2^2 - 0.33C_3^2$$

Where XL_3 was xylitol conversion of xylose-purple guinea grass (% of initial xylose), C_1 was xylose concentration (g/L), C_2 was glucose concentration (g/L) and C_3 was yeast extract concentration (g/L). Based on the ANOVA statistical significant model (Appendix J), the equation exhibited 96% of the observed response at R^2 value (0.96). The model was significant with $p = 0.0064$ whereas lack of fit was not significant ($p = 0.07$), suggesting that the regression model could accurately predict the response. Moreover, a low coefficient of variation (CV = 19.73%) indicated the precision and reliability of the experiments. The RSM assessment showed the optimum condition of a medium containing 54.73 g/L xylose concentration, 5.31 g/L glucose concentration and 3.57 g/L yeast extract concentration which could produce the xylitol with xylitol conversion efficiency at 27.92 % of initial xylose. Xylitol production from xylose-purple guinea grass was performed under the suggested condition to confirm the prediction. The result showed that xylitol conversion at 26.69 ± 1.05 % of initial xylose ($p=0.56$) was not significantly different from the predicted value, recommended that the equations were accurate. Using this optimized condition, the xylitol conversion from xylose-purple guinea grass was 1.44-fold higher than that with the unoptimized condition.

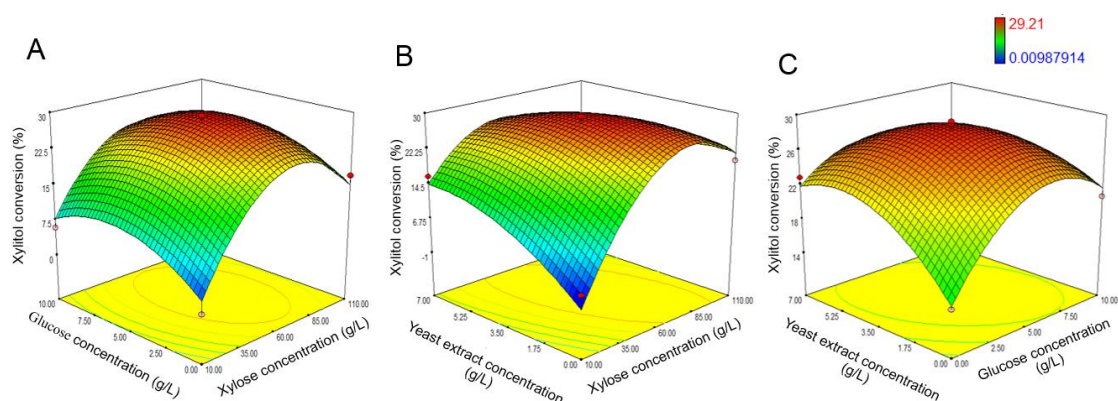


Figure 37 Response surface plots for optimal condition of xylitol conversion from xylose-purple guinea grass. (A) Effect of xylose and glucose concentrations, (B) Effect of xylose and yeast extract concentrations and (C) Effect of glucose and yeast extract concentrations

Table 34 BBD and RSM predicted the percentages of xylitol conversion from xylose-purple guinea grass

Run	Code level			Actual level			Xylitol conversion (%)	
	C ₁	C ₂	C ₃	Xylose concentration (g/L)	Glucose concentration (g/L)	Yeast extract concentration (g/L)	Predicted	Observed*
1	-1	-1	0	10	0	3.5	2.70	0.01±0.02
2	+1	-1	0	110	0	3.5	14.99	17.01±0.78
3	-1	+1	0	10	10	3.5	7.87	5.85±0.21
4	+1	+1	0	110	10	3.5	12.80	15.49±1.09
5	-1	0	-1	10	5	0	0.00	2.24±0.19
6	+1	0	-1	110	5	0	21.46	19.80±1.60
7	-1	0	+1	10	5	7	14.51	16.17±1.14
8	+1	0	+1	110	5	7	9.46	6.41±0.89
9	0	-1	-1	60	0	0	14.46	14.10±0.43
10	0	+1	-1	60	10	0	21.68	20.66±0.22
11	0	-1	+1	60	0	7	21.84	22.86±0.22
12	0	+1	+1	60	10	7	17.51	17.97±1.34
13	0	0	0	60	5	3.5	28.46	28.96±1.53
14	0	0	0	60	5	3.5	28.46	27.21±0.45
15	0	0	0	60	5	3.5	28.46	29.21±1.64

*Mean ± SD derived from three replicates

4.9.2.4 Xylose-napier grass

The response surface plots for xylitol production from xylose-napier grass were shown in Figure 38. BBD with 3 levels of 3 variable factors was used and the response values were presented in Table 35. The data based on a second order polynomial could be expressed by following equation:

$$XL_4 = -17.63 + 0.86C_1 + 2.65C_2 + 4.86C_3 - 0.005C_1C_2 - 0.04C_1C_3 - 0.12C_2C_3 - 0.005C_1^2 - 0.20C_2^2 - 0.31C_3^2$$

Where XL_4 was xylitol conversion of xylose-napier grass (% of initial xylose), C_1 was xylose concentration (g/L), C_2 was glucose concentration (g/L) and C_3 was yeast extract concentration (g/L). Based on the ANOVA statistical significant model (Appendix J), the equation exhibited 94% of the observed response at R^2 value (0.94). The model was significant with $p = 0.0149$ whereas lack of fit was not significant ($p = 0.09$), suggesting that the regression model could accurately predict the response. Moreover, a low coefficient of variation ($CV = 23.81\%$) indicated the precision and reliability of the experiments. The RSM assessment showed that the optimum condition could be achieved when adjusting 54.38 g/L xylose concentration, 5.80 g/L glucose concentration and 4.01 g/L yeast extract concentration with xylitol conversion at 27.04 % of initial xylose. Xylitol production from xylose-napier grass was performed under the suggested condition to confirm the prediction. The result showed that xylitol conversion at 24.62 ± 1.98 % of initial xylose ($p=0.37$) was not significantly different from the predicted value, recommended that the equations were accurate. Using this optimized condition, the xylitol conversion from xylose-napier grass was 1.38-fold higher than that with the unoptimized condition.

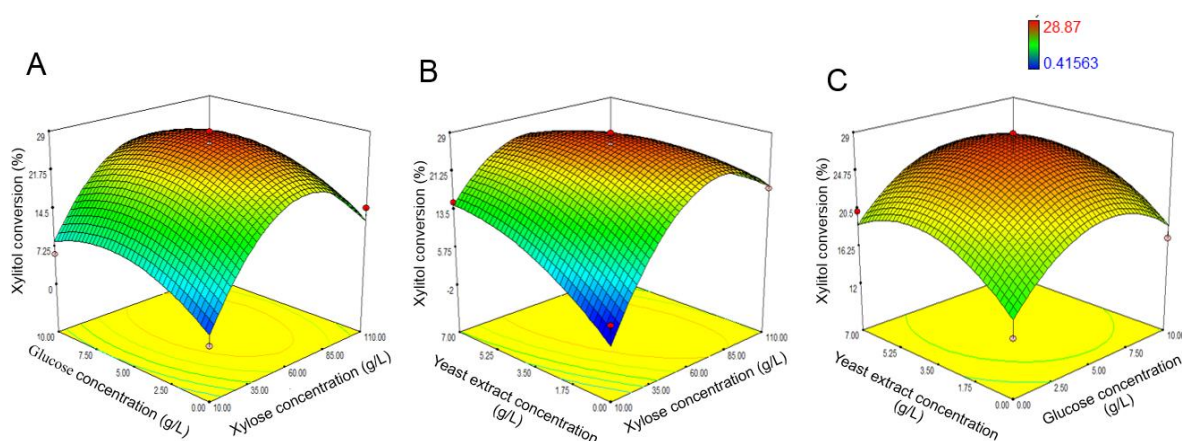


Figure 38 Response surface plots for optimal condition of xylitol conversion from xylose-napier grass. (A) Effect of xylose and glucose concentrations, (B) Effect of xylose and yeast extract concentrations and (C) Effect of glucose and yeast extract concentrations

Table 35 BBD and RSM predicted the percentages of xylitol conversion from xylose-napier grass

Run	Code level			Actual level			Xylitol conversion (%)	
	C ₁	C ₂	C ₃	Xylose concentration (g/L)	Glucose concentration (g/L)	Yeast extract concentration (g/L)	Predicted	Observed*
1	-1	-1	0	10	0	3.5	2.41	0.42±0.01
2	+1	-1	0	110	0	3.5	12.31	14.79±0.60
3	-1	+1	0	10	10	3.5	8.33	5.85±0.16
4	+1	+1	0	110	10	3.5	13.26	15.25±0.86
5	-1	0	-1	10	5	0	0.00	2.46±0.23
6	+1	0	-1	110	5	0	18.46	17.93±0.21
7	-1	0	+1	10	5	7	14.53	15.06±0.30
8	+1	0	+1	110	5	7	9.41	5.46±0.11
9	0	-1	-1	60	0	0	14.84	12.88±0.20
10	0	+1	-1	60	10	0	18.70	17.23±0.50
11	0	-1	+1	60	0	7	18.75	20.21±0.25
12	0	+1	+1	60	10	7	21.76	23.72±0.29
13	0	0	0	60	5	3.5	27.18	26.12±0.60
14	0	0	0	60	5	3.5	27.18	26.55±0.23
15	0	0	0	60	5	3.5	27.18	28.87±2.03

*Mean ± SD derived from three replicates

Chapter V

Discussion

5.1 Xylan extraction

Xylan has been reported to be extracted from hardwood, softwood and agricultural residues (Kämpfi et al., 2010; Deutschmann and Dekker, 2012; Hauli et al., 2013; Salmén, 2022). However, these biomass sources revealed a slow growth that could impact on biomass availability. Hardwoods and softwoods such as aspen, eucalyptus, beechwood, larch have been harvested in the range between 5 and 7 ton/ha (Rodriguez et al., 1997; Pastor and Bockheim, 2011; Peng et al., 2018; Muhdi et al., 2019). While, agricultural residues such as wheat straw, corn stover and corncob were harvested in the range between 1 and 7 ton/ha (Morey et al., 2010; Kafilzadeh et al., 2012; Mensah et al., 2021). Effective biomass availability could affect logistic cost and profit for large scale production (Wang et al., 2020). Comparing to grasses, they were fast growing weeds which were available throughout the year in every region with biomass availability higher than 7 ton/ha (Mohapatra, 2017). Therefore, grass-like weeds were considered to be a more attractive material for xylan extraction. According to biomass availability of grasses in Appendix B, ten grass samples in this study were selected which based on their biomass availability in the range of 12 - 46 ton/ha. They were higher than other grasses such as tropical carpet grass, whip grass, cairo grass, mission grass, communist grass, bana grass, signal grass and plicatum grass with the biomass availability in the range of 7 - 10 ton/ha.

Xylan can be extracted from biomasses by using different methods such as alkaline extraction, acid extraction, ultrasound-assisted extraction and microwave-assisted extraction (Kaur and Mankoo, 2021). In the acid extraction method, there was the releasing of furfural that inhibited the microbial activity (Akobi et al., 2017). For ultrasound and microwave-assisted extraction, these methods needed to operate in the high operation cost with modified process. Therefore, alkaline extraction was the suitable method because it was lower operation cost and structural xylan degradation (Cheng et al., 2010). Among the alkaline extraction, NaOH showed the higher solubility of xylan and it extracted the xylan with a greater degree of enzymatic hydrolysis than other alkaline extraction (Samanta et al., 2012; Modenbach and Nokes, 2014). Due to

the complex linkages of cell wall, this alkaline method assisted with steam method was applied to improve the efficiency of xylan extraction. NaOH, alkaline hydrolyzed ester linkages from biomass followed by extracting them into alkaline fraction. Steam with autoclaving softened the lignin protective network in plant biomass (Peng et al., 2012). For the xylan extraction in this study, the highest relative xylan recovery were detected in sugarcane leaf, purple guinea grass, napier grass, sabi grass and napier grass that corresponded to their hemicellulose and lignin contents (Table 17). They contained the highest ratio of hemicellulose content to lignin content.

According to ANOVA for response surface quadratic model in Appendix G, the model revealed that NaOH concentration ($p = 0.0009$), steaming time ($p = 0.0037$) and liquid-to-solid ratio ($p < 0.0001$) had significant impact on xylan recovery from sugarcane leaf. The response surface plots (Figure 13) suggested that NaOH concentration and liquid-to-solid ratio ($p = 0.0030$) and steaming time and liquid-to-solid ratio ($p = 0.0002$) showed a strong interaction effect on xylan recovery. For xylan extraction from napier grass, all 3 variables ($p < 0.0081$) exhibited a significant impact on xylan recovery. The response surface plots (Figure 14) exhibited NaOH concentration and steaming time ($p = 0.0257$) and NaOH concentration and liquid-to-solid ratio ($p = 0.0303$) to be a strong interaction effect on xylan recovery. Moreover, only liquid-to-solid ratio ($p < 0.0002$) was a significant variable on xylan recovery from purple guinea grass and vetiver grass. The interaction of NaOH concentration and liquid-to-solid ratio ($p = 0.0467$) exhibited a strong effect on xylan recovery from vetiver grass (Figure 16). For sabi grass, steaming time ($p = 0.0487$) and liquid-to-solid ratio ($p < 0.0001$) were significant variables to impact on xylan recovery. After optimization, the xylans were improved for the relative xylan recovery in the range between 88 and 99% which were higher than the previous reports by using similar extraction method with the relative xylan recovery in the range of 75-85 % from switch grass (Stoklosa and Hodge, 2012; Geng, 2018) and 69 % from vetiver grass (Patipong et al., 2019).

According to the results of sugar composition and structural analysis, the major component of xylans were (glucurono)arabinoxylan for napier grass, purple guinea grass, sabi grass and vetiver grass xylans and arabinoxylan for sugarcane leaf xylan. Similar to the previous reports, (glucurono)arabinoxylan was determined in the xylans from switch grass (Smith et al., 2017), Chinese silver grass (Tryfona et al., 2019) and stiff brome grass (Duan et al., 2021). However, there was the different xylan component of

sugarcane leaf that Morais de Carvalho et al. (2017) reported the major component of sugarcane leaf xylan as acetylated glucuronoarabinoxylan. This difference was probably occurred from the the extraction method and raw materials used (Morais de Carvalho et al., 2017; Ahmad Sobri et al., 2019).

5.2 Endoxylanase and β -xylosidase production

In the xylanases production, these enzymes could be produced by bacteria and fungi. There were limitations of the production including the cost of substrates and purification process (Nasr et al., 2013; Chakdar et al., 2016). However, *A. pullulans* has been reported as a good xylanase producer to produce the cellulose-free enzymes using the low cost substrates including agricultural wastes such as corn cobs (Leathers, 1986; Nasr et al., 2013; Bankeeree et al., 2014). Moreover, the most conditions of enzymatic xylan hydrolysis were conducted under temperature at least 50°C and pH at least 5 with a large enzyme dosage (>50 U/g substrate) (Brienzo et al., 2010; Boonchuay et al., 2014; Bankeeree et al., 2018; Wang et al., 2018; Li et al., 2020). Therefore, screening of *A. pullulans* xylanases with highly stable under incubation condition was required

For endoxylanase production in this study, the selected enzyme from *A. pullulans* NRRL 58523 exhibited the activity at 22 U/mL which was higher the previous reports on endoxylanases activity at 2 U/mL from *A. pullulans* SN 090 (Nasr et al., 2013) and 5 U/mL from *A. pullulans* CBS 135684 (Bankeeree et al., 2014). At the optimal temperature and pH of this enzyme were at 50°C and pH 4 which were similar to other fungal endoxylanases at temperature (40-60°C) and pH (pH 4-7) (Zhou et al., 2013; Sakthiselvan et al., 2014; Guan et al., 2016; Bakri et al., 2020; Otero et al., 2021). For the thermostability at optimal temperature (50°C), *A. pullulans* NRRL 58523 endoxylanase remained activity about 50% of its initial activity after 12 h which was more stable than fungal endoxylanases from *A. pullulans* CBS 135684 (Bankeeree et al., 2014), *A. flavus* (Silva et al., 2016) and *A. awamori* (Solórzano et al., 2000), remaining the activity between 35 and 60% of their initial activity after 2 to 5 h.

For the screening of β -xylosidase production, the highest enzyme activity was detected in *A. pullulans* NRRL 58559 with the optimal temperature at 70°C and pH 4. However, this enzyme exhibited lower activity and thermostability than the enzyme

previously reported for the strain CBS 135684 (Bankeeree et al., 2018). To achieve the high efficiency for enzymatic hydrolysis, this enzyme was selected for complete hydrolysis in this study. *A. pullulans* CBS135684 β -xylosidase showed the similar optimal conditions with the strain NRRL 58559 at 70 °C and pH 4. Comparing to previous report, β -xylosidases from this strain exhibited higher than *A. pullulans* CBS 58479 with the activity at 0.9 U/mg (Dobberstein and Emeis, 1991). At the optimal temperature and pH, this enzyme exhibited similar to other fungal β -xylosidase at temperature in the range of 50-75 and pH from 3.5-6 (Ohta et al., 2010; Knob and Carmona, 2012; Fanchini Terrasan et al., 2013; Zimbardi et al., 2013; Xia et al., 2015). For the thermostability at optimal temperature, *A. pullulans* CBS135684 β -xylosidase exhibited higher stability (remaining 88% of its initial activity after 12 h) than fungal β -xylosidases from *P. sclerotiorum* (Knob and Carmona, 2012), *H. insolens* (Xia et al., 2015) and *C. graminicola* (Zimbardi et al., 2013) which lost most activity at this temperature after 1 h.

Therefore, the crude xylanases from *A. pullulans* NRRL 58523 and CBS 135684 showed the promising potential for partial and complete hydrolysis.

5.3 Molecular weight, average DP and viscosity property

The molecular weight of xylans showed the large molecular weight. For the low molecular weight, it probably caused by alkaline extraction according to the previous report (Poletto et al., 2020). These differences were affected by xylan types and extraction methods that impact on xylan structure and degree of substitution (Sporck et al., 2017). The molecular weight of xylans in this study fell in wider range than previous reports from sugarcane bagasse (65,000-212,000 g/mol) (Khaleghipour et al., 2021), wheat bran (470,000-600,000 g/mol) (Koegelenberg and Chimphango, 2017) and switch grass (47,700-64,300 g/mol) (Farhat et al., 2017). For the DP and molecular weight, both of them exhibited a positive correlation. This was in accordance with the reports of Zimmermann et al. (2010), Chun et al. (2011) and Djafaripetroudy et al. (2014).

For the study of viscosity property, The viscosity was affected by molecular size and chain length (Raghee et al., 2001). In this study, the viscosity and DP values of xylans decreased with an increasing of endoxylanase loading. Enzymatic method to reduce xylan viscosity was also reported in wheat (Sorensen et al., 2006) and rye (Ravn

et al., 2016). Therefore, enzymatic method was more attractive to reduce the viscosity because it was high specific to reduce chain length with eco-friendly process and no undesirable product (Sorensen et al., 2006; Tian et al., 2020). The viscosity values were considered for the xylan applications. Xylans with higher viscosity could be applied as film/gel-like compounds for packaging films, coatings, cellular immobilizations, acoustic insulations and drug carriers (Ebringerová and Hromádková, 1999; Pääkkönen et al., 2016). At low viscosity of xylans, they were applied as food hydrocolloids and improvement of paper strength (Sedlmeyer, 2011; Cheng et al., 2018). For the low viscosity of xylans in this study, they were affected by a xylan structure which more branch or side chain of xylan exhibited lower viscosity than lower side chain or linear structure (Geng, 2018). At these viscosity ranges has been reported to be applied for the improvement of paper strengthening property and food texture (Qin et al., 2005; Cheng et al., 2018; Xu et al., 2019).

5.4 Enzymatic xylan hydrolysis

Xylan could be hydrolyzed by acid and enzymatic hydrolysis methods. In the acid hydrolysis method, there were limitations including the releasing of undesirable by product such as furfural (Sorensen et al., 2006). It could inhibit the microbial activity (Akobi et al., 2017). Comparing to enzymatic hydrolysis method, it reacted specifically and did not generate harsh, eroding condition to the equipment (Akpinar et al., 2010). Therefore, enzymatic hydrolysis method was considered for the xylan hydrolysis. Both of partial and complete hydrolysis revealed the maximum product yield in commercial beechwood xylan. Due to lignin containing in the three extracted xylans, it limited the enzyme access to xylan (Kellock et al., 2022). Among the extracted xylans, the maximal hydrolysate yield was detected in sugarcane leaf. According to the structural xylan in this study, purple guinea grass and napier grass xylan as (glucurono) arabinoxylan showed more complex components than sugarcane leaf xylan as arabionoxylan. More branching xylan structure resisted accessible enzyme to reduce the releasing of hydrolysate products (Liu et al., 2021).

For XO_s production after optimization, the three xylans yielded XO_s products including xylobiose and xylotriose in the range of between 0.11 and 0.24 g/g initial xylan under optimal conditions including endoxylanase concentration from 65 to 75 U/g

substrate and incubation time from 53 to 64 h. XOs including xylobiose and xylotriose had higher market values because they exhibited higher prebiotic properties and commercial functional food products (Guido et al., 2019). According to ANOVA for response surface quadratic model in Appendix H, the model revealed that endoxylanase concentration ($p = 0.0021$) had significant impact on XOs production from sugarcane leaf. For napier grass and purple guinea grass, enzyme concentration ($p < 0.0002$) and incubation time ($p < 0.0035$) showed significant variables for the releasing of XOs product. Comparing to the previous reports on XOs production including xylobiose and xylotriose, the products in this study showed similar yields to XOs yields at 0.18 g/g initial xylan from sehima grass (Samanta et al., 2012), 0.33 g/g initial xylan from oil palm (Siti-Normah et al., 2012), 0.11 g/g initial xylan from corncob (Boonchuay et al., 2014) and 0.13 g/g initial xylan from vetiver grass (Patipong et al., 2019)

For xylose production, the cocktail process with the mixture of endoxylanase and β -xylosidase yielded higher xylose monomer than stepwise process. In the stepwise process, endoxylanase hydrolyzes the xylan to release XOs before β -xylosidase loading. Accumulation of XOs may react as inhibitor to endoxylanase that can limit XOs yield. This consequence affects substrate volumes for hydrolysis via β -xylosidase to release xylose products. To alleviate this limitation, the cocktail enzymes lead to improve the efficiency of xylose releasing (Li et al., 2020). After optimization via the mixture of endoxylanase and β -xylosidase, the xylans yielded xylose products from 0.13 to 0.20 g/g initial xylan at endoxylanase concentration from 68 to 70 U/g substrate, β -xylosidase from 63 to 70 U/g substrate and incubation time from 17 to 18 h. According to ANOVA for response surface quadratic model in Appendix I, the model revealed that endoxylanase concentration ($p < 0.0152$), β -xylosidase concentration ($p < 0.0337$) and incubation time ($p < 0.0087$) had significant impact on xylose production from hydrolysis of 3 xylans. Comparing to the previous reports, the products in this study exhibited similar yield to xylose product at 0.15 g/g initial xylan from walnut shell (Tran et al., 2004) and 0.22 g/g initial xylan from poplar sawdust (Li et al., 2020) at endoxylanase concentration from 60 to 500 U/g substrate, β -xylosidase concentration from 10 to 100 U/g substrate and incubation time from 18 to 72 h. However, there were higher xylose yield from pistachio shell at 0.36 g/g initial xylan (Cho et al., 2002) and sugarcane bagasse at 0.46 g/g initial xylan (Martins et al., 2018) at from 10 to 3,000 U/g substrate

endoxyylanase concentration, from 16 to 33 U/g substrate β -xylosidase concentration for 72 h.

In the term of the economic value for enzymatic hydrolysis process (Appendix K), the investment cost for the production of xylanase enzymes in this study was 0.30 Bath/Unit enzyme. Moreover, the investment cost of xylan extractions were 19.15 Bath/g xylan from grass samples in this study. The investment for production cost of XOs including xylobiose and xylotriose in this study were from 0.3 to 0.6 and 0.5 to 1.6 Bath/mg, respectively. Comparing to the market price of commercial products were 780 Bath/mg of xylobiose (Sigma-aldrich, USA) and 735 Bath/mg of xylotriose (Megazyme, Ireland). For the xylose production, the production cost in this study was 0.2 bath/mg. While, the selling price of commercial xylose in the market was 74 Bath/mg (Sigma-aldrich, USA). However, the investment production in this study was estimated according to lab scale production. To apply as commercial product, investigation of further upscale production and the purification process cost should be included for the cost estimation.

5.5 Prebiotic property

According to the prebiotic properties, the produced XOs from the xylans significantly stimulated all 3 strains of *Lactobacillus* growth in a species-specific characteristic comparing to glucose. However, there was no significant prebiotic activity in *Bifidobacterium* strain. This species-specific prebiotic activity toward *Lactobacillus* spp. including *L. plantarum* S2, *L. casei* TISTR 390, *L. brevis* TISTR 868 and *L. viridiscens* NCIM 167 have been reported in XOs from corncob and vetiver grass (Samanta et al., 2012; Yu et al., 2015; Patipong et al., 2019). Moreover, Ananieva et al. (2012) investigated the utilization of commercial XOs to enhance *L. plantarum* (2 strains), *L. brevis* (3 strains) and *L. sakei* (4 strains). There was the specific growth of *L. brevis* S8, S27 and S38 which were higher than glucose. Jaichakan et al. (2021) also investigated the growth of 10 strains *Lactobacillus* spp. including *L. reuteri* KUB-AC5, *L. bulgaricus* JCM 1002, *L. lactis* KA-FF1-4, *L. johnsonii* KUNN19-2, *L. plantarum* JCM 1149T, *L. fermentum* KUB-D18, *L. crispatus* JCM 8780, *L. casei* TISTR 1340, *L. sakei* JCM 1157 and *L. brevis* TISTR 860 by using XOs from rice straw and rice husk. The result showed that the growth of *L. sakei* JCM 1157 and *L. brevis* TISTR 860 were

promoted strongly. Moreover, XOs from corncob have been reported to stimulate the growth of *L. plantarum* MTT 2621. However, they failed to enhance the growth of *B. adolescentis* NCDC 236 (Thakuria and Sheth, 2019).

Lactobacillus spp. have been reported as the major probiotic bacteria in the market, and they have been *Lactobacillus*-containing products to exhibit the potential for the prevention of diseases and diarrhea (Sniffen et al., 2018; Śliżewska and Chlebicz-Wójcik, 2020). Moreover, *Lactobacillus* spp. exhibit more stable in the gastrointestinal tract than *Bifidobacterium* spp. (Agah et al., 2019). According to the previous report on the effect of probiotic bacteria in gut of obese mice (Bubnov et al., 2017), *L. casei* IMV B-7280 exhibited the higher efficiency for decreasing cholesterol level and restoring the liver morphology, compared with *B. animalis* VKB and *B. animalis* VKL.

5.6 Antioxidant activity

XOs from the three xylans showed insignificant antioxidant activity via DPPH inhibition method with IC_{50} concentration in the range between 6.58 and 15.61 mg/mL which were higher than ascorbic acid and gallic acid. XOs from sugarcane leaf exhibited the lowest IC_{50} concentration comparing to the other two XOs. Different characteristics and efficiencies of antioxidant was depended on type of antioxidant XOs including DP, substitution and its concentration (Yu et al., 2015; Si et al., 2020). Comparing to the previous on antioxidant property of XOs via DPPH assay, the three XOs in this study showed the similar IC_{50} concentration at 11 mg/mL from wheat bran (Bian et al., 2013) and 20 mg/mL from sugarcane bagasse (Sanarat et al., 2021). Whereas, XOs from sugarcane bagasse, corncob and wheat bran showed significant antioxidant activity with IC_{50} concentration from 0.6 to 1 mg/mL (Gowdhaman and Ponnusami, 2015; Huang et al., 2020; Si et al., 2020).

5.7 Xylitol production

In the industrial scale, xylitol can be produced through chemical hydrogenation of xylose with a nickel catalyst at high temperature and pressure. This process needs to be extensive for separation and purification processes. The resultant product is very expensive. Comparing to microbial process through yeast fermentation, it is highly attractive alternatives that produce a high-quality and cost-effective product. Xylitol-

producing yeasts have been studied in the last few decades (Rafiqul and Sakinah, 2013).

In this study, the maximum xylitol conversion was obtained from commercial xylose which was higher than xylose hydrolysates from the xylans. Due to phenolic compounds as lignin containing in the hydrolysates, it influenced negatively the performance of yeast for xylitol production. These compounds reacted as toxic on the yeast in the inhibition of xylitol production (Zhang et al., 2012). For the influence of process variables: xylose, glucose and yeast extract concentrations were evaluated by RSM. For xylose concentration as the substrate to be xylitol, the increasing quantity of initial xylose concentration let to produce a higher xylitol product. However, high quantity of xylose could cause high osmotic pressure condition that inhibited the microbial growth (Ramesh et al., 2013). For the use of glucose as co-substrate, the fermentation medium containing low concentration of glucose stimulated the cell growth and affected to increase xylitol production via contribution of NADPH cofactor through HMP pathway to enhance the xylose reductase. On the other hand, the medium containing high concentration of glucose impacted on utilization of xylose because yeasts consumed glucose before xylose toward respiratory chain that caused the low efficiency of xylitol production (Horitsu et al., 1992; Tochampa et al., 2005). For yeast extraction concentration, it enhanced the growth and biomass of the yeast (Siriwattanawimolchai et al., 2013). However, high concentration of yeast extract increased NAD^+ cofactor to enhance xylitol dehydrogenase that reduced xylitol yield via conversion of xylitol to xylulose (Evans et al., 2010). After the optimization, xylitol conversion efficiency at 29% from sugarcane leaf, 27% from purple guinea grass and 25% from napier grass under optimum medium from the prediction of RSM were lower than trial run no. 15 in Table 33, no. 13-15 in Table 34 and no. 13-15 in Table 35, respectively. However, they were not significantly different. In term of investment cost, the medium under optimal conditions from three xylose hydrolysates were in the range of 12.62 – 13.16 Bath/mL which were lower than the medium in the trial runs at 13.92 Bath/mL. Therefore, xylitol production under optimum medium was suitable for actual production. Comparing to the previous reports on the xylitol production from other agricultural biomasses using *Candida* yeasts, xylitol conversion efficiency in this study showed the similar trend from corncob at 24 % of initial xylose (Arifan and Nuswantari, 2020) and sugarcane bagasse at 29 % of initial xylose (Wannawilai and

Sirisansaneeyakul, 2015). However, there were higher xylitol conversion efficiency at 46 % of initial xylose from big bluestem grass (West, 2009), 47 % of initial xylose from sugarcane bagasse (Thancharoen et al., 2016) by using activated carbon absorption and 59 % of initial xylose from wheat straw by using fed-batch condition (Canilha et al., 2008).



Chapter VI

Conclusion and prospect

In this study, grasses showed the potential source for xylan extraction by using a simple sodium hydroxide method that yielded a nearly complete xylan recovery. After optimization, the highest xylan recovery at 99.42, 95.85 and 93.49% were detected in sugarcane leaf, purple guinea grass and napier grass, respectively. From the analysis of xylan structure and sugar composition, the major xylan from sugarcane leaf was arabinoxylan, and the other grass samples were (glucurono)arabinoxylan.

For the xylanases production, the highest activity of crude endoxylanase at 22.43 U/mL was detected in *A. pullulans* NRRL 58523 with the optimal pH and temperature at pH 4 and 50 °C, respectively. endoxylanase was selected with the highest activity. While, crude β -xylosidase from the strain CBS 135684 has been reported to exhibit higher enzyme activity and stability with the optimal pH and temperature at pH 4 and 70 °C, respectively. Moreover, both crude enzymes exhibited high stability at their optimal temperature. Therefore, they were selected for enzymatic xylan hydrolysis.

For the determination of molecular weight, the three xylans exhibited the large molecular weight size. Moreover, average DP values showed the relation with molecular weight. To disrupt the xylan fragments, it was feasible method to reduce viscosity and average DP for further xylan utilization with specific application.

For enzymatic xylan hydrolysis, the partial xylan hydrolysis was investigated for XO's production at 50 °C and pH 4. The highest reducing sugar at 0.27 g/g xylan was detected in sugarcane leaf following by purple guinea grass and napier grass at 0.17 g/g xylan. For complete hydrolysis after optimization via cocktail protocol at 50 °C and pH 4, the xylose yields at 0.20, 0.17 and 0.13 g/g xylan were detected in sugarcane leaf, purple guinea grass and napier grass, respectively.

For prebiotic and antioxidant properties, the produced XO's from three xylans showed species –specific prebiotic activity toward *Lactobacillus* spp., which they have high potential in functional food products. The result showed that three strains of *Lactobacillus* spp. could be enhanced by three produced XO's, whereas they failed to stimulate the growth of three *Bifidobacterium* strains. For antioxidant property, there was insignificant antioxidant activity from three produced XO's via DPPH assay.

Among 14 strains of xylitol-producing yeasts, *C. tropicalis* FS10 was selected for optimization of xylitol production under optimal temperature at 35 °C and 48-h incubation time. Under optimal production medium, The highest xylitol conversion efficiency at 89.15 % of initial xylose was detected in the medium containing commercial xylose. For the hydrolysates from three xylans, sugarcane leaf, purple guinea grass and napier grass yielded the xylitol product with conversion efficiency at 28.78, 26.69 and 24.62 % of initial xylose, respectively.

For the perspective study, the investigation of XO_s, xylose and xylitol production in this study will be further pursued to study the upscale optimization for enhancement of sugar products from grass biomasses and the purification process for investigation of human clinical trial for food product application.



REFERENCES

- Aditya, S., Srinivasan, R., Brooks, J. and Sharma, C. 2015. *In vitro* prebiotic bacterial growth properties of xylooligosaccharides produced by autohydrolysis of corn fiber. *International Journal of Poultry Science* 14: 305-311
- Agah, S., et al. 2019. More protection of *Lactobacillus acidophilus* than *Bifidobacterium bifidum* probiotics on azoxymethane-induced mouse colon cancer. *Probiotics Antimicrob Proteins* 11: 857-864
- Ahmad Sobri, N., Harun, S., Ishak, N. S., Jahim, J. and Mohammad, A. 2019. Enhancement of high xylan recovery from black liquor of alkaline pretreated oil palm frond and its physicochemical properties. *Bioresources* 14: 5400-5421
- Akobi, C., Hafez, H. and Nakhla, G. 2017. Impact of furfural on biological hydrogen production kinetics from synthetic lignocellulosic hydrolysate using mesophilic and thermophilic mixed cultures. *International Journal of Hydrogen Energy* 42: 12157-12172
- Akpinar, O., Erdoğ̃an-Tokatlı, K., Bakir, U. and Yilmaz, L. 2010. Comparison of acid and enzymatic hydrolysis of tobacco stalk xylan for preparation of xylooligosaccharides. *LWT - Food Science and Technology* 43: 119-125
- Akpinar, O., Erdogan, K. and Bostanci, S. 2009. Enzymatic production of xylooligosaccharide from selected agricultural wastes. *Food and Bioproducts Processing* 87: 145-151
- Amadou, I., Amza, T., Shi, Y. and Le, G. 2011. Chemical analysis and antioxidant properties of foxtail millet bran extracts. *Songklanakarın Journal of Science and Technology* 35: 509-515
- Anand, A., Kumar, V. and Satyanarayana, T. 2012. Characteristics of thermostable endoxylanase and β -xylosidase of the extremely thermophilic bacterium *Geobacillus thermodenitrificans* TSAA1 and its applicability in generating xylooligosaccharides and xylose from agro-residues. *Extremophiles* 17: 357-366
- Ananieva, M., Mandadzhieva, T., Stojanovski, S., Iliev, I. and Ivanova, I. 2012. Utilization of xylooligosaccharides from different *Lactobacillus* strains. *Journal of BioScience and Biotechnology* SE/ONLINE: 147-150
- Arifan, F. and Nuswantari, S. 2020. The xylitol production efficiency from corn cob waste

- by using stirred tank bioreactor-tubular loop liquid emulsion membrane (LEM).
IOP Conference Series: Earth and Environmental Science 448: 012023
- Atlas, R. M. (1993). *Handbook of micrological media*. Boca Raton, CRC Press
- Bai, L., Hu, H. and Xu, J. 2012. Influences of configuration and molecular weight of hemicelluloses on their paper-strengthening effects. *Carbohydrate Polymers* 88: 1258-1263
- Bailey, M. J., Biely, P. and Poutanen, K. 1992. Interlaboratory testing of methods for assay of xylanase activity. *Journal of Biotechnology* 23: 257-270
- Bakri, Y., Akeed, Y., Jawhar, M. and Arabi, M. 2020. Evaluation of xylanase production from filamentous fungi with different lifestyles *Acta Alimentaria* 49: 197-203
- Banka, A., Komolwanich, T. and Wongkasemjit, S. 2014. Potential Thai grasses for bioethanol production. *Cellulose* 22: 9-29
- Bankeeree, W., Akada, R., Lotrakul, P., Punnapayak, H. and Prasongsuk, S. 2018. Enzymatic hydrolysis of black liquor xylan by a novel xylose-tolerant, thermostable β -xylosidase from a tropical strain of *Aureobasidium pullulans* CBS 135684. *Applied Biochemistry and Biotechnology* 184: 919-934
- Bankeeree, W., et al. 2014. Effect of polyols on thermostability of xylanase from a tropical isolate of *Aureobasidium pullulans* and its application in prebleaching of rice straw pulp. *Springerplus* 3: 37
- Bankeeree, W., Lotrakul, P., Prasongsuk, S., Kim, S. and Punnapayak, H. 2016. Enhanced production of cellulase-free thermoactive xylanase using corncob by a black yeast, *Aureobasidium pullulans* CBS 135684. *Korean Chemical Engineering Research* 54: 822-829
- Beg, Q., Kapoor, M., Mahajan, L. and Hoondal, G. S. 2001. Microbial xylanases and their industrial applications: A review. *Applied Microbiology and Biotechnology* 56: 326-338
- Benassi, V., Coutinho de Lucas, R., Jorge, J. and Polizeli, M. d. L. 2014. Screening of thermotolerant and thermophilic fungi aiming β -xylosidase and arabinanase production. *Brazilian journal of microbiology* 45: 1459-1467
- Bhalla, A., Bischoff, K. and Sani, R. 2014. Highly thermostable GH39 β -xylosidase from a *Geobacillus* sp. strain WSUCF1. *BMC biotechnology* 14: 106
- Bian, J., et al. 2013. Structural features and antioxidant activity of xylooligosaccharides enzymatically produced from sugarcane bagasse. *Bioresource Technology*

127: 236-241

- Bian, J., Peng, F., Xu, F., Sun, R.-C. and Kennedy, J. F. 2010. Fractional isolation and structural characterization of hemicelluloses from *Caragana korshinskii*. *Carbohydrate Polymers* 80: 753-760
- Boonchuay, P., Techapun, C., Seesuriyachan, P. and Chaiyaso, T. 2014. Production of xylooligosaccharides from corncob using a crude thermostable endo-xylanase from *Streptomyces thermovulgaris* TISTR1948 and prebiotic properties. *Food Science and Biotechnology* 23: 1515-1523
- Brienzo, M., Carvalho, W. and Milagres, A. M. F. 2010. Xylooligosaccharides production from alkali-pretreated sugarcane bagasse using xylanases from *Thermoascus aurantiacus*. *Applied Biochemistry and Biotechnology* 162: 1195-1205
- Broeckx, G., et al. 2019. Effects of initial cell concentration, growth phase, and process parameters on the viability of *Lactobacillus rhamnosus* GG after spray drying. *Drying Technology* 38: 1-19
- Bubnov, R. V., et al. 2017. Comparative study of probiotic effects of *Lactobacillus* and *Bifidobacteria* strains on cholesterol levels, liver morphology and the gut microbiota in obese mice. *EPMA Journal* 8: 357-376
- Buthelezi, S. P., Olaniran, A. O. and Pillay, B. 2011. Sawdust and digestive bran as cheap alternate substrates for xylanase production. *African Journal of Microbiology Research* 5: 742-752
- Canilha, L., Carvalho, W., Felipe, M. and de Almeida e Silva, J. 2008. Xylitol production from wheat straw hemicellulosic hydrolysate: Hydrolysate detoxification and carbon source used for inoculum preparation. *Brazilian Journal of Microbiology* 39: 333-336
- Carvalho, A. F. A., Neto, P. d. O., da Silva, D. F. and Pastore, G. M. 2013. Xylooligosaccharides from lignocellulosic materials: chemical structure, health benefits and production by chemical and enzymatic hydrolysis. *Food Research International* 51: 75-85
- Carvalho, D. M., et al. 2015. Assessment of chemical transformations in eucalyptus, sugarcane bagasse and straw during hydrothermal, dilute acid, and alkaline pretreatments. *Industrial Crops and Products* 73: 118-126
- Chakdar, H., et al. 2016. Bacterial xylanases: biology to biotechnology. *3 Biotech* 6: 150
- Chantorn, S., et al. 2016. Suitable conditions for xylanases activities from *Bacillus* sp.

- GA2(1) and *Bacillus* sp. GA1(6) and their properties for agricultural residues hydrolysis. *Songklanakarin Journal of Science and Technology* 38: 177-182
- Chapla, D., Pandit, P. and Shah, A. 2012. Production of xylooligosaccharides from corncob xylan by fungal xylanase and their utilization by probiotics. *Bioresource Technology* 115: 215-221
- Chen, M.-H., et al. 2016. *Miscanthus* × *giganteus* xylooligosaccharides: Purification and fermentation. *Carbohydrate Polymers* 140: 96-103
- Chen, X., Jiang, Z., Chen, S. and Qin, W. 2010. Microbial and bioconversion production of D-xylitol and its detection and application. *International Journal of Biological Sciences* 6: 834-844
- Cheng, H., Ford, C., Kolpak, F. and Wu, Q. 2018. Preparation and characterization of xylan derivatives and their blends. *Journal of Polymers and the Environment* 26: 1-10
- Cheng, H., Zhan, H., FU, S. and Lucia, L. A. 2010. Alkali extraction of hemicellulose from depithed corn stover and effects on soda-aq pulping. *BioResources* 11: 196-206
- Cho, C., Hatsu, M. and Takamizawa, K. 2002. The production of D-xylose by enzymatic hydrolysis of agricultural wastes. *Water Science and Technology : A Journal of The International Association on Water Pollution Research* 45: 97-102
- Choojit, S., Kamesak, P., Rayayoi, S. and Saikaew, S. 2017. Statistical optimization for alkali extraction of xylan from sugarcane bagasse by surface response methodology. *International Journal of Advanced Research in Science, Engineering and Technology* 6: 42-47
- Christov, L. P., Myburgh, J., van Tonder, A. and Prior, B. A. 1997. Hydrolysis of extracted and fibre-bound xylan with *Aureobasidium pullulans* enzymes. *Journal of Biotechnology* 55: 21-29
- Chun, S.-J., Lee, S., Doh, G.-H., Lee, S. and Kim, J. 2011. Preparation of ultra-strength nanopaper using cellulose nanofibrils *Journal of Industrial and Engineering Chemistry* 17: 521-526
- Collins, T., Gerday, C. and Feller, G. 2005. Xylanases, xylanase families and extremophilic xylanases. *FEMS Microbiology Reviews* 29: 3-23
- Coman, G. and Bahrim, G. 2011. Optimization of xylanase production by *Streptomyces* sp. P12-137 using response surface methodology and central composite design. *Annals of Microbiology* 61: 773-779

- Cooke, W. B. 1959. An ecological life history of *Aureobasidium pullulans* (De Bary) Arnaud. *Mycopathologia et mycologia applicata* 12: 1-45
- Corrêa, J. M., et al. 2016. High levels of β -xylosidase in *Thermomyces lanuginosus*: potential use for saccharification. *Brazilian Journal of Microbiology* 47: 680-690
- de Hoog, G. S. 1993. Evolution of black yeasts: possible adaptation to the human host. *Antonie van Leeuwenhoek* 63: 105-109
- De Man, J., Rogosa, M. A. and Sharpe, M. 2008. A medium for the cultivation of lactobacilli. *Journal of Applied Microbiology* 23: 130-135
- Deutschmann, R. and Dekker, R. F. 2012. From plant biomass to bio-based chemicals: latest developments in xylan research. *Biotechnology Advance* 30: 1627-40
- Devi, S., Dwivedi, D. and Bhatt, A. K. 2022. Utilization of agroresidues for the production of xylanase by *Bacillus safensis* XPS7 and optimization of production parameters. *Fermentation* 8: 221-238
- Djafaripetroudy, S., Ghasemian, A., Resalati, H., Syverud, K. and Chinga Carrasco, G. 2014. The effect of xylan on the fibrillation efficiency of DED bleached soda bagasse pulp and on nanopaper characteristics. *Cellulose* 22: 385-395
- Dobberstein, J. and Emeis, C. C. 1991. Purification and characterization of β -xylosidase from *Aureobasidium pullulans*. *Applied Microbiology and Biotechnology* 35: 210-215
- Du, J., Liu, P., Liu, Z.-h., Sun, D.-g. and Tao, C.-y. 2010. Fast pyrolysis of biomass for bio-oil with ionic liquid and microwave irradiation. *Journal of Fuel Chemistry and Technology* 38: 554-559
- Duan, J., et al. 2019. Investigation into electrospinning water-soluble xylan: developing applications from highly absorbent and hydrophilic surfaces to carbonized fiber. *Cellulose* 26: 413-427
- Duan, P., et al. 2021. Xylan structure and dynamics in native *Brachypodium* grass cell walls investigated by solid-state NMR spectroscopy. *ACS Omega* 6: 15460-15471
- Ebringerová, A. and Hromádková, Z. 1999. Xylans of industrial and biomedical importance. *Journal of Genetic Engineering and Biotechnology* 16: 325-346
- Ebringerová, A. 2006. Structural diversity and application potential of hemicelluloses. *Macromolecular Symposia* 232: 1-12
- Evans, C., et al. 2010. NAD⁺ metabolite levels as a function of vitamins and calorie

- restriction: Evidence for different mechanisms of longevity. *BMC chemical biology* 10: 2-12
- Falck, P., Linares-Pastén, J. A., Adlercreutz, P. and Karlsson, E. N. 2015. Characterization of a family 43 β -xylosidase from the xylooligosaccharide utilizing putative probiotic *Weissella* sp. strain 92. *Glycobiology* 26: 193-202
- Fanchini Terrasan, C. R., Temer, B., Sarto, C., da Silva Júnior, F. and Carmona, E. 2013. Xylanase and β -xylosidase from *Penicillium janczewskii*: Production, physico-chemical properties, and application of the crude extract to pulp biobleaching. *BioResources* 8: 1292-1305
- Farhat, W., et al. 2017. Hemicellulose extraction and characterization for applications in paper coatings and adhesives. *Industrial Crops and Products* 107: 370-377
- Faryar, R., et al. 2015. Production of prebiotic xylooligosaccharides from alkaline extracted wheat straw using the K80R-variant of a thermostable alkali-tolerant xylanase. *Food and Bioproducts Processing* 93: 1-10
- Geng, A., Wang, H., Wu, J., Xie, R. and Sun, J. 2017. Characterization of a β -Xylosidase from *Clostridium clariflavum* and its application in xylan hydrolysis. *BioResources* 12: 9253-9262
- Geng, W. 2018. Effect of delignification on hemicellulose extraction from switchgrass, poplar, and pine and its effect on enzymatic convertibility of cellulose-rich residues. *Bioresources* 13: 4946-4963
- Goering, H. K. and Van Soest, P. J. (1970). Forage fiber analysis (apparatus, reagent, producers and some applications). Washington DC, Agriculture Research Service USDA
- Govender, L., Naidoo, L. and Setati, M. 2009. Isolation of hydrolase producing bacteria from Sua Pan solar salterns and the production of endo-1, 4- β -xylanase from a newly isolated haloalkaliphilic *Nesterenkonia* sp. *African Journal of Biotechnology* 8: 5458-5466
- Gowdhaman, D. and Ponnusami, V. 2015. Production and optimization of xylooligosaccharides from corncob by *Bacillus aerophilus* KGJ2 xylanase and its antioxidant potential. *International Journal of Biological Macromolecules* 79: 595-600
- Guan, G. Q., et al. 2016. Production and partial characterization of an alkaline xylanase from a novel fungus *Cladosporium oxysporum*. *BioMed Research International*

2016: 4575024

- Guido, E. S., Silveira, J. and Kalil, S. J. 2019. Enzymatic production of xylooligosaccharides from beechwood xylan: effect of xylanase preparation on carbohydrate profile of the hydrolysates. *International Food Research Journal* 26: 713-721
- Gullón Estévez, P., et al. 2008. Assessment on the fermentability of xylooligosaccharides from rice husks by probiotic bacteria. *Journal of Agricultural and Food Chemistry* 56: 7482-7487
- Haqiqi, M. T., et al. 2021. Antioxidant and UV-blocking properties of a carboxymethyl cellulose–lignin composite film produced from oil palm empty fruit bunch. *ACS Omega* 6: 9653-9666
- Hauli, I., Sarkar, B., Mukherjee, T., Chattopadhyay, A. and Mukhopadhyay, S. K. 2013. Alkaline extraction of xylan from agricultural waste, for the cost effective production of xylooligosaccharides, using thermoalkaline xylanase of thermophilic *Anoxybacillus* sp. Ip-C. *International Journal of Pure and Applied Bioscience* 1: 126-131
- Heinze, S., et al. 2017. Identification of endoxylanase XynE from *Clostridium thermocellum* as the first xylanase of glycoside hydrolase family GH141. *Scientific Reports* 7: 11178
- Ho, D. P., Ngo, H. H. and Guo, W. 2014. A mini review on renewable sources for biofuel. *Bioresource Technology* 169: 742-749
- Hood, E. E., Nelson, P. and Powell, R. (2011). Plant biomass conversion. Oxford, John Wiley & Sons Inc.
- Horitsu, H., et al. 1992. Production of xylitol from D-xylose by *Candida tropicalis*: optimization of production rate. *Biotechnology and Bioengineering* 40: 1085-1091
- Hrůzová, K., et al. 2020. Second-generation biofuel production from the marine filter feeder *Ciona intestinalis*. *ACS Sustainable Chemistry and Engineering* 8: 8373-8380
- Huang, C., et al. 2020. Production performances and antioxidant activities of laying hens fed *Aspergillus oryzae* and phytase co-fermented wheat bran. *Asian-Australasian Journal of Animal Sciences* 34: 371-384
- Ja'afaru, M. 2013. Screening of fungi isolated from environmental samples for xylanase

- and cellulase production. *ISRN Microbiology* 2013: 283423
- Jaichakan, P., et al. 2021. Two-stage processing for xylooligosaccharide recovery from rice by-products and evaluation of products: Promotion of lactic acid-producing bacterial growth and food application in a high-pressure process. *Food Research International* 147: 110529
- Jain, I., Kumar, V. and Satyanarayana, T. 2015. Xylooligosaccharides: An economical prebiotic from agroresidues and their health benefits. *Indian Journal of Experimental Biology* 53: 131-142
- Jang, M. and Kim, M. D. 2011. β -1,4-Xylosidase activity of *leuconostoc* lactic acid bacteria isolated from kimchi. *Korean Journal of Food Science and Technology* 43: 169-175
- Jayathilake, C., Rizliya, V. and Liyanage, R. 2016. Antioxidant and free radical scavenging capacity of extensively used medicinal plants in Sri Lanka. *Procedia Food Science* 6: 123-126
- Kačuráková, M., et al. 1999. Characterisation of xylan-type polysaccharides and associated cell wall components by FT-IR and FT-Raman spectroscopies. *Food Hydrocolloids* 13: 35-41
- Kafilzadeh, F., Heidari, N. and Bahraminejad, S. 2012. Variety effect on composition, kinetics of fermentation and *in vitro* digestibility of oat (*Avena sativa* L.) straw and its neutral detergent fibre. *South African Journal Of Animal Science* 42: 406-415
- Kamoga, O. L., Byaruhanga, J. K. and Kirabira, J. B. 2013. A review on pulp manufacture from non wood plant materials. *International Journal of Chemical Engineering and Applications* 4: 144-148
- Kämpfi, R., Leponiemi, A., Höhammer, H. and van Heiningen, A. 2010. Pre-extraction and PSAQ pulping of Siberian larch. *PAPTAC 95th Annual Meeting* 25: 255-259
- Kanjanapruthipong, J. 2006. Dairy herd management. *Publisher* www. puechkaset.com/ หน้าชนน: Accessed 18 October 2022
- Karni, M., Deopurkar, R. L. and Rale, V. B. 1993. β -Xylanase production by *Aureobasidium pullulans* grown on sugars agricultural residues. *World Journal of Microbiology and Biotechnology* 9: 476-478
- Kaur, P. and Mankoo, R. K. 2021. Optimization of xylan extraction process from rice straw for production of autohydrolysates rich in prebiotic xylooligosaccharides

Cellulose Chemistry and Technology 55: 1001-1017

- Kaur, R., Uppal, S. K. and Sharma, P. 2019. Production of xylooligosaccharides from sugarcane bagasse and evaluation of their prebiotic potency in vitro. *Waste Biomass Valori* 10: 2627-2635
- Kellock, M., et al. 2022. Inhibitory effect of lignin on the hydrolysis of xylan by thermophilic and thermolabile GH11 xylanases. *Biotechnology for Biofuels and Bioproducts* 15: 49
- Khaleghipour, L., et al. 2021. Extraction of sugarcane bagasse arabinoxylan, integrated with enzymatic production of xylo-oligosaccharides and separation of cellulose. *Biotechnol Biofuels* 14: 153-172
- Khasin, A., Alchanati, I. and Shoham, Y. 1993. Purification and characterization of a thermostable xylanase from *Bacillus stearothermophilus* T-6. *Applied and Environmental Microbiology* 59: 1725-1730
- Khat-udomkiri, N., et al. 2018. Optimization of alkaline pretreatment and enzymatic hydrolysis for the extraction of xylooligosaccharide from rice husk. *AMB express* 8: 115
- Kholis, M., Yopi, Y. and Meryandini, A. 2015. Xylooligosaccharide production from tobacco stalk xylan using xylanase *Streptomyces* sp. BO 3.2. *Makara Journal of Science* 19: 49-54
- Kim, J., Park, J., Jang, S. and Ha, S. 2015. Enhanced xylitol production by mutant *Kluyveromyces marxianus* 36907-FMEL1 due to improved xylose reductase activity. *Applied Biochemistry and Biotechnology* 176: 1975-1984
- Knob, A. and Carmona, E. C. 2012. Purification and properties of an acid β -xylosidase from *Penicillium sclerotiorum*. *Annals of Microbiology* 62: 501-508
- Ko, B. S., Kim, J. and Kim, J. H. 2006. Production of xylitol from d-xylose by a xylitol dehydrogenase gene-disrupted mutant of *Candida tropicalis*. *Applied and Environmental Microbiology* 72: 4207-4213
- Koegelenberg, D. and Chimphango, A. F. A. 2017. Effects of wheat-bran arabinoxylan as partial flour replacer on bread properties. *Food Chemistry* 221: 1606-1613
- Kucharska, K., Stupek, E., Cieślński, H. and Kamiński, M. 2020. Advantageous conditions of saccharification of lignocellulosic biomass for biofuels generation via fermentation processes. *Chemical Papers* 74: 1199-1209
- Kumar, P., Barrett, M. P., Delwiche, M. J. and Stroeve, P. 2009. Methods for pretreatment

- of lignocellulosic biomass for efficient hydrolysis and biofuel production. *Industrial and Engineering Chemistry Research* 48: 3713–3729
- Kumari, D. and Singh, R. 2022. Rice straw structure changes following green pretreatment with petha wastewater for economically viable bioethanol production. *Scientific Reports* 12: 10443
- Kundu, D. and Banerjee, T. 2019. Carboxymethyl cellulose–xylan hydrogel: Synthesis, characterization, and in vitro Release of vitamin B 12. *ACS Omega* 4: 4793-4803
- Kurrataa'Yun, Yopi and Meryandini, A. 2015. Characterization of xylanase activity produced by *Paenibacillus* sp. XJ18 from TNBD Jambi, Indonesia. *HAYATI Journal of Biosciences* 22: 20-26
- Leathers, T. D. 1986. Color variants of *Aureobasidium pullulans* overproduce xylanase with extremely high specific activity. *Applied and Environmental Microbiology* 52: 1026-1030
- Leathers, T. D., Kurtzman, C. P. and Detroy, R. W. 1984. Overproduction and regulation of xylanase in *Aureobasidium pullulans* and *Cryptococcus albidus*. *Biotechnology and Bioengineering Symposium* 14: 225-240
- Li, Q., Jiang, Y., Tong, X., Zhao, L. and Pei, J. 2020. Co-production of xylooligosaccharides and xylose from poplar sawdust by recombinant endo-1,4- β -xylanase and β -xylosidase mixture hydrolysis. *Frontiers in Bioengineering and Biotechnology* 8: 637397
- Li, Q., et al. 2018. Characterization of a novel thermostable and xylose-tolerant GH 39 β -xylosidase from *Dictyoglomus thermophilum*. *BMC Biotechnology* 18: 29-40
- Liang, Y. Y., Halis, R., Lai, O. M. and Mohamed, R. 2012. Conversion of lignocellulosic biomass from grass to bioethanol using materials pretreated with alkali and the white rot fungus, *Phanerochaete chrysosporium*. *Bioresources* 7: 5500-5513
- Liu, J., Liu, Z., Chi, Z., Zhang, L. and Zhang, D. 2009. Intraspecific diversity of *Aureobasidium pullulans* strains from different marine environments. *Journal of Ocean University of China* 8: 241-246
- Liu, J., Sun, D., Zhu, J., Liu, C. and Liu, W. 2021. Carbohydrate-binding modules targeting branched polysaccharides: overcoming side-chain recalcitrance in a non-catalytic approach. *Bioresources and Bioprocessing* 8: 28-39
- Lotrakul, P., Deenarn, P., Prasongsuk, S. and Punnapayak, H. 2009. Isolation of

- Aureobasidium pullulans* from bathroom surfaces and their antifungal activity against some Aspergilli. *African Journal of Microbiology Research* 3: 253-257
- Mafuleka, S. and Kana, E. B. G. 2015. Modelling and optimization of xylose and glucose production from napier grass using hybrid pre-treatment techniques. *Biomass and Bioenergy* 77: 200-208
- Mahmoudi, F., Miloud, H., Bettache, G. and Mebrouk, K. 2013. Identification and physiological properties of *Bifidobacterium* strains isolated from different origin. *Journal of Food Science and Engineering* 3: 196-206
- Mäkeläinen, H., Saarinen, M., Stowell, J., Rautonen, N. and Ouwehand, A. C. 2010. Xylo-oligosaccharides and lactitol promote the growth of *Bifidobacterium lactis* and *Lactobacillus* species in pure cultures. *Beneficial Microbes* 1: 139-48
- Manitchotpisit, P., et al. 2009. Multilocus phylogenetic analyses, pullulan production and xylanase activity of tropical isolates of *Aureobasidium pullulans*. *Mycological Research* 113: 1107-1120
- Mansor, A. M., Lim, J. S., Ani, F., Hashim, H. and Ho, W. S. 2019. Characteristics of cellulose, hemicellulose and lignin of MD2 pineapple biomass. *Chemical Engineering Transactions* 72: 79-84
- Mardawati, E., Kresnowati, P., Purwadi, R., Bindar, Y. and Setiadi, T. 2018. Fungal production of xylanase from oil palm empty fruit bunches via solid state cultivation. *International Journal on Advanced Science, Engineering and Information Technology* 8: 2539-2546
- Maria, A., Margarita, T., Iliev, I. and Ivanova, I. 2014. Gene expression of enzymes involved in utilization of xylooligosaccharides by *Lactobacillus* strains. *Biotechnology and Biotechnological Equipment* 28: 941-948
- Martins, D., Oliveira, O. M. M. F., Gomes, E. and Da Silva, R. 2005. Use of sugarcane bagasse and grass hydrolysates as carbon sources for xylanase production by *Bacillus circulans* D1 in submerged fermentation. *Process Biochemistry* 40: 3653-3659
- Martins, M., et al. 2018. The β -xylosidase from *Ceratocystis fimbriata* RM35 improves the saccharification of sugarcane bagasse. *Biocatalysis and Agricultural Biotechnology* 13: 291-298
- Mensah, M. B., Jumpah, H., Boadi, N. O. and Awudza, J. A. M. 2021. Assessment of quantities and composition of corn stover in Ghana and their conversion into

- bioethanol. *Scientific African* 12: e00731
- Mesquita, A., et al. 2017. Metabolism and physiology of Lactobacilli: a review. *Journal of Environmental Analysis and Progress* 2: 125-136
- Mhetras, N., Liddell, S. and Gokhale, D. 2016. Purification and characterization of an extracellular β -xylosidase from *Pseudozyma hubeiensis* NCIM 3574 (PhXyl), an unexplored yeast. *AMB Express* 6: 73-84
- Michelin, M., et al. 2012. Xylanase and beta-xylosidase production by *Aspergillus ochraceus*: new perspectives for the application of wheat straw autohydrolysis liquor. *Applied Biochemistry and Biotechnology* 166: 336-47
- Miller, G. L. 1959. Use of dinitrosalicylic acid reagent for determination of reducing sugar. *Analytical Chemistry* 31: 426-428
- Miret, C., Chazara, P., Montastruc, L., Negny, S. and Domenech, S. 2016. Design of bioethanol green supply chain: Comparison between first and second generation biomass concerning economic, environmental and social criteria. *Computers and Chemical Engineering* 85: 16-35
- Miyazaki, K., Hirase, T., Kojima, Y. and Flint, H. J. 2005. Medium- to large-sized xylo-oligosaccharides are responsible for xylanase induction in *Prevotella bryantii* B₄. *Microbiology* 151: 4121-4125
- Mmango-Kaseke, Z., Okaiyeto, K., Nwodo, U., Mabinya, L. and Okoh, A. 2016. Optimization of cellulase and xylanase production by *Micrococcus* species under submerged fermentation. *Sustainability* 8: 1168-1183
- Modenbach, A. A. and Nokes, S. 2014. Effects of sodium hydroxide pretreatment on structural components of biomass. *American Society of Agricultural and Biological Engineers* 57: 1187-1198
- Mohamad, N. L., Kamal, S. M. M., Abdullah, N. and Ismail, I. 2013. Evaluation of fermentation conditions by *Candida tropicalis* for xylitol production from sago trunk cortex. *Bioresources* 8: 2499-2509
- Mohamad, N. L., Mustapa Kamal, S. M. and Mokhtar, M. N. 2015. Xylitol biological production: A review of recent studies. *Food Reviews International* 31: 74-89
- Mohapatra, S. 2017. Application of pretreatment, fermentation and molecular techniques for enhancing bioethanol production from grass biomass – A review. *Renewable and Sustainable Energy Reviews* 78: 1007-1032
- Morais de Carvalho, D., et al. 2017. Isolation and characterization of acetylated

- glucuronoarabinoxylan from sugarcane bagasse and straw. *Carbohydrate Polymers* 156: 223-234
- Morey, R., Kaliyan, N., Tiffany, D. and Schmidt, D. 2010. A corn stover supply logistics system. *Agecon Search, Miscellaneous Papers* 26: 455-461
- Morthensen, S. T., Luo, J., Meyer, A. S., Jørgensen, H. and Pinelo, M. 2015. High performance separation of xylose and glucose by enzyme assisted nanofiltration. *Journal of Membrane Science* 492: 107-115
- Muhdi, M., Sahar, A., Hanafiah, D., Zaitunah, A. and Nababan, F. 2019. Analysis of biomass and carbon potential on eucalyptus stand in industrial plantation forest, North Sumatra, Indonesia. *IOP Conference Series: Earth and Environmental Science* 374: 012054
- Mumcu, A. S. and Temiz, A. 2014. Effects of prebiotics on growth and acidifying activity of probiotic bacteria. *GIDA* 39: 71-77
- Naik, S. N., Goud, V. V., Rout, P. K. and Dalai, A. K. 2010. Production of first and second generation biofuels: A comprehensive review. *Renewable and Sustainable Energy Reviews* 14: 578-597
- Nascimento, R., et al. 2020. A thermotolerant xylan-degrading enzyme is produced by *Streptomyces malaysiensis* AMT-3 using by-products from the food industry. *Brazilian Archives of Biology and Technology* 63: 20190243
- Nasr, S., Soudi, M. R., Hatef Salmanian, A. and Ghadam, P. 2013. Partial optimization of endo-1, 4-**B**-xylanase production by *Aureobasidium pullulans* using agro-industrial residues. *Iranian Journal of Basic Medical Sciences* 16: 1245-1253
- Natividad, C., Santiago and Alías Gallego, J. 2020. Quantification of the antioxidant activity of plant extracts: analysis of sensitivity and hierarchization based on the method used. *Antioxidants* 9: 76
- Nieto Domínguez, M., et al. 2017. Prebiotic effect of xylooligosaccharides produced from birchwood xylan by a novel fungal GH11 xylanase. *Food Chemistry* 232: 105-113
- Noda, K., Teerawatsakul, M., Prakongvongs, C. and Chaiwiratnukul, L. (1994). Major weed in Thailand. Bangkok, Ministry of Agriculture and cooperative
- Ohta, K., Fujimoto, H., Fujii, S. and Wakiyama, M. 2010. Cell-associated beta-xylosidase from *Aureobasidium pullulans* ATCC 20524: Purification, properties, and characterization of the encoding gene. *Journal of Bioscience and*

Bioengineering 110: 152-157

- Okazaki, M., Fujikawa, S. and Matsumoto, N. 1990. Effect of xylooligosaccharide on the growth of bifidobacteria. *Bifidobacteria and Microflora* 9: 77-86
- Oliveira, M., et al. 2014. *Trichoderma atroviride* 102C1 mutant: a high endoxylanase producer for assisting lignocellulosic material degradation. *Journal of Microbial & Biochemical Technology* 6: 236-241
- Olivieri, G., Wijffels, R. H., Marzocchella, A. and Russo, M. E. 2021. Bioreactor and bioprocess design issues in enzymatic hydrolysis of lignocellulosic biomass. *Catalysts* 11: 680
- Olszowy, M. and Dawidowicz, A. 2017. Is it possible to use the DPPH and ABTS methods for reliable estimation of antioxidant power of colored compounds? *Chemical Papers* 72: 393-400
- Otero, D. M., Cavalcante Braga, A. R. and Kalil, S. J. 2021. Diversification of nitrogen sources as a tool to improve endo-xylanase enzyme activity produced by *Cryptococcus laurentii*. *Biocatalysis and Agricultural Biotechnology* 32: 101941
- Pääkkönen, T., et al. 2016. Effect of xylan in hardwood pulp on the reaction rate of TEMPO-mediated oxidation and the rheology of the final nanofibrillated cellulose gel. *Cellulose* 23: 277-293
- Parameswaran, B., Gnansounou, E., Raveendran, S. and Pandey, A. 2018. Enzymes for second generation biofuels: Recent developments and future perspectives. *Bioresource Technology Reports* 5: 317-325
- Pastor, J. and Bockheim, J. G. 2011. Biomass and production of an aspen-mixed hardwood-spodosol ecosystem in northern Wisconsin. *Aspen Bibliography* 11: 132-138
- Pathania, S. 2012. Optimization of cellulase-free xylanase produced by a potential thermoalkalophilic *Paenibacillus* sp. N1 isolated from hot springs of Northern Himalayas in India. *Journal of microbiology, biotechnology and food sciences* 2: 1-24
- Patipong, T., et al. 2019. Enzymatic hydrolysis of tropical weed xylans using xylanase from *Aureobasidium melanogenum* PBUAP46 for xylooligosaccharide production. *3 Biotech* 9: 56
- Pechak, D. G. and Crang, R. 1977. An analysis of *Aureobasidium pullulans* developmental stages by means of scanning electron microscopy. *Mycologia* 69: 783-792

- Peng, F., Peng, P., Xu, F. and Sun, R.-C. 2012. Fractional purification and bioconversion of hemicelluloses. *Biotechnology Advances* 30: 879-903
- Peng, F., et al. 2009. Fractional study of alkali-soluble hemicelluloses obtained by graded ethanol precipitation from sugarcane bagasse. *Journal of Agricultural and Food Chemistry* 58: 1768-1776
- Peng, G. F., et al. 2009. Comparative study of hemicelluloses obtained by graded ethanol precipitation from sugarcane bagasse. *Journal of Agricultural and Food Chemistry* 57: 6305–6317
- Peng, H., et al. 2013. Fractionation and characterization of hemicelluloses from young bamboo (*Phyllostachys pubescens* Mazel) leaves. *Carbohydrate Polymers* 95: 262-271
- Peng, W., Pukkala, T., Jin, X. and Li, F. 2018. Optimal management of larch (*Larix olgensis* A. Henry) plantations in Northeast China when timber production and carbon stock are considered. *Annals of Forest Science* 75: 63-78
- Penksza, P., et al. 2018. Utilization of xylo-oligosaccharides as prebiotics in yoghurt. *Journal of Hygienic Engineering and Design* 22: 66-71
- Pereira, M. A. F., et al. 2020. Deconstruction of banana peel for carbohydrate fractionation. *Bioprocess and Biosystems Engineering*
- Peterson, S., Manitchotpisit, P. and Leathers, T. 2013. *Aureobasidium thailandense* sp. nov. isolated from leaves and wooden surfaces. *International Journal of Systematic and Evolutionary Microbiology* 63: 790–795
- Ping, Y., Ling, H.-Z., Song, G. and Ge, J.-P. 2013. Xylitol production from non-detoxified corncob hemicellulose acid hydrolysate by *Candida tropicalis*. *Biochemical Engineering Journal* 75: 86-91
- Poletto, P., et al. 2020. Xylooligosaccharides: Transforming the lignocellulosic biomasses into valuable 5-carbon sugar prebiotics. *Process Biochemistry* 91: 352-363
- Poltam, S., Kaewrueng, S. and Duangpatra, P. 2018. Assessment of biomass loss and air pollution caused by pre-harvest sugarcane burning using the closed loop combustion system model. *Environment Asia* 11: 1-8
- Prakash, G., Varma, A. J., Prabhune, A., Shouche, Y. and Rao, M. 2011. Microbial production of xylitol from d-xylose and sugarcane bagasse hemicellulose using newly isolated thermotolerant yeast *Debaryomyces hansenii*. *Bioresource Technology* 102: 3304-3308

- Prasongsuk, S., Lotrakul, P., Ali, I., Bankeeree, W. and Punnapayak, H. 2018. The current status of *Aureobasidium pullulans* in biotechnology. *Folia Microbiologica* 63: 129-140
- Punnapayak, H., Sudhadham, M., Prasongsuk, S. and Pichayangkura, S. 2003. Characterization of *Aureobasidium pullulans* isolated from airborne spores in Thailand. *Journal of industrial microbiology & biotechnology* 30: 89-94
- Qin, L., Xu, S.-y. and Zhang, W.-b. 2005. Effect of enzymatic hydrolysis on the yield of cloudy carrot juice and the effects of hydrocolloids on color and cloud stability during ambient storage. *Journal of the Science of Food and Agriculture* 85: 505-512
- Rafiqul, I. S. M. and Sakinah, A. M. M. 2013. Processes for the production of xylitol-a review. *Food Reviews International* 29: 127-156
- Raghee, S. M., Campbell, G. L., Scoles, G. J., MeLeod, J. G. and Tyler, R. T. 2001. Studies on rye (*Secale cereale* L.) lines exhibiting a range of extract viscosities. 1. composition, molecular weight distribution of water extracts, and biochemical characteristics of purified water-extractable arabinoxylan. *Journal of Agricultural and Food Chemistry* 49: 2437-2445
- Rai, A., et al. 2022. Recent developments in lignocellulosic biofuels, a renewable source of bioenergy. *Fermentation* 8: 161
- Raj, A., Kumar, S. and Singh, S. K. 2013. A highly thermostable xylanase from *Stenotrophomonas maltophilia*: Purification and partial characterization. *Enzyme Research* 2013: 429305
- Ramesh, S., Muthuvelayudham, R., Rajesh Kannan, R. and Viruthagiri, T. 2013. Enhanced production of xylitol from corncob by *Pachysolen tannophilus* using response surface methodology. *International Journal of Food Science* 2013: 514676
- Ramos, S. and García Acha, I. 1975. A vegetative cycle of *Pullularia pullulans*. *Transactions of the British Mycological Society* 64: 129-135
- Rao, L. V., Goli, J. K., Gentela, J. and Koti, S. 2016. Bioconversion of lignocellulosic biomass to xylitol: An overview. *Bioresource Technology* 213: 299-310
- Rashad, M. M., et al. 2016. Production of antioxidant xylooligosaccharides from lignocellulosic materials using *Bacillus amyloliquifaciens* NRRL B-14393 xylanase. *Journal of Applied Pharmaceutical Science* 6: 30-36
- Ravn, J. L., Martens, H. J., Pettersson, D. and Pedersen, N. R. 2016. A commercial GH 11

- xylanase mediates xylan solubilisation and degradation in wheat, rye and barley as demonstrated by microscopy techniques and wet chemistry methods. *Animal Feed Science and Technology* 219: 216-225
- Ribeiro, L., et al. 2014. A novel thermostable xylanase GH10 from *Malbranchea pulchella* expressed in *Aspergillus nidulans* with potential applications in biotechnology. *Biotechnol Biofuels* 7: 115
- Rodriguez, I., Tarazona, T. and Calvo, R. 1997. Aboveground biomass in a beech forest and a scots pine plantation in the Sierra de la Demanda area of northern Spain. *Annals of Forest Science* 54: 261-269
- Ruthes, A., Martínez-Abad, A., Tan, H.-T., Bulone, V. and Vilaplana, F. 2017. Sequential fractionation of feruloylated hemicelluloses and oligosaccharides from wheat bran using subcritical water and xylanolytic enzymes. *Green Chemistry* 19: 1919-1931
- Sakthiselvan, P., Naveena, B. and Partha, N. 2014. Molecular characterization of a xylanase-producing fungus isolated from fouled soil. *Brazilian Journal of Microbiology* 45: 1293-302
- Salmén, L. 2022. On the organization of hemicelluloses in the wood cell wall. *Cellulose* 29: 1349-1355
- Samanta, A. K., et al. 2015. Xylooligosaccharides as prebiotics from agricultural by-products: Production and applications. *Bioactive Carbohydrates and Dietary Fibre* 5: 62-71
- Samanta, A. K., et al. 2013. Application of pigeon pea (*Cajanus cajan*) stalks as raw material for xylooligosaccharides production. *Applied Biochemistry and Biotechnology* 169: 2392-2404
- Samanta, A. K., et al. 2012. Enzymatic production of xylooligosaccharides from alkali solubilized xylan of natural grass (*Sehima nervosum*). *Bioresource Technology* 112: 199-205
- Samanta, A. K., et al. 2016. Value addition of corn husks through enzymatic production of xylooligosaccharides. *Brazilian Archives of Biology and Technology* 59:
- Sanarat, P., Motham, P., Thonpho, A. and Srihanam, P. 2021. Phytochemicals and antioxidant activity in sugarcane (*Saccharum officinarum* L.) bagasse extracts. *Suan Sunandha Science and Technology Journal* 8: 26-35
- Santana, N. B., et al. 2018. Production of xylitol and bio-detoxification of cocoa pod husk

- hemicellulose hydrolysate by *Candida boidinii* XM02G. *PLOS ONE* 13: e0195206
- Schoch, C. L., et al. 2006. A multigene phylogeny of the Dothideomycetes using four nuclear loci. *Mycologia* 98: 1041-1052
- Sedlmeyer, F. B. 2011. Xylan as by-product of biorefineries: Characteristics and potential use for food applications. *Food Hydrocolloids* 25: 1891-1898
- Sevanan, M., Arnold, D., Pongiya, U. and Narayanan, P. M. 2011. Production of xylanase from *Arthrobacter* sp. MTCC 6915 using saw dust as substrate under solid state fermentation. *Enzyme research* 2011: 696942
- Shao, W., et al. 2011. Characterization of a novel α -xylosidase, XylC, from *Thermoanaerobacterium saccharolyticum* JW/SL-YS485. *Applied and environmental microbiology* 77: 719-726
- Sharma, K., Khaire, K. C., Thakur, A., Moholkar, V. S. and Goyal, A. 2020. Acacia xylan as a substitute for commercially available xylan and its application in the production of xylooligosaccharides. *ACS Omega* 5: 13729-13738
- Si, D., et al. 2020. Production and characterization of functional wheat bran hydrolysate rich in reducing sugars, xylooligosaccharides and phenolic acids. *Biotechnology Reports* 27: e00511
- Silva, P., et al. 2016. Production of cellulase-free xylanase by *Aspergillus flavus*: Effect of polyols on the thermostability and its application on cellulose pulp biobleaching. *African Journal of Biotechnology* 14: 3368-3373
- Singh, R., et al. 2015. *Aureobasidium pullulans* - An industrially important pullulan producing black yeast. *International Journal of Current Microbiology and Applied Sciences* 4: 605-622
- Singhania, R. R., et al. 2022. Advances and challenges in biocatalysts application for high solid-loading of biomass for 2nd generation bio-ethanol production. *Catalysts* 12: 615
- Siriwattanawimolchai, C., Ruamkratok, T., Chamninawakun, N., Poejamseen, W. and Chaim, K. 2013. Screening and characterization of yeasts from fruits and utilization in the food industry. *Thai Journal of Genetics* 1: 425
- Siti-Normah, M. D. S., Sabiha-Hanim, S. and Noraishah, A. 2012. Effects of pH, Temperature, Enzyme and substrate concentration on xylooligosaccharides production. *International Journal of Innovative Science Engineering and*

Technology 6: 1181-1185

- Śliżewska, K. and Chlebicz-Wójcik, A. 2020. Growth kinetics of probiotic *Lactobacillus* strains in the alternative, cost-efficient semi-solid fermentation medium. *Biology* 9: 423
- Smith, P. J., Wang, H.-T., York, W. S., Peña, M. J. and Urbanowicz, B. R. 2017. Designer biomass for next-generation biorefineries: leveraging recent insights into xylan structure and biosynthesis. *Biotechnology for Biofuels* 10: 286
- Sniffen, J., McFarland, L., Evans, C. and Goldstein, E. 2018. Choosing an appropriate probiotic product for your patient: An evidence-based practical guide. *PLoS ONE* 13: e0209205
- Solórzano, L., P.S. B., Ebole, S. and Pereira Jr, N. 2000. Thermal stability of xylanases produced by *Aspergillus awamori*. *Brazilian Journal of Microbiology* 31: 206-211
- Song, M., et al. 2015. Characterization of selected *Lactobacillus* Strains for use as probiotics. *Korean Journal for Food Science of Animal Resources* 35: 551-556
- Sorensen, H. R., Pedersen, S. and Meyer, A. S. 2006. Optimization of reaction conditions for enzymatic viscosity reduction and hydrolysis of wheat arabinoxylan in an industrial ethanol fermentation residue. *Biotechnology Progress* 22: 505-513
- Sousa, F., et al. 2017. Physicochemical properties of edible seed hemicelluloses. *Open Access Library Journal* 04: 1-14
- Sporck, D., et al. 2017. Xylan extraction from pretreated sugarcane bagasse using alkaline and enzymatic approaches. *Biotechnology for Biofuels* 10: 296
- Srinorasing, T., Laohakunjit, N., Keardchoecheun, O. and Matta, F. B. 2016. Comparison of conventional and ultrasound pretreatment for extracted of xylan from riceberry bran. *Agricultural Science Journal* 47: 689-692
- Sripoon, S. Effect of close cutting on yields and quality of eight forage grass species. Master's Thesis, Department of Animal Science, Graduate School, 1992.
- Stoklosa, R. J. and Hodge, D. B. 2012. Extraction, recovery, and characterization of hardwood and grass hemicelluloses for integration into biorefining processes. *Industrial and Engineering Chemistry Research* 51: 11045-11053
- Sun, J. X., Sun, X. F., Sun, R. C. and Su, Y. Q. 2004. Fractional extraction and structural characterization of sugarcane bagasse hemicelluloses. *Carbohydrate Polymers* 56: 195-204

- Tada, K., Kanno, T. and Horiuchi, J.-I. 2012. Enhanced Production of Xylitol from Corn Cobs by *Candida magnoliae*. *Industrial and Engineering Chemistry Research* 51: 10008–10014
- Tayyab, M., et al. 2017. Bioethanol production from lignocellulosic biomass by environment-friendly pretreatment methods: A review. *Applied Ecology and Environmental Research* 16: 225-249
- Teeravivattanakit, T., et al. 2016. Novel trifunctional xylanolytic enzyme Axy43A from *Paenibacillus curdlanolyticus* strain B-6 exhibiting endo-xylanase, β -D-xylosidase, and arabinoxylan arabinofuranohydrolase activities. *Applied and Environmental Microbiology* 82: 6942-6951
- Thakuria, A. and Sheth, M. 2019. An In vitro study of the prebiotic properties of xylooligosaccharide (XOS) and organoleptic evaluation of XOS added *Prawn patia* and black rice kheer. *Bioactive Compounds in Health and Disease* 3: 1-14
- Thancharoen, K., Deeseenthum, S. and Vichitphan, K. 2016. Potential of xylose-fermented yeast isolated from sugarcane bagasse waste for xylitol production using hydrolysate as carbon source. *Songklanakarin Journal of Science and Technology* 38: 473-483
- Tian, D., et al. 2020. Potential of xylanases to reduce the viscosity of micro/nanofibrillated bleached kraft pulp. *ACS Applied Bio Materials* 3: 2201-2208
- Tochampa, W., et al. 2005. A model of xylitol production by the yeast *Candida mogii*. *Bioprocess and Biosystems Engineering* 28: 175-183
- Tran, L. H., et al. 2004. The production of xylitol by enzymatic hydrolysis of agricultural wastes. *Biotechnology and Bioprocess Engineering* 9: 223-228
- Tryfona, T., et al. 2019. Development of an oligosaccharide library to characterise the structural variation in glucuronoarabinoxylan in the cell walls of vegetative tissues in grasses. *Biotechnology for Biofuels* 12: 109-128
- Tsutsui, S., Sakuragi, K., Igarashi, K., Samejima, M. and Kaneko, S. 2020. Evaluation of ammonia pretreatment for enzymatic hydrolysis of sugarcane bagasse to recover xylooligosaccharides. *Journal of Applied Glycoscience* 67: 17-22
- Tudsri, S. (1997). Tropical forage. Bangkok, Kasetsart University
- Tunc, M. S., Lawoko, M. and Heiningen, A. V. 2010. Understanding the limitations of removal of hemicelluloses during autohydrolysis of a mixture of southern

- hardwoods. *Bioresources* 5: 356-371
- Tuncer, M. and Ball, A. 2003. Co-operative actions and degradation analysis of purified xylan-degrading enzymes from *Thermomonospora fusca* BD25 on oat-spelt xylan. *Journal of applied microbiology* 94: 1030-1035
- Ünlü, C. H., Kutlu, M. and Atıcı, O. G. 2015. Mannich reaction of polysaccharides: Xylan functionalization in aqueous basic medium. *Carbohydrate Polymers* 127: 19-27
- Vacher, C., et al. 2016. The phyllosphere: microbial jungle at the plant–climate interface. *Annual Review of Ecology, Evolution, and Systematics* 47: 1-24
- Veenashri, B. R. and Muralikrishna, G. 2011. *In vitro* anti-oxidant activity of xylo-oligosaccharides derived from cereal and millet brans – A comparative study. *Food Chemistry* 126: 1475-1481
- Vena, P., García-Aparicio, M., Brienzo, M., Görgens, J. and Rypstra, T. 2013. Effect of alkaline hemicellulose extraction on kraft pulp fibers from *Eucalyptus grandis*. *Journal of Wood Chemistry and Technology* 33: 157–173
- Vlasova, A., Kandasamy, S., Chattha, K., Rajashekara, G. and Saif, L. 2016. Comparison of probiotic lactobacilli and bifidobacteria effects, immune responses and rotavirus vaccines and infection in different host species. *Veterinary Immunology and Immunopathology* 172: 72–84
- Wang, T.-H. and Lu, S. 2013. Production of xylooligosaccharide from wheat bran by microwave assisted enzymatic hydrolysis. *Food Chemistry* 138: 1531-1535
- Wang, Y., et al. 2018. Evaluation of xylooligosaccharide production from residual hemicelluloses of dissolving pulp by acid and enzymatic hydrolysis. *RSC Advances* 8: 35211-35217
- Wang, Y., et al. 2020. Optimization of harvest and logistics for multiple lignocellulosic biomass feedstocks in the northeastern United States. *Energy* 197: 117260
- Wannawilai, S. and Sirisansaneeyakul, S. 2015. Economical production of xylitol from *Candida magnoliae* TISTR 5663 using sugarcane bagasse hydrolysate. *Kasetsart Journal : Natural Science* 49: 583-596
- Wawro, A., Batog, J. and Gieparda, W. 2019. Chemical and enzymatic treatment of hemp biomass for bioethanol production. *Applied Sciences* 9: 5348
- Wei, L., Yan, T., Wu, Y., Chen, H. and Zhang, B. 2018. Optimization of alkaline extraction of hemicellulose from sweet sorghum bagasse and its direct application for the production of acidic xylooligosaccharides by *Bacillus subtilis* strain MR44.

PLOS ONE 13: e0195616

- Wen, X., et al. 2016. Exceptional hexose-fermenting ability of the xylitol-producing yeast *Candida guilliermondii* FTI 20037. *Journal of Bioscience and Bioengineering* 121: 631-637
- West, T. P. 2009. Xylitol production by *Candida* species grown on a grass hydrolysate. *World Journal of Microbiology and Biotechnology* 25: 913-916
- Williams, C. L., Westover, T. L., Emerson, R. M., Tumuluru, J. S. and Li, C. 2016. Sources of biomass feedstock variability and the potential impact on biofuels production. *BioEnergy Research* 9: 1-14
- Wipusaree, N., Sihanonth, P., Piapukiew, J., Sangvanich, P. and Karnchanata, A. 2011. Purification and characterization of a xylanase from the endophytic fungus *Alternaria alternata* isolated from the Thai medicinal plant, *Croton oblongifolius* Roxb. *African Journal of Microbiology Research* 5: 5697-5712
- Wu, J., et al. 2020. Enhancing enzyme-mediated hydrolysis of mechanical pulps by deacetylation and delignification. *ACS Sustainable Chemistry and Engineering* 8: 5847-5855
- Wu, J., et al. 2018. Single-cell protein and xylitol production by a novel yeast strain *Candida intermedia* FL023 from lignocellulosic hydrolysates and xylose. *Applied Biochemistry and Biotechnology* 185: 163-178
- Wu, Y.-R. and He, J. 2015. Characterization of a xylanase-producing *Cellvibrio mixtus* strain J3-8 and its genome analysis. *Scientific Reports* 5: 10521
- Xia, W., et al. 2015. High level expression of a novel family 3 neutral β -xylosidase from *Humicola insolens* Y1 with high tolerance to D-xylose. *PLoS One* 10: e0117578
- Xie, Y., et al. 2020. Efficient extraction and structural characterization of hemicellulose from sugarcane bagasse pith. *Polymers* 12: 608
- Xu, G.-B., Kong, W.-Q., Liu, C.-F., Sun, R.-C. and Ren, J.-L. 2017. Synthesis and characteristic of xylan-grafted-polyacrylamide and application for improving pulp properties. *Materials* 10: 971-983
- Xu, G., Song, T., He, B., Chang, M. and Ren, J. 2019. Preparation and application of a xylan-based antibacterial additive agent against *Escherichia Coli* bacteria. *BioResources* 15: 4781-4801
- Yamani, L., Kristanti, A. N. and Puspaningsih, N. N. 2016. The preliminary study of antioxidant activity from xylo-oligosaccharide of corncob (*Zea mays*) hydrolysis

- product with endo- β -xylanase enzyme. *International Journal of Infectious Diseases* 3: 112-117
- Yang, C.-H., Yang, S.-F. and Liu, W.-H. 2007. Production of xylooligosaccharides from xylans by extracellular xylanases from *Thermobifida fusca*. *Journal of agricultural and food chemistry* 55: 3955-3959
- Yanwisetpakdee, B., et al. 2016. Associations among halotolerance, osmotolerance and exopolysaccharide production of *Aureobasidium melanogenum* strains from habitats under salt stress. *Pakistan Journal of Botany* 48: 1229-1239
- Ye, Y., Li, X. and Zhao, J. 2017. Production and Characteristics of a Novel Xylose- and Alkali-tolerant GH 43 β -xylosidase from *Penicillium oxalicum* for Promoting Hemicellulose Degradation. *Scientific Reports* 7: 11600
- Yu, X., et al. 2015. Prebiotic potential of xylooligosaccharides derived from corn cobs and their in vitro antioxidant activity when combined with *Lactobacillus*. *Journal of Microbiology and Biotechnology* 25: 1084-1092
- Yurlova, N. A. and de Hoog, G. S. 1997. A new variety of *Aureobasidium pullulans* characterized by exopolysaccharide structure, nutritional physiology and molecular features. *Antonie Van Leeuwenhoek* 72: 141-147
- Yutthagosa, W. 2017. Utilization of vetiver grass in agricultural areas. PUblisher. www3.rdi.ku.ac.th/?p=38094. Accessed 18 October 2022
- Zhang, J., Geng, A., Yao, C., Lu, Y. and Li, Q. 2012. Effects of lignin-derived phenolic compounds on xylitol production and key enzyme activities by a xylose utilizing yeast *Candida athensensis* SB18. *Bioresource technology* 121: 369-378
- Zhou, J., et al. 2013. Production and characterization of ethanol- and protease-tolerant and xylooligosaccharides-producing endoxylanase from *Humicola* sp. Ly01. *Journal of Microbiology and Biotechnology* 23: 794-801
- Zimbardi, A. L., et al. 2013. Optimization of β -glucosidase, β -xylosidase and xylanase production by *Colletotrichum graminicola* under solid-state fermentation and application in raw sugarcane trash saccharification. *International Journal of Molecular Sciences* 14: 2875-2902
- Zimmermann, T., Bordeanu, N. and Strub, E. 2010. Properties of nanofibrillated cellulose from different raw materials and its reinforcement potential. *Carbohydrate Polymers* 79: 1086-1093



จุฬาลงกรณ์มหาวิทยาลัย
CHULALONGKORN UNIVERSITY



APPENDIX

จุฬาลงกรณ์มหาวิทยาลัย
CHULALONGKORN UNIVERSITY

APPENDIX A
Culture mediums

1. Yeast Malt Agar (YMA) (Atlas, 1993)		
Yeast extract	5	g
Malt extract	5	g
Peptone	5	g
Glucose	20	g
Agar	15	g
Distilled H ₂ O	1,000	mL
2. Yeast Extract-Peptone-Xylose Agar (YPX agar) (Ping et al., 2013)		
Xylose	20	g
Yeast extract	10	g
Peptone	20	g
Agar	15	g
Distilled H ₂ O	1,000	mL
3. Xylanase Production Medium (Bankeeree, 2014)		
Corn cob	1	%
Yeast-nitrogen base	6.7	g
L-Asparagine	2	g
KH ₂ PO ₄	5	g
Glucose	0.5	%
Distilled H ₂ O	1,000	mL
4. de Man Rogosa Sharpe (MRS) Agar (De Man , Rogosa and Sharpe, 1960)		
Peptone	10	g
Beef extract	10	g
Yeast extract	5	g
Glucose	20	g
Tween 80	1	mL
K ₂ HPO ₄	2	g

Sodium acetate	5	g
Tri-ammonium citrate	2	g
MgSO ₄ ·7H ₂ O	0.2	g
MnSO ₄ ·H ₂ O	0.02	g
Distilled H ₂ O	1,000	mL

5. Xylitol Production Medium (Ping et al., 2013)

- Xylose	45	g
- Glucose	5	g
- Yeast extract	2	g
- KH ₂ PO ₄	5	g
- MgSO ₄	0.4	g
- (NH ₄) ₂ SO ₄	2	g
- Distilled H ₂ O	1,000	mL

Note that: sterile xylose should be prepared separately and added after autoclaving to prevent caramelization.



APPENDIX B
Samples collection

1. Ten grass samples



Pangola grass



Ruzi grass



Para grass



Napier Pakchong 1 grass



Vetiver grass



Sugarcane leaf



Rhodes grass



Purple guinea grass



Sabi grass



Barnyard grass

2. Sample collection at Phetburi Animal Nutrition Research and Development Center



3. Sample collection at Pakchong Technology Research and Training Center



4. Sample collection at Nakhon Ratchasima Animal Nutrition Research and Development Center



CHULALONGKORN UNIVERSITY

5. Sample collection at Department of Agronomy, Kasetsart University



6. Biomass availability of grasses

Grass samples	Biomass availability (ton/ha)	Source
<u>Ten grass samples in this study</u>		
Napier grass	46	Banka et al. (2014)
Purple guinea grass	19	Banka et al. (2014)
Vetiver grass	18	Yutthagosa (2017)
Sabi grass	12	Sripoon (1992)
Ruzi grass	14	Banka et al. (2014)
Pangola grass	38	Banka et al. (2014)
Para grass	31	Kanjanapruthipong (2006)
Barnyard grass	18	Noda et al. (1994)
Rhode grass	16	Tudsri (1997)
Sugarcane leaf	17	Poltam et al. (2018)
<u>Other grasses</u>		
Tropical carpet grass	7	Teerawattanapong et al. (2018)
Whip grass	7	Teerawattanapong et al. (2018)
Cairo grass	10	Sa Kaeo Provincial Agriculture and Cooperatives Office (2017)
Signal grass	9	
Plicatulum grass	8	
Mission grass	11	Usanakornkul and Leenanruksa (1977)
Bana grass	8	Banka et al. (2014)
Communist grass	11	Jamroenprugksa (1984)

APPENDIX C

Determination of biomass composition

(Goering and Van Soest, 1970)

1. Chemicals preparation for determination of biomass composition

1.1 Neutral detergent solution

Sodium lauryl sulphate	30	g
Disodium ethylenediamine tetraacetate (EDTA) dehydrate	16.18	g
Sodium borate decahydrate ($\text{Na}_2\text{B}_4\text{O}_7 \cdot 10\text{H}_2\text{O}$)	6.81	g
Na_2HPO_4	4.56	g
2-Ethoxyethanol (ethylene glycol monoethyl ether)	10	mL

Put EDTA and $\text{Na}_2\text{B}_4\text{O}_7 \cdot 10\text{H}_2\text{O}$ in some of the distilled water, and heat until dissolved. Then, to solution containing sodium lauryl sulfate and 2-ethoxyethanol. Put Na_2HPO_4 in some of the distilled water, and heat until dissolved. Then, add to solution containing other ingredients. Adjust volume to 1 L. Check pH to rang 6.9 to 7.1.

1.2 Acid detergent solution

Sulfuric acid (%assay = 100)	49.04	g
Cetyl trimethylammonium bromide (CTAB)	20	g

Weigh sulfuric acid and make up to volume with distilled water. Check normality (N) by titration until 1 N. Then, add CTAB and stir in some of the distilled water, and heat until dissolved. Add to solution containing the other ingredient. Adjust volume to 1 L.

1.3 Saturated potassium permanganate

KMnO_4	50	g
Ag_2SO_4	0.05	g

Dissolve KMnO_4 and Ag_2SO_4 in distilled water. Keep out from sunlight.

1.4 Lignin buffer solution

Fe(NO ₃) ₃ ·9H ₂ O	6	g
AgNO ₃	0.15	g
Potassium acetate	5	g
Acetic acid, glacial	500	mL
Tertiary butyl alcohol	400	mL

Dissolve Fe(NO₃)₃·9H₂O and AgNO₃ in distilled water. Mix with acetic acid and potassium acetate. Then, add Tertiary butyl alcohol and mix.

1.5 Combined permanganate solution

Mix saturated potassium permanganate and lignin buffer solution in the ratio of 2:1 (v/v) before use. The mix solution may be kept about a week in a refrigerator in the absence of light. Old solutions change to a red color and should be discarded.

1.6 Demineralizing solution

Oxalic acid dehydrate	50	g
95% Ethanol	700	mL
Hydrochloric acid (HCl)	50	mL
Distilled H ₂ O	250	mL

Dissolve oxalic acid dehydrate in 95% ethanol. Add HCl and distilled water and mix.

จุฬาลงกรณ์มหาวิทยาลัย
CHULALONGKORN UNIVERSITY

2. Procedures for determination of biomass composition

2.1 Neutral detergent procedure

1) Dry sintered glass crucibles in the oven at 100 °C for 1 h. Oven-dry crucibles were placed in desiccator for cooling and then weight.

2) Weight 1 g dry samples ground to pass 20-30 mesh (1 mm.) into a beaker. Add 100 mL of neutral detergent solution, 2 mL of decarhydronephthalene and 0.5 g of sodium sulfite. Heat the mixture to boil in 5 to 10 minutes. Reduce heat to avoid foaming. Adjust boiling to an even level and reflux for 1 h.

3) After reflux, place the samples into sintered glass crucible. Rinse samples with hot water (90-100 °C) 3-4 times. Wash twice with acetone. Liquid solutions were removed by vacuum pump. Then, dry crucibles at 100 °C for 12 h.

4) Oven-dry crucibles were placed in desiccator for cooling and then weight. Increased weight is volume of neutral detergent fiber (NDF).

5) Calculate %NDF:

$$\%NDF = \frac{(B-A) \times 100}{S}$$

Where: S = weight of sample

A = weight of crucible

B = weight of crucible and NDF

2.2 Acid detergent procedure

1) Put samples extracted by neutral detergent solution into a beaker. Add 100 mL of acid detergent solution and 2 mL of decarhydronephthalene. Heat the mixture to boil in 5 to 10 minutes. Reduce heat to avoid foaming. Adjust boiling to an even level and reflux for 1 h.

2) After reflux, place the samples into sintered glass crucible. Rinse samples with hot water (90-100 °C) 3-4 times. Wash twice with 80% ethanol. Liquid solutions were removed by vacuum pump. Then, dry crucibles at 100 °C for 12 h.

3) Oven-dry crucibles were placed in desiccator for cooling and then weight. The gathering result is weight of acid detergent fiber (ADF). The difference between NDF and ADF is weight of hemicellulose.

4) Calculate %ADF and % Hemicellulose:

$$\%ADF = \frac{(C-A) \times 100}{S}$$

Where: S = weight of sample

A = weight of crucible

C = weight of crucible and ADF

5) Calculate % Hemicellulose:

$$\% \text{ Hemicellulose} = \% \text{ NDF} - \% \text{ ADF}$$

2.3 Determination of permanganate lignin (PML)

1) Add 25 mL of combined permanganate to crucibles that had samples extracted by acid detergent solution in the pan containing high level (2-3 cm.) of cold water for 45 min. Each crucible was placed by glass rod to stir content for distribution of permanganate to wet all particles. Then, the solution was removed by vacuum pump.

2) Add 25 mL of combined permanganate to crucibles again for 45 min. Remove solution by vacuum pump.

3) Add demineralizing solution to crucible for 5 min and remove the solution by vacuum pump. Repeat until the samples were white within 20-30 min. Then, wash twice with 80% ethanol and acetone. Liquid solutions were removed by vacuum pump. Then, dry crucibles at 100 °C for 12 h.

5) Oven-dry crucibles were placed in desiccator for cooling and then weight. The weight of samples extracted by combined permanganate was weight of lignin.

6) Calculate % Lignin:

$$\% \text{ Lignin} = \frac{(C-D) \times 100}{S}$$

Where: S = weight of sample

C = weight of crucible and ADF

D = weight of crucible and samples extracted by permanganate

2.4 Determination of cellulose

1) Burn crucible from extraction with combined permanganate in the furnace at 500 °C for 3 h.

2) Then, place crucibles in desiccator for cooling and then weight. The different weight of burning samples and crucibles was the weight of ash. For the weight of cellulose, it was the difference between weight of samples extracted by combined permanganate and weight of samples after burning.

3) Calculate % Cellulose.

$$\% \text{ Cellulose} = \frac{(D-E) \times 100}{S}$$

Where: S = weight of sample

D = weight of crucible and samples extracted by permanganate

E = weight of crucible and samples after burning

APPENDIX D
Xylanases assay

1. Chemical preparation

1.1 Dinitrosalicylic acid solution (DNS) (Miller, 1959)

3,5-Dinitrosalicylic acid	7.49	g
NaOH	13.98	g
Rochelle salt (sodium potassium tartrate)	216.10	g
Phenol solution	5.37	g
Sodium metabisulphate	5.86	g
Distilled H ₂ O	1,000	mL

1.2 Citrate buffer

1) 0.1 M citrate buffer (pH 3.0)

Citric acid	1.7	g
Tri-sodium citrate	0.5	g
Distilled H ₂ O	100	mL

2) 0.1 M citrate buffer (pH 4.0)

Citric acid	1.2	g
Tri-sodium citrate	1.2	g
Distilled H ₂ O	100	mL

1.3 Sodium acetate buffer

1) 0.1 M sodium acetate buffer (pH 4.0)

Acetic acid	0.5	mL
Sodium acetate	0.2	g
Distilled H ₂ O	99.5	mL

2) 0.1 M sodium acetate buffer (pH 5.0)

Acetic acid	0.2	mL
Sodium acetate	1	g
Distilled H ₂ O	99.8	mL

1.4 Sodium phosphate buffer

1) 0.1 M sodium phosphate buffer (pH 5.0)

Disodium hydrogen phosphate	0.1	g
Sodium dihydrogen phosphate	1.6	g
Distilled H ₂ O	100	mL

2) 0.1 M sodium phosphate buffer (pH 6.0)

Disodium hydrogen phosphate	0.2	g
Sodium dihydrogen phosphate	1.4	g
Distilled H ₂ O	100	mL

3) 0.1 M sodium phosphate buffer (pH 7.0)

Disodium hydrogen phosphate	1.1	g
Sodium dihydrogen phosphate	0.6	g
Distilled H ₂ O	100	mL

4) 0.1 M sodium phosphate buffer (pH 8.0)

Disodium hydrogen phosphate	1.7	g
Sodium dihydrogen phosphate	0.1	g
Distilled H ₂ O	100	mL

1.5 Tris-HCl buffer

1) 0.1 M Tris-HCl buffer (pH 8.0)

Tris (Hydroxymethyl) Methylamine	1.2	g
Hydrochloric acid	0.2	mL
Distilled H ₂ O	99.8	mL

2) 0.1 M Tris-HCl buffer (pH 9.0)

Tris (Hydroxymethyl) Methylamine	1.2	g
Hydrochloric acid	0.05	mL
Distilled H ₂ O	99.8	mL

1.6 Na₂HPO₄-NaOH buffer

1) 0.1 M Na₂HPO₄-NaOH (pH 9.0)

Na ₂ HPO ₄	1.4	g
NaOH	0.01	g
Distilled H ₂ O	100	mL

2) 0.1 M Na₂HPO₄-NaOH (pH 10.0)

Na ₂ HPO ₄	1.4	g
NaOH	0.03	g
Distilled H ₂ O	100	mL

3) 0.1 M Na₂HPO₄-NaOH (pH 11.0)

Na ₂ HPO ₄	1.4	g
NaOH	0.04	g
Distilled H ₂ O	100	mL

CHULALONGKORN UNIVERSITY

2. Standard curves

2.1 Standard curves for endoxylanase assay

Xylose concentrations from 0.00 to 0.07 mg/mL were prepared in distilled water. A 125 µL of each xylose concentration was added with 125 µL distilled water, 250 µL different buffers and 750 µL DNS and boiled for 5 min. A 1.5 mL distilled water was added and measured at the absorbance 540 nm. The amount of released xylose in an enzyme reaction was calculated by using the following standard xylose curves in different buffers as a reference.

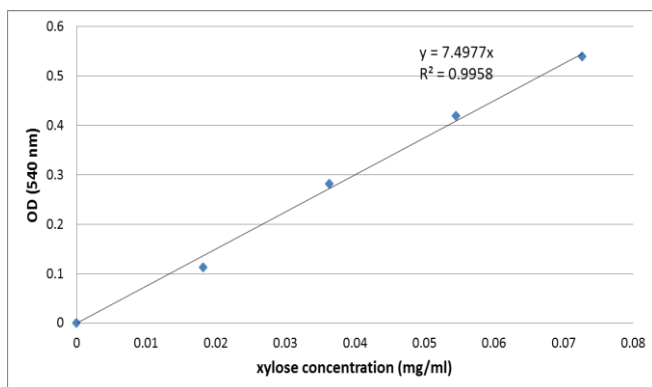


Fig 1D Xylose standard curve in Citrate buffer pH 3.0

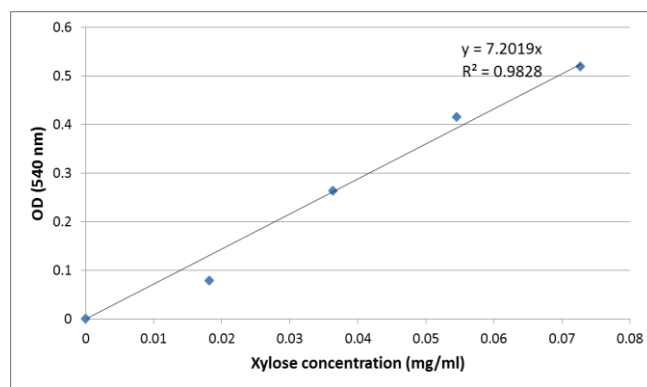


Fig 2D Xylose standard curve in Citrate buffer pH 4.0

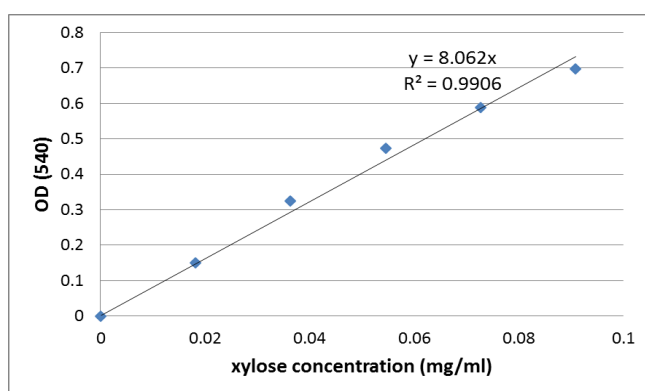


Fig 3D Xylose standard curve in sodium acetate buffer pH 4.0

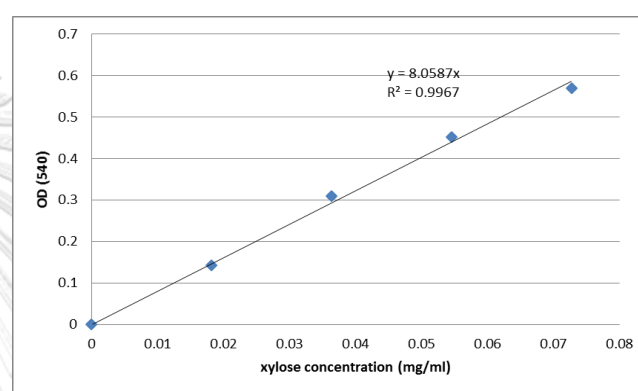


Fig 4D Xylose standard curve in sodium acetate buffer pH 5.0

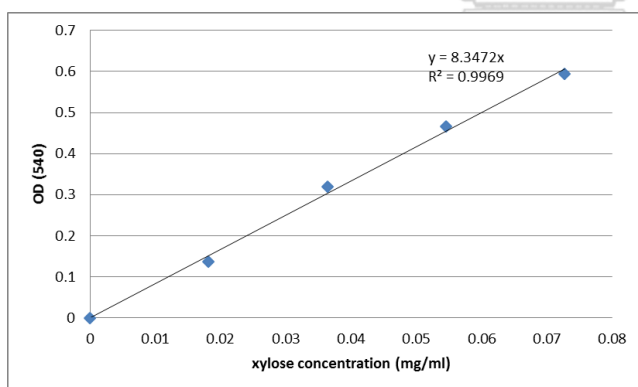


Fig 5D Xylose standard curve in sodium phosphate buffer pH 5.0

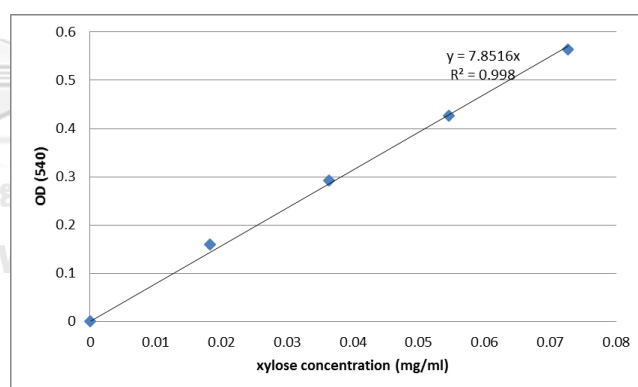


Fig 6D Xylose standard curve in sodium phosphate buffer pH 6.0

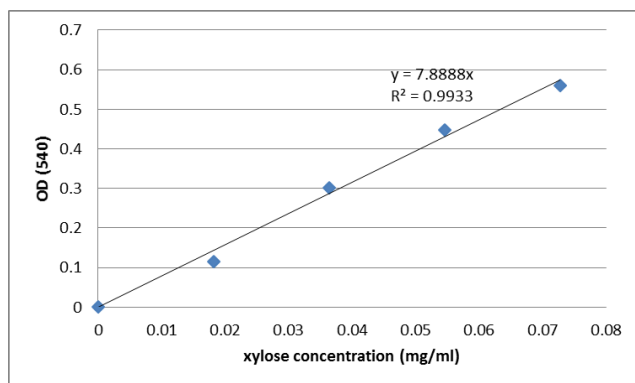


Fig 7D Xylose standard curve in sodium phosphate buffer pH 7.0

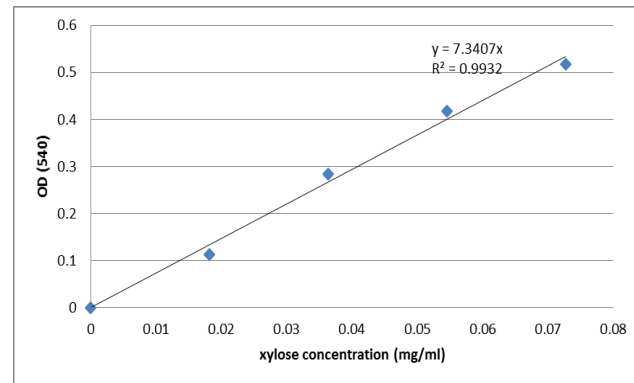


Fig 8D Xylose standard curve in sodium phosphate buffer pH 8.0

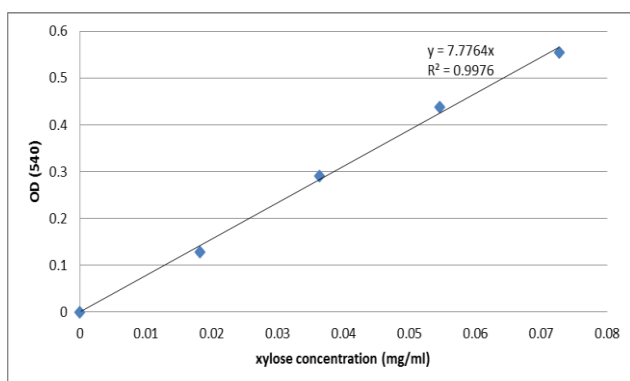


Fig 9D Xylose standard curve in Tris-HCl buffer pH 8.0

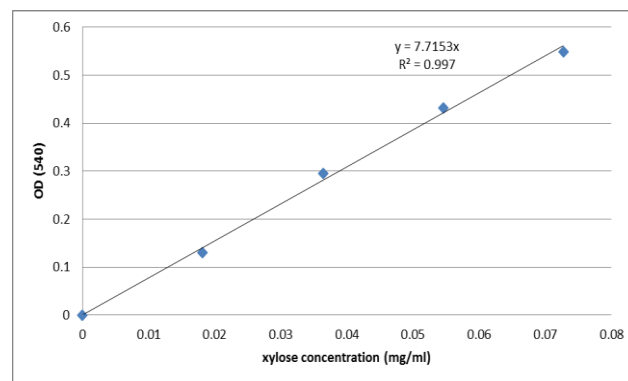


Fig 10D Xylose standard curve in Tris-HCl buffer pH 9.0

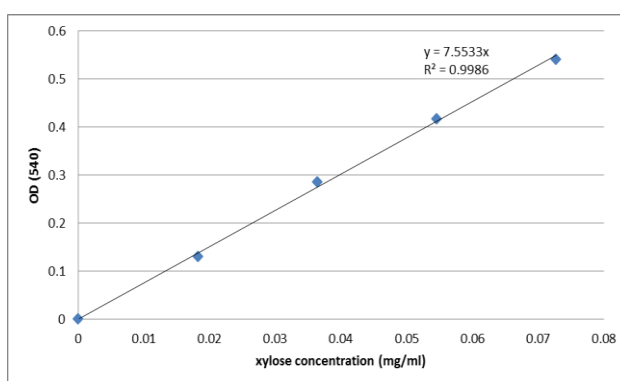


Fig 11D Xylose standard curve in Na₂HPO₄-NaOH buffer pH 9.0

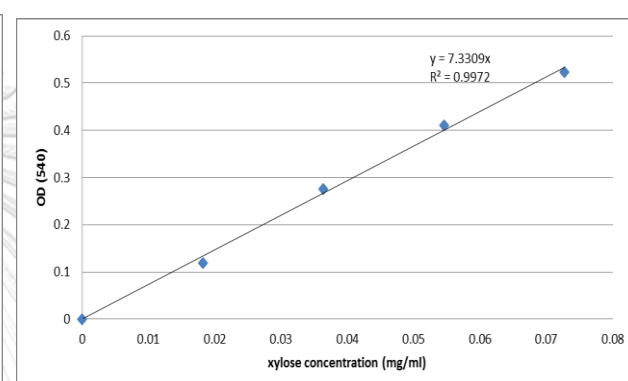


Fig 12D Xylose standard curve in Na₂HPO₄-NaOH buffer pH 10.0

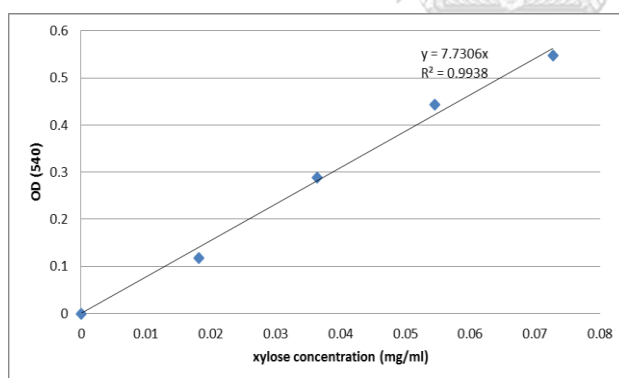


Fig 13D Xylose standard curve in Na₂HPO₄-NaOH buffer pH 11.0

2.2 Standard curves for β -xylosidase assay

p-nitrophenol between 0.00 and 0.01 μ mol were prepared in distill water. A 10 μ L each *p*-nitrophenol was added with 90 μ L distill water and 100 μ L different buffers in an eppendof. Then, 200 μ L 0.1 M Na₂CO₃ was added and measured at the absorbance 405 nm. The amount of released *p*-nitrophenol in an enzyme reaction was calculated by using the following standard *p*-nitrophenol curves in different buffers as a reference.

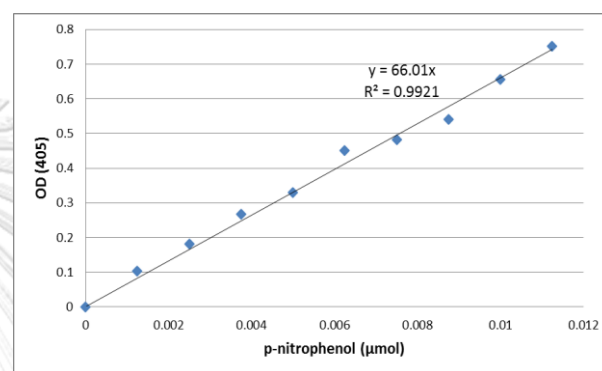
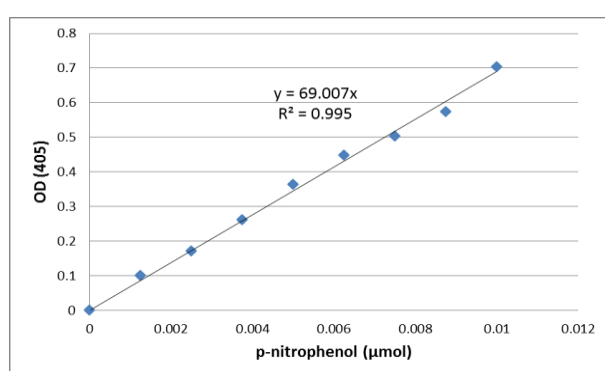
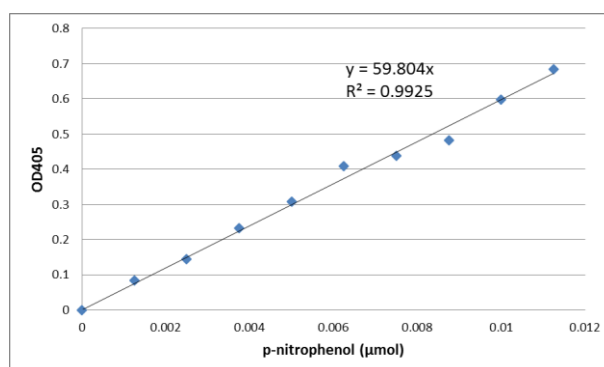
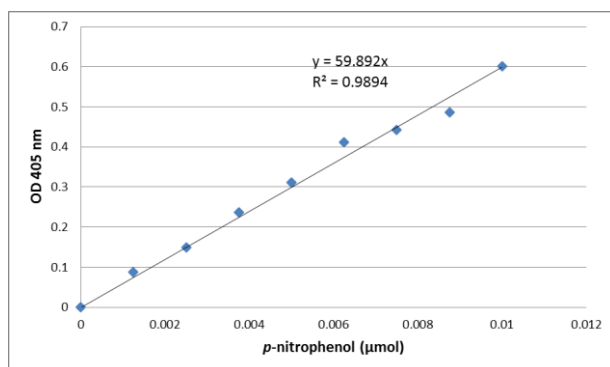


Fig 16D *p*-nitrophenol standard curve in sodium acetate buffer pH 4.0 Fig 17D *p*-nitrophenol standard curve in sodium acetate buffer pH 5.0

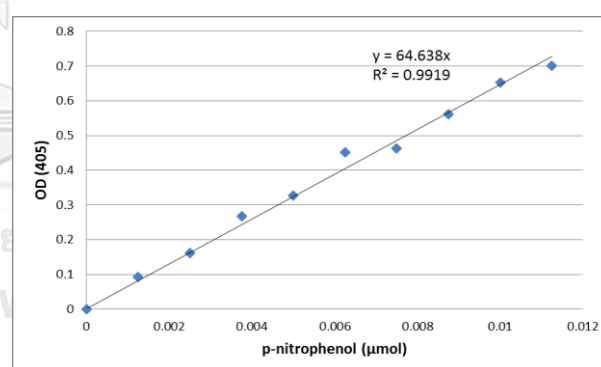
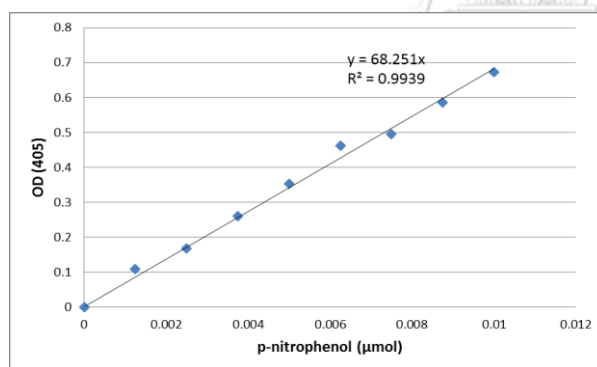


Fig 18D *p*-nitrophenol standard curve in sodium phosphate buffer pH 5.0

Fig 19D *p*-nitrophenol standard curve in sodium phosphate buffer pH 6.0

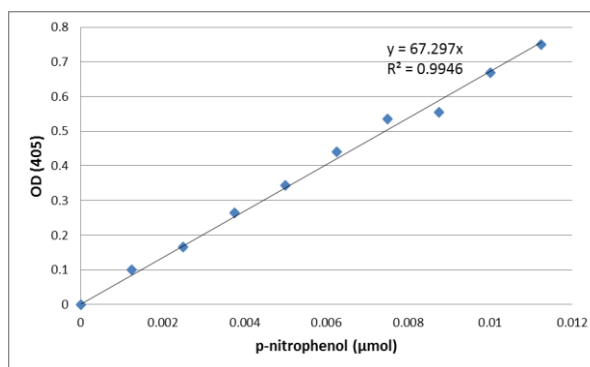


Fig 20D *p*-nitrophenol standard curve in sodium phosphate buffer pH 7.0

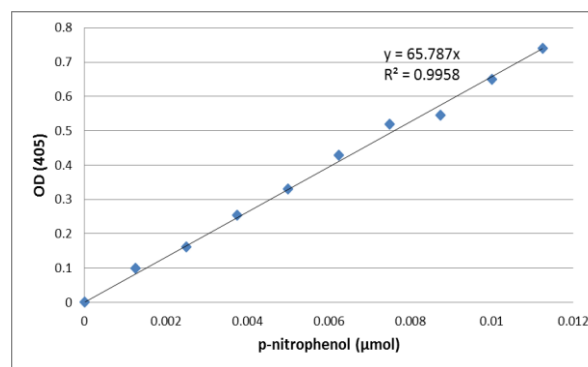


Fig 21D *p*-nitrophenol standard curve in sodium phosphate buffer pH 8.0

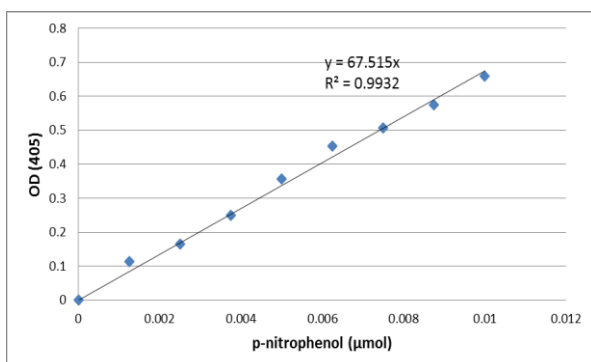


Fig 22D *p*-nitrophenol standard curve in Tris-HCl buffer pH 8.0

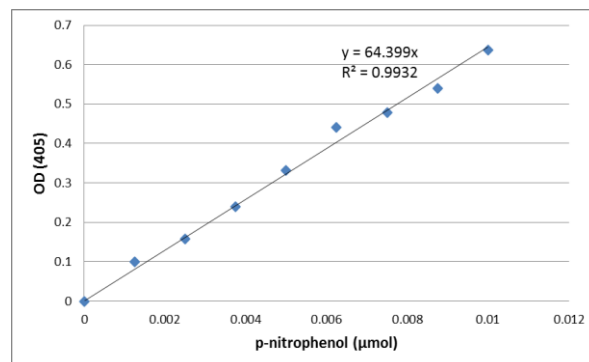


Fig 23D *p*-nitrophenol standard curve in Tris-HCl buffer pH 9.0

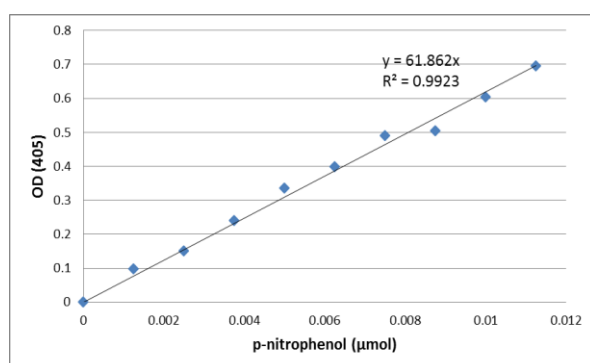


Fig 24D *p*-nitrophenol standard curve in Na₂HPO₄-NaOH buffer pH 9.0

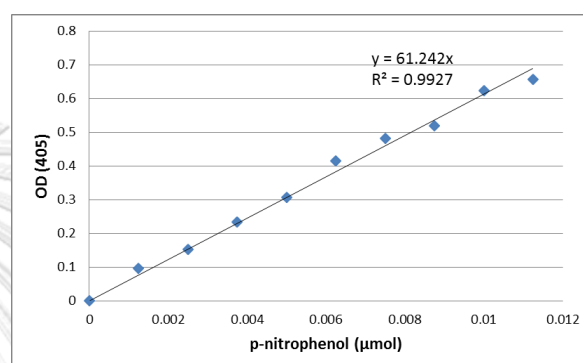


Fig 25D *p*-nitrophenol standard curve in Na₂HPO₄-NaOH buffer pH 10.0

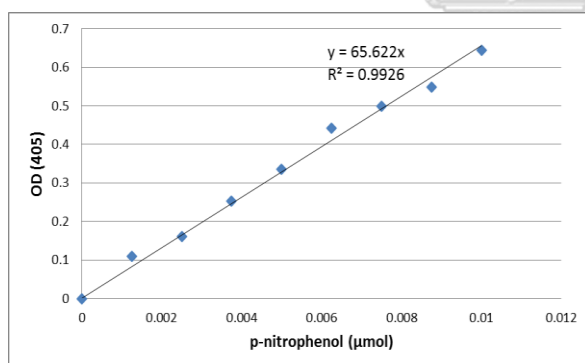


Fig 26D *p*-nitrophenol standard curve in Na₂HPO₄-NaOH buffer pH 11.0

3. Enzyme activity calculation

3.1 Endoxylanase activity

$$\text{Endoxylanase activity (Unit/ml)} = \frac{\text{Xylose concentration (mg/ml)} \times 1000 \times \text{enzyme dilution factor}}{\text{MW of xylan (g/mol)} \times \text{incubation (min)} \times \text{enzyme volume (ml)}}$$

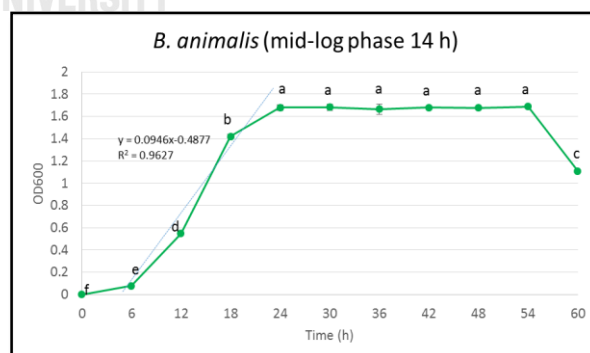
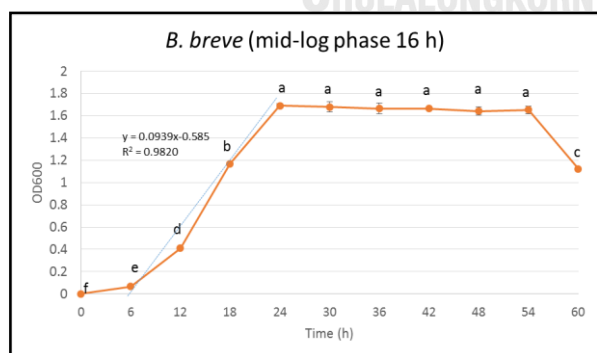
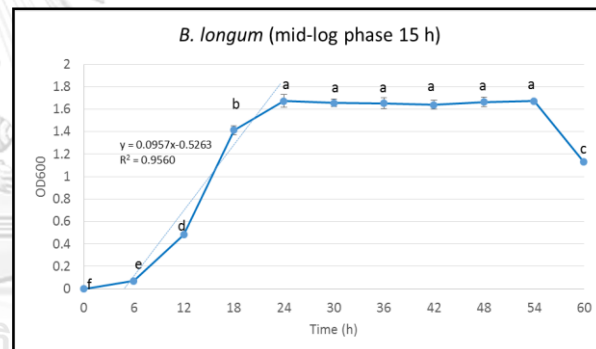
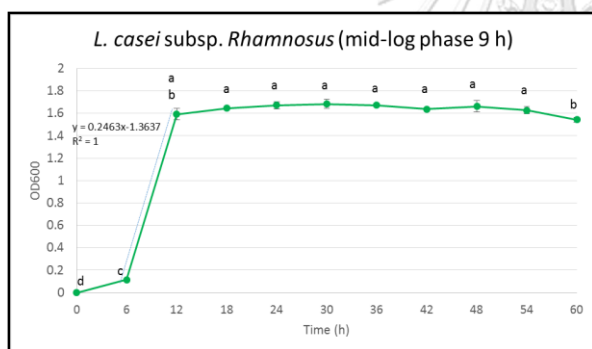
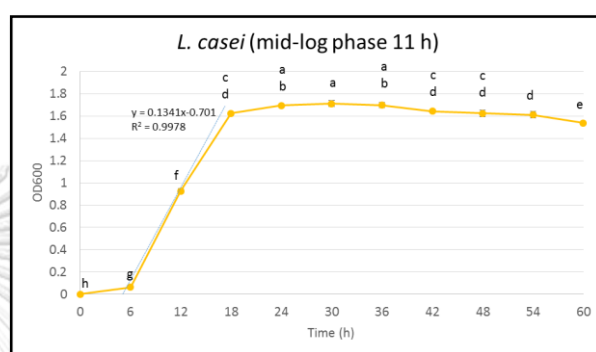
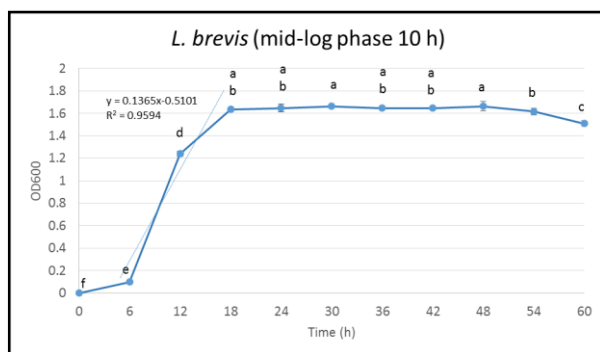
3.2 β -xylosidase activity

$$\beta\text{-xylosidase activity (Unit/g)} = \frac{p\text{-nitrophenol } (\mu\text{mol}) \times \text{enzyme dilution factor} \times \text{suspended volume (ml)}}{\text{incubation (min)} \times \text{enzyme volume (ml)} \times \text{cell dry weight (g)}}$$

APPENDIX E

Growth curve of probiotic bacteria in this study

Six strains of probiotic bacteria were cultivated in MRS broth containing glucose as the carbon source and measure cell growth every 6 h until 60 h by spectrophotometer at 600 nm of optical density.



APPENDIX F

The estimation of the average DP

(Miyazaki et al., 2005)

The average DP of each hydrolysate xylans were calculated the following equation:

$$\text{The average DP} = \frac{\text{Xylose equivalent in the xylan via Orcinol test}}{\text{Reducing sugars content via DNS method}}$$

1. Xylose equivalents by Orcinol test

- Orcinol Reagent- Dissolve 0.1g of ferric chloride in 100 mL of concentrated HCl and add 3.5 mL of 6% w/v orcinol in 95% ethanol.
- Pipette each hydrolysate xylans, each xylose concentrations and water as blank at 200 μL in test tubes.
- Add 400 μL of orcinol reagent to each test tubes.
- Mix the contents of the tubes by vortexing / shaking the tubes and heat on a boiling water bath for 20 min.
- Then cool the contents and record the absorbance at 665 nm against blank.
- Then plot the standard curve (Fig 1F) by taking concentration of xylose along X-axis and absorbance at 665 nm along Y-axis.

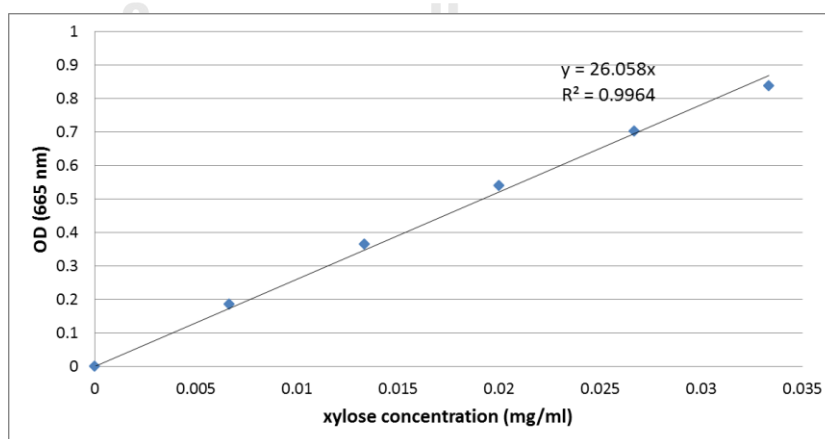


Fig 1F Xylose standard curve via Orcinol test

- Xylose equivalent of each samples were calculated by xylose concentration (mg/mL) x dilution factor.

2. Reducing sugar contents by DNS method

- Pipette each hydrolysate xylans and water as blank at 125 μL in test tubes.
- Add 125 μL of distilled water and 250 μL of sodium citrate buffer (pH 4)
- 750 μL DNS was added and the mixtures boiled for 5 min.
- Distilled water (1.5 mL) was then added and the absorbance was measured at 540 nm.
- Reducing sugar contents were calculated by xylose concentration (mg/mL) comparing with standard curve (Fig 2D) x dilution factor.



APPENDIX G

ANOVA for response surface quadratic model of optimization of xylan extraction

1. Sugarcane leaf

Source	Sum of squares	Mean square	F-value	p-value	
Model	7946.3	882.9	179.0	<0.0001	Significant
X ₁ -NaOH concentration	243.6	243.6	49.4	0.0009	
X ₂ -Steaming time	130.1	130.1	26.4	0.0037	
X ₃ -Liquid-to-solid ratio	4199.5	4199.5	851.6	<0.0001	
X ₁ X ₂	16.1	16.1	3.26	0.1309	
X ₁ X ₃	142.9	142.9	29.0	0.0030	
X ₂ X ₃	456.5	456.5	92.6	0.0002	
X ₁ ²	289.7	289.7	58.8	0.0006	
X ₂ ²	9.8	9.8	1.98	0.2187	
X ₃ ²	2581.8	2581.8	523.5	<0.0001	
Residual	24.6	4.93			
Lack of fit	23.4	7.81	12.6	0.0746	Not significant
Pure error	1.20	0.62			
Cor Total	7970.9				

Relative xylan recovery: R² = 0.99, R² (adjacent) = 0.99, CV = 2.85%

2. Napier (Pakchong 1)

Source	Sum of squares	Mean square	F-value	p-value	
Model	14156.64	1572.96	341.24	< 0.0001	Significant
X ₁ -NaOH concentration	83.21	83.21	18.05	0.0081	
X ₂ -Steaming time	112.73	112.73	24.46	0.0043	
X ₃ -Liquid-to-solid ratio	11643.03	11643.03	2525.85	< 0.0001	
X ₁ X ₂	45.42	45.42	9.85	0.0257	
X ₁ X ₃	41.35	41.35	8.97	0.0303	
X ₂ X ₃	17.51	17.51	3.80	0.1088	
X ₁ ²	105.82	105.82	22.96	0.0049	
X ₂ ²	9.53	9.53	2.07	0.2100	
X ₃ ²	2167.20	2167.20	470.15	< 0.0001	
Residual	23.05	4.61			
Lack of fit	18.25	6.08	2.54	0.2955	Not significant
Pure error	4.80	2.40			
Cor Total	14179.69				

Relative xylan recovery: R² = 0.99, R² (adjacent) = 0.99, CV = 3.70%

3. Purple guinea

Source	Sum of squares	Mean square	F-value	p-value	
Model	11067.29	1229.70	14.55	0.0044	Significant
X ₁ -NaOH concentration	295.10	295.10	3.49	0.1206	
X ₂ -Steaming time	18.86	18.86	0.22	0.6565	
X ₃ -Liquid-to-solid ratio	7909.90	7909.90	93.59	0.0002	
X ₁ X ₂	0.10	0.10	0.001	0.9737	
X ₁ X ₃	125.84	125.84	1.49	0.2768	
X ₂ X ₃	24.80	24.80	0.29	0.6113	
X ₁ ²	8.82	8.82	0.10	0.7597	
X ₂ ²	73.34	73.34	0.87	0.3943	
X ₃ ²	2669.70	2669.70	31.59	0.0025	
Residual	422.58	84.52			
Lack of fit	406.82	135.61	17.21	0.0554	Not significant
Pure error	15.76	7.88			
Cor Total	11489.87				

Relative xylan recovery: $R^2 = 0.96$, R^2 (adjacent) = 0.90, CV = 12.22%

4. Vetiver

Source	Sum of squares	Mean square	F-value	p-value	
Model	11725.13	1302.79	39.89	0.0004	Significant
X ₁ -NaOH concentration	99.94	99.94	3.06	0.1407	
X ₂ -Steaming time	0.34	0.34	0.010	0.9232	
X ₃ -Liquid-to-solid ratio	8357.03	8357.03	255.87	< 0.0001	
X ₁ X ₂	4.39	4.39	0.13	0.7288	
X ₁ X ₃	225.35	225.35	6.90	0.0467	
X ₂ X ₃	10.01	10.01	0.31	0.6036	
X ₁ ²	58.08	58.08	1.78	0.2399	
X ₂ ²	14.88	14.88	0.46	0.5296	
X ₃ ²	2838.65	2838.65	86.91	0.0002	
Residual	163.31	32.66			
Lack of fit	132.32	44.11	2.85	0.2706	Not significant
Pure error	30.99	15.49			
Cor Total	11888.44				

Relative xylan recovery: $R^2 = 0.98$, R^2 (adjacent) = 0.96, CV = 8.06%

5. Sabi

Source	Sum of squares	Mean square	F-value	p-value	
Model	6957.92	773.10	29.44	0.0008	Significant
X ₁ -NaOH concentration	69.64	69.64	2.65	0.1644	
X ₂ -Steaming time	176.52	176.52	6.72	0.0487	
X ₃ -Liquid-to-solid ratio	5563.57	5563.57	211.84	< 0.0001	
X ₁ X ₂	0.73	0.73	0.028	0.8738	
X ₁ X ₃	9.73	9.73	0.37	0.5693	
X ₂ X ₃	11.74	11.74	0.45	0.5333	
X ₁ ²	87.58	87.58	3.33	0.1274	
X ₂ ²	68.82	68.82	2.62	0.1664	
X ₃ ²	1050.03	1050.03	39.98	0.0015	
Residual	131.31	26.26			
Lack of fit	124.80	41.60	12.76	0.0735	Not significant
Pure error	6.52	3.26			
Cor Total	7089.24				

Relative xylan recovery: $R^2 = 0.98$, R^2 (adjacent) = 0.95, CV = 7.25%

APPENDIX H

ANOVA for response surface quadratic model of optimization of XO's production

1. Sugarcane leaf xylan

Source	Sum of squares	Mean square	F-value	p-value	
Model	0.015	2.973E-003	10.60	0.0108	Significant
A ₁ -Endoxylanase dosage	9.516E-003	9.516E-003	33.93	0.0021	
A ₂ -Incubation time	1.542E-003	1.542E-003	5.50	0.0660	
A ₁ A ₂	2.489E-005	2.489E-005	0.089	0.7777	
A ₁ ²	2.270E-003	2.270E-003	8.10	0.0360	
A ₂ ²	2.617E-003	2.617E-003	9.33	0.0283	
Residual	1.402E-003	2.804E-004			
Lack of fit	1.343E-003	4.478E-004	15.22	0.0623	Not significant
Pure error	5.884E-005	2.942E-005			
Cor Total	0.016				

Reducing sugars: R² = 0.91, R² (adjacent) = 0.83, CV = 6.94%

2. Purple guinea grass xylan

Source	Sum of squares	Mean square	F-value	p-value	
Model	7.286E-003	1.457E-003	831.43	< 0.0001	Significant
A ₁ -Endoxylanase dosage	4.928E-003	4.928E-003	2811.78	< 0.0001	
A ₂ -Incubation time	1.394E-003	1.394E-003	795.51	< 0.0001	
A ₁ A ₂	1.129E-005	1.129E-005	6.44	0.0520	
A ₁ ²	8.001E-004	8.001E-004	456.48	< 0.0001	
A ₂ ²	4.048E-004	4.048E-004	230.94	< 0.0001	
Residual	8.764E-006	1.753E-006			
Lack of fit	7.741E-006	2.580E-006	5.04	0.1699	Not significant
Pure error	1.023E-006	5.115E-007			
Cor Total	7.295E-003				

Reducing sugars: R² = 0.99, R² (adjacent) = 0.99, CV = 0.94%

3. Napier grass xylan

Source	Sum of squares	Mean square	F-value	p-value	
Model	5.851E-003	1.170E-003	26.73	0.0013	Significant
A ₁ -Endoxylanase dosage	4.002E-003	4.002E-003	91.41	0.0002	
A ₂ -Incubation time	1.175E-003	1.175E-003	26.84	0.0035	
A ₁ A ₂	6.471E-005	6.471E-005	1.48	0.2783	
A ₁ ²	5.476E-004	5.476E-004	12.51	0.0166	
A ₂ ²	2.087E-004	2.087E-004	4.77	0.0807	
Residual	2.189E-004	4.378E-005			
Lack of fit	1.794E-004	5.979E-005	3.03	0.2581	Not significant
Pure error	3.951E-005	1.976E-005			
Cor Total	6.070E-003				

Reducing sugars: $R^2 = 0.96$, R^2 (adjusted) = 0.93, CV = 4.66%

APPENDIX I

ANOVA for response surface quadratic model of optimization of xylose production

1. Sugarcane leaf xylan

Source	Sum of squares	Mean square	F-value	p-value	
Model	3.474E-003	3.860E-004	8.29	0.0157	Significant
B ₁ -endoxylanase concentration	6.579E-004	6.579E-004	14.13	0.0132	
B ₂ - β -xylosidase concentration	7.480E-004	7.480E-004	16.06	0.0102	
B ₃ -Incubation time	1.487E-003	1.487E-003	31.94	0.0024	
B ₁ B ₂	7.057E-006	7.057E-006	0.15	0.7131	
B ₁ B ₃	8.885E-007	8.885E-007	0.019	0.8955	
B ₂ B ₃	2.763E-005	2.763E-005	0.59	0.4759	
B ₁ ²	3.121E-005	3.121E-005	0.67	0.4502	
B ₂ ²	1.106E-006	1.106E-006	0.024	0.8835	
B ₃ ²	5.296E-004	5.296E-004	11.37	0.0198	
Residual	2.328E-004	4.657E-005			
Lack of fit	1.853E-004	6.176E-005	2.60	0.2902	Not significant
Pure error	4.756E-005	2.378E-005			
Cor Total	3.707E-003				

Xylose product: R² = 0.94, R² (adjacent) = 0.82, CV = 3.61%

2. Purple guinea grass xylan

Source	Sum of squares	Mean square	F-value	p-value	
Model	4.111E-003	4.568E-004	6.02	0.0311	Significant
B ₁ -endoxylanase concentration	9.953E-004	9.953E-004	13.12	0.0152	
B ₂ - β -xylosidase concentration	6.393E-004	6.393E-004	8.42	0.0337	
B ₃ -Incubation time	1.324E-003	1.324E-003	17.45	0.0087	
B ₁ B ₂	1.307E-004	1.307E-004	1.72	0.2464	
B ₁ B ₃	1.334E-005	1.334E-005	0.18	0.6924	
B ₂ B ₃	1.066E-005	1.066E-005	0.14	0.7232	
B ₁ ²	8.112E-004	8.112E-004	10.69	0.0222	
B ₂ ²	1.990E-005	1.990E-005	0.26	0.6304	
B ₃ ²	1.216E-004	1.216E-004	1.60	0.2614	
Residual	3.794E-004	7.588E-005			
Lack of fit	3.639E-004	1.213E-004	15.62	0.0608	Not significant
Pure error	1.553E-005	7.763E-006			
Cor Total	4.490E-003				

Xylose product: R² = 0.91, R² (adjacent) = 0.76, CV = 6.31%

3. Napier grass xylan

Source	Sum of squares	Mean square	F-value	p-value	
Model	2.030E-003	2.256E-004	27.59	0.0010	Significant
B ₁ -endoxylanase concentration	4.327E-004	4.327E-004	52.92	0.0008	
B ₂ - β -xylosidase concentration	2.510E-004	2.510E-004	30.70	0.0026	
B ₃ -Incubation time	1.145E-003	1.145E-003	140.08	< 0.0001	
B ₁ B ₂	2.025E-006	2.025E-006	0.25	0.6398	
B ₁ B ₃	1.777E-005	1.777E-005	2.17	0.2005	
B ₂ B ₃	3.994E-005	3.994E-005	4.89	0.0781	
B ₁ ²	8.370E-006	8.370E-006	1.02	0.3581	
B ₂ ²	2.106E-007	2.106E-007	0.026	0.8788	
B ₃ ²	1.270E-004	1.270E-004	15.53	0.0109	
Residual	4.088E-005	8.177E-006			
Lack of fit	3.200E-005	1.067E-005	2.40	0.3074	Not significant
Pure error	8.878E-006	4.439E-006			
Cor Total	2.071E-003				

Xylose product: $R^2 = 0.98$, R^2 (adjacent) = 0.94, CV = 2.24%

APPENDIX J

ANOVA for response surface quadratic model of optimization of xylitol production

1. Commercial xylose

Source	Sum of squares	Mean square	F-value	p-value	
Model	14053.87	1561.54	18.06	0.0027	Significant
C ₁ -Xylose concentration	1484.10	1484.10	17.17	0.0090	
C ₂ - Glucose concentration	0.49	0.49	5.650E-003	0.9430	
C ₃ -Yeast extract concention	7339.47	7339.47	84.90	0.0003	
C ₁ C ₂	56.48	56.48	0.65	0.4556	
C ₁ C ₃	397.05	397.05	4.59	0.0850	
C ₂ C ₃	1.85	1.85	0.021	0.8893	
C ₁ ²	1440.63	1440.63	16.66	0.0095	
C ₂ ²	583.19	583.19	6.75	0.0484	
C ₃ ²	3341.99	3341.99	38.66	0.0016	
Residual	432.25	86.45			
Lack of fit	417.66	139.22	19.09	0.0502	Not significant
Pure error	14.58	7.29			
Cor Total	14486.12				

Xylitol conversion: $R^2 = 0.97$, R^2 (adjacent) = 0.92, CV = 20.66%

2. Xylose-sugarcane leaf

Source	Sum of squares	Mean square	F-value	p-value	
Model	1316.00	146.22	7.91	0.0174	Significant
C ₁ -Xylose concentration	180.06	180.06	9.74	0.0262	
C ₂ - Glucose concentration	12.17	12.17	0.66	0.4542	
C ₃ -Yeast extract concention	24.28	24.28	1.31	0.3038	
C ₁ C ₂	8.95	8.95	0.48	0.5177	
C ₁ C ₃	220.44	220.44	11.92	0.0182	
C ₂ C ₃	7.83	7.83	0.42	0.5440	
C ₁ ²	816.65	816.65	44.16	0.0012	
C ₂ ²	78.23	78.23	4.23	0.0948	
C ₃ ²	14.18	14.18	0.77	0.4213	
Residual	92.47	18.49			
Lack of fit	84.87	28.29	7.44	0.1208	Not significant
Pure error	7.60	3.80			
Cor Total	1408.47				

Xylitol conversion: $R^2 = 0.93$, R^2 (adjacent) = 0.82, CV = 24.37%

3. Xylose-purple guinea grass

Source	Sum of squares	Mean square	F-value	p-value	
Model	1147.49	127.50	12.39	0.0064	Significant
C ₁ -Xylose concentration	148.23	148.23	14.40	0.0127	
C ₂ - Glucose concentration	4.46	4.46	0.43	0.5393	
C ₃ -Yeast extract concentration	5.47	5.47	0.53	0.4986	
C ₁ C ₂	13.57	13.57	1.32	0.3029	
C ₁ C ₃	186.53	186.53	18.12	0.0080	
C ₂ C ₃	32.83	32.83	3.19	0.1342	
C ₁ ²	653.56	653.56	63.49	0.0005	
C ₂ ²	114.34	114.34	11.11	0.0207	
C ₃ ²	59.03	59.03	5.73	0.0620	
Residual	51.47	10.29			
Lack of fit	49.10	16.37	13.83	0.0682	Not significant
Pure error	2.37	1.18			
Cor Total	1198.96				

Xylitol conversion: $R^2 = 0.96$, R^2 (adjacent) = 0.88, CV = 19.73%

4. Xylose-napier grass

Source	Sum of squares	Mean square	F-value	p-value	
Model	1043.20	115.91	8.49	0.0149	Significant
C ₁ -Xylose concentration	109.91	109.91	8.05	0.0364	
C ₂ - Glucose concentration	23.62	23.62	1.73	0.2455	
C ₃ -Yeast extract concentration	24.32	24.32	1.78	0.2395	
C ₁ C ₂	6.19	6.19	0.45	0.5306	
C ₁ C ₃	157.17	157.17	11.51	0.0194	
C ₂ C ₃	0.18	0.18	0.013	0.9133	
C ₁ ²	642.71	642.71	47.07	0.0010	
C ₂ ²	89.06	89.06	6.52	0.0510	
C ₃ ²	52.20	52.20	3.82	0.1079	
Residual	68.26	13.65			
Lack of fit	63.89	21.30	9.73	0.0946	Not significant
Pure error	4.38	2.19			
Cor Total	1111.47				

Xylitol conversion: $R^2 = 0.94$, R^2 (adjacent) = 0.83, CV = 23.81%

APPENDIX K
The production cost

1. The cost for xylan production in 1 g

Materials	Cost	Source	The used volume	The cost in this study
NaOH	0.52 Bath/g	Ajex Finechem	2.38 g	1.24 Bath
Acetic acid	0.44 Bath/mL	Merck	2.5 mL	1.10 Bath
95% Ethanol	0.20 Bath/mL	Excise Department	42 mL	8.40 Bath
Distilled water	0.08 Bath/mL	B smart Science Co.,Ltd	14 mL	1.12 Bath
Electricity utility	4.42 Bath/unit	Metropolitan Electricity Authority	1.65 unit	7.29 Bath
The production cost of 1 g xyan				19.15 Bath

2. The cost for xylanases production medium in 1 L

Materials	Cost	Source	The used volume	The cost in this study
Glucose	0.5 Bath/g	Ajex Finechem	5 g	2.5 Bath
Yeast Nitrogen Base	24 Bath/g	Hi-Media	6.7 g	160.8 Bath
L-Asparagine	24 Bath/g	Hi-Meida	2 g	48 Bath
KH ₂ PO ₄	0.98 Bath/g	Ajex Finechem	5 g	4.9 Bath
Distilled water	0.08 Bath/mL	B smart Science Co.,Ltd	1,000 mL	80 Bath
Electricity utility	4.42 Bath/unit	Metropolitan Electricity Authority	6.50 unit	28.73 Bath
The production cost of 1 L medium				324.13 Bath
Preparation of xylanase activity				10 U/mL
The cost of 1 unit xylanase enzymes				0.03 Bath

3. The production cost of partial and complete xylan hydrolysis

Product	Hydrolysis condition				Cost (Bath)				Production cost (Bath/mg)
	Endoxylanase (U/g substrate)	β -xylosidase (U/g substrate)	Incubation time (h)	Yield (g/g initial xylan)	Endo xylanase	β -xylosidase	Electricity	Xylan	
<u>Xylobiose</u>									
Sugarcane leaf	65.32	0	52.89	0.16	1.96	0.00	21.10	19.15	0.26
Purple guinea grass	74.86	0	64.3	0.09	2.25	0.00	25.66	19.15	0.52
Napier grass	74.88	0	64.4	0.08	2.25	0.00	25.70	19.15	0.59
<u>Xylotriase</u>									
Sugarcane leaf	65.32	0	52.89	0.08	1.96	0.00	21.10	19.15	0.53
Purple guinea grass	74.86	0	64.3	0.04	2.25	0.00	25.66	19.15	1.18
Napier grass	74.88	0	64.4	0.03	2.25	0.00	25.70	19.15	1.57
<u>Xylose</u>									
Sugarcane leaf	69.93	67.85	17.71	0.2	2.10	2.04	7.07	19.15	0.15
Purple guinea grass	69.9	70	17.71	0.17	2.10	2.10	7.07	19.15	0.18
Napier grass	68.05	63.1	17.38	0.13	2.04	1.89	6.94	19.15	0.23

VITA

NAME Acting SubLt.Sorawit Na Nongkhai

DATE OF BIRTH 10 August 1984

PLACE OF BIRTH Bangkok

INSTITUTIONS ATTENDED Chiang Mai University, Chiang Mai, Thailand
(2003-2006): B.S. in Microbiology, Graduated with First Class Honors

Asian Institute of Technology (AIT), Bangkok, Thailand
(2007- 2009): M.S. in Natural Resource Management

HOME ADDRESS 509/447, Phetchaburi Road, Thanon Phaya Thai, Ratchathewi, Bangkok, 10400

AWARD RECEIVED - First Class Honor, Chiang Mai University, 2006
- Academic Achievement Award, Department of Biology, Faculty of Science, Chiang Mai University, 2005